Tailoring Molecular Sieves' Dielectric and Electric Properties for Efficient Microwave and Resistive Heating Regeneration

by

Pooya Shariaty

A thesis submitted in partial fulfillment of the requirements for the degree of

Doctor of Philosophy

in

Environmental Engineering

Department of Civil and Environmental Engineering

University of Alberta

ABSTRACT

Adsorption onto molecular sieve adsorbents is a well-developed technique in the industry for gaseous pollutants emission control. Loaded adsorbents must then be regenerated for reuse in further adsorption cycles. Microwave and resistive heating have been introduced as potential alternatives to conventional thermal regeneration methods due to lower energy consumption, higher desorption rate, and shorter duration. Their performances mainly depend on adsorbent's permittivity (dielectric properties) and electrical resistivity for microwave and resistive heating, respectively. In general, molecular sieves have relatively low permittivity and high resistivity which can pose challenges for microwave and resistive heating regeneration. However, tuning the dielectric and electric properties of molecular sieves, can allow for more effective microwave heating regeneration and possibility of implementing resistive heating regeneration. The objective of this thesis is to provide a suitable method to tune these properties in molecular sieves without compromising their adsorption properties.

Firstly, the effect of ion-exchange of Engelhard Titanosilicate, ETS-10, (test molecular sieve), on its dielectric, adsorption and microwave regeneration properties was investigated using water (polar adsorbate). Monovalent and divalent cations (Li^+, K^+, Ca^{2+}, Cu^{2+}, Ba^{2+}) were used for ion-exchanging. The analysis of ion-exchanged samples showed decreased dielectric properties, which reduced microwave absorbance during regeneration. This effect along with increased water adsorption capacity led to up to 27% more adsorbent regeneration efficiency, suggesting more effective process due to direct adsorbate heating. Li-ETS-10 was the most suitable candidate for microwave regeneration when loaded with polar adsorbate, based on adsorption capacity, desorption efficiency, and energy consumption.

Secondly, effect of different methods for carbon addition to dealuminated zeolite Y (highly resistive molecular sieve) on its resistivity and adsorption properties was studied. Carbon was added by thermal decomposition of polyvinyl-alcohol, catalytic CH_4 decomposition, ethanol/benzene chemical vapor deposition, and physical mixing with powdered carbon. Elemental analyses and scanning electron micrographs confirmed addition of carbon to the zeolite which reduced its resistivity by up to 8 orders of magnitude. Resistivity reduction was greatest when carbon was added directly to the zeolite's surface. Catalyzed CH_4 decomposition resulted in 31wt% carbon addition in the form of carbon nanotube (CNT) reduced its resistivity from $>10^7\Omega$.m to 0.7Ω.m, but decreased its adsorption capacity by 32%.

Optimum condition for CNT deposition on dealuminated zeolite Y was then investigated aiming for minimizing the effect on its adsorption properties while suitably reducing its resistivity. Different thermal conditions were tested for this purpose. CNT addition using low temperature (as low as 400°C) and short (1hour) duration was achieved. SEM images revealed lower temperature resulted in less and smaller CNT deposition minimizing the effect on adsorption properties, while effectively reduced resistivity (to 1.1 Ω.m). The results suggested potential use of low-temperature procedure to tailor the adsorbents resistivity with minor effect on their adsorption properties.

Additionally, adsorption/thermal regeneration cycles were completed to evaluate the performance of resistive heating compared to conventional conduction-convention heating. The samples were completely regenerated using a constant power of 70 W and 4.25 W for conventional and resistive heating, respectively. Resistive heating regeneration demonstrated 94% less energy consumption, 4 times higher heating rate, and 4 times higher desorption rate compared to conventional heating.

Finally, adsorption/microwave heating regeneration performance of the modified sample was evaluated, aiming for improved dielectric properties with respect to microwave and conventional heating regeneration of original zeolite. The modification increased (>1 order of magnitude) the dielectric constant and loss factor of the zeolite resulting in higher heating rate (~10 times) and power absorption (~3 times) during microwave heating. Faster heating (16 and 5 times) and desorption rate (4 and 8 times) were obtained for microwave regeneration of modified zeolite compared to microwave and conventional regeneration of original zeolite. Modified zeolite required less time (half) and energy (7.4 times) for complete microwave regeneration compared to original zeolite. Also, modified sample showed similar microwave regeneration performance for both polar and non-polar adsorbates.

In summary, a method for tailoring the dielectric and electric properties of molecular sieves with low permittivity and high resistivity was developed. The method allows for enhanced microwave and resistive heating regeneration of molecular sieves which provides shorter regeneration duration, faster desorption, and lower energy consumption compared to conventional thermal regeneration.

PREFACE

The research completed in this dissertation was planned, designed, conducted, analyzed, interpreted, and compiled by myself, and was fully reviewed and supervised by Dr. Zaher Hashisho in the Department of Civil and Environmental Engineering at the University of Alberta. My colleagues in the Air Quality Characterization and Control Lab in the Department of Civil and Environmental Engineering at the University of Alberta, and collaborators from Dr. Steven Kuznicki group at Department of Chemical & Materials Engineering at the University of Alberta, Dr. Mojgan Daneshmand group at Department of Electrical & Computer Engineering, and Microwave Properties North assisted me in the following areas:

Chapter 3:

A version of this chapter has been published as: Shariaty P., Jahandar Lashaki M., Hashisho Z., Sawada J., Kuznicki S., Hutcheon R.; Effect of ETS-10 ion exchange on its dielectric properties and adsorption/microwave regeneration. *Separation and Purification Technology* **2017**, *179, 420-427*.

- Dr. Masoud Jahandar Lashaki assisted me in completing some of the adsorption experiments.
- Dr. Steven Kuznicki and Dr. James Sawada helped me in editing the manuscript.
- Dr. Ron Hutcheon contributed to dielectric properties measurements

Chapter 4:

- Dr. John D. Atkinson helped me in experimental design.

Chapter 5:

A version of this chapter was published as a conference paper: Shariaty, P. and Hashisho. Z.; Tailoring the Electric Resistivity of a Molecular Sieve Adsorbent for Electrothermal Regeneration. *In proceedings of 2016 AIChE Annual Meeting*, San Francisco, CA, 2016.

I dedicate this dissertation to my beloved family.

A special gratitude to my loving parents, Reza and Esmat, for their invaluable support and encouragement throughout my life.

Special feeling of gratitude goes to my sister, Pardiss, for continuous motivation to pursue my higher education, and being a great example to follow throughout my life.

Last but not least, I dedicate this dissertation to my lovely wife, Samineh, for her help, support, encouragement, and advice within the course of my PhD studies.

ACKNOWLEDGEMENTS

First and foremost, I would like to express my deepest appreciation to my supervisor, Dr. Zaher Hashisho, for his continuous guidance, generous support, and invaluable comments and feedbacks during my PhD studies. This work could not be accomplished without his experience, knowledge, and passion.

I am grateful to my funders, particularly Alberta Innovates Graduate Student Scholarship, Helmholtz-Alberta Initiative, Air & Waste Management Association (Dave Benferado Scholarship and Air Quality Study and Research Scholarship), Canadian Prairies and Northern Section of the Air & Waste Management Association (Scholarship Award and Graduate Student Travel Award), the Faculty of Graduate Studies and Research at the University of Alberta (Andrew Stewart Memorial Graduate Prize, Lehigh Inland Cement Graduate Scholarship in Environmental Studies, and Graduate Travel Award), the Graduate Students Association at the University of Alberta (Graduate Student Research Assistant Award and Professional Development Award), Shell Enhanced Learning Fund, and the Department of Civil and Environmental Engineering at the University of Alberta (Gordon R. Finch Memorial Graduate Scholarship in Environmental Engineering) for their financial support.

I also acknowledge my defense committee members, Dr. Steven Kuznicki, Dr. Yaman Boluk, Dr. Tong Yu and Dr. Nader Mahinpey as well as my former committee members, Dr. Mojgan Daneshmand and Dr. Selma Guigard, for their contributions to this work.

I highly appreciate the contribution of my co-authors: Dr. Zaher Hashisho, Dr. John Atkinson, Dr. Masoud Jahandar Lashaki, Dr. James Sawada, Dr. Ron Hutcheon, and Dr. Steven Kuznicki.

I would also like to express my gratitude to Dr. John D. Atkinson and Dr. Mohammad H. Zarifi, during their postdoctoral fellowship in our research group, for their support, comments, recommendations, and availability.

Thank you to the technicians in the Department of Civil and Environmental Engineering for their support and availability: Chen Liang, Elena Dlusskaya, Yupeng (David) Zhao, and Jela Burkus. Also, I would like to acknowledge infrastructure and instruments grants from Canada Foundation for Innovation, NSERC of Canada, and Alberta Advanced Education and Technology.

Special thanks to Samineh Kamravaei for the help and support she provided not only as a college but also as a wonderful wife.

Last but not least, I am very thankful to my friends and colleagues in the Air Quality Characterization & Control Lab.

TABLE OF CONTENTS

LIST OF TABLES

LIST OF FIGURES

LIST OF ABBREVIATIONS AND SYMBOLS

ACB	Activated Carbon Beads
ACFC	Activated Carbon Fiber Cloth
ACM	Activated Carbon Monolith
BET	Braunauer, Emmett, and Teller
BSEM	Back Scattered Scanning Electron Microscopy
CBV-901	Dealuminated Zeolite Y
CCS	Carbon Capture and Storage
CNT	Carbon Nanotube
CVD	Chemical Vapor Deposition
d_E	Penetration Depth
DAC	Data Acquisition and Control
DFT	Density Functional Theory
E(z)	Electric Field Strength
EDX	Energy Dispersive X-Ray Spectroscopy
ETS	Engelhard Titanosilicate
f	Frequency
FAU	Faujasite
f-CNT	Functionalized Carbon Nanotube
FID	Flame Ionization Detector
I	Electric Current
LUB	Length of Unused Bed
MEK	Methyl Ethyl Ketone

MW	Microwave
MWCNT	Multi Wall Carbon Nanotube
P	Power
$P(z)_{ave}$	Volumetric Power Density
pH_{PZC}	pH of Point of Zero Charge
PSR	Pressure Swing Regeneration
PVA	Polyvinyl Alcohol
PVDF	Poly(Vinylidene Fluoride)
R	Electric Resistance
RH	Relative Humidity
SEM	Scanning Electron Microscopy
SLPM	Standard Liter Per Minute
SWCNT	Single Wall Carbon Nanotube
tanδ	Loss Tangent
TMB	1,2,4-Trimethlbenzene
TPR	Throughput Ratio
TSR	Temperature Swing Regeneration
VNA	Vector Network Analyzer
VOCs	Volatile Organic Compounds
W_{AA}	Weight of Adsorbent Bed After Adsorption
W_{BA}	Weight of Adsorbent Bed Before Adsorption
XRD	X-Ray Diffraction
ε*	Complex Permittivity

ε'	Dielectric Constant
ε''	Dielectric Loss Factor
ε_0	Free Space Permittivity
λ_0	Wavelength in Vacuum

Chapter 1. INTRODUCTION AND RESEARCH OBJECTIVES

1.1. General Introduction

Adsorptive separation using molecular sieve adsorbents is a well-developed method in the industry for controlling gaseous pollutants and greenhouse gas emissions (e.g. zeolite 13x, ETS-10, and zeolite Y for controlling CO_2, CH_4, and volatile organic compounds (VOCs) emissions, respectively (Anson et al. 2009, Ling et al. 2015, Nigar et al. 2015). In this technique, however, following adsorption, loaded adsorbent must be regenerated to be used in further adsorption cycles. Conventional temperature and pressure swing regeneration (TSR and PSR) are established techniques for the regeneration of loaded adsorbents. These methods, however, have some drawbacks such as high energy consumption, long regeneration duration, and deterioration of the adsorbents (Al-Baghli and Loughlin 2005, Ania et al. 2005, Cherbański and Molga 2009, Cherbański et al. 2011, Chowdhury et al. 2012).

Microwave and resistive heating are proposed as potential alternatives for conventional thermal regeneration methods. Compared to conventional methods (e.g. hot gas, steam) these techniques are faster, can have higher desorption efficiency, and require less energy to achieve a desired desorption efficiency (Petkovska et al. 1991, Luo et al. 2006, Shi et al. 2010, Chowdhury et al. 2012, Chowdhury et al. 2013, Fayaz et al. 2015).

During microwave heating, microwave energy dissipates in an adsorbent and/or adsorbate as thermal energy or heat according to its complex permittivity (ε^*) consisting of dielectric constant (ε', real) and dielectric loss factor (ε'', imaginary), also known as dielectric properties. Dielectric

constant is related to material's ability to store energy, and dielectric loss factor describes dissipation of energy as heat. Loss tangent ($\tan\frac{\varepsilon''}{\varepsilon'}$) is also commonly used to describe the losses within the material as a result of formation of the internal field within the affected medium by microwaves penetration, a consequence of which is volumetric heating.

Resistive (also known as ohmic, electrothermal, or Joule) heating is a heating technique, whereby electric current is passed through a material with sufficiently low resistivity and heat is generated by the Joule effect (Russell and Cohn 2012). The electric current (I) that can pass through a material is inversely related to its electrical resistance (R). As the electric current passes through the material, the electrical energy dissipates into heat due to its inherent electrical resistance. The power dissipated is directly proportional to the square of electric current and electrical resistance of heated media ($\sim I^2R$).

Effective implementation of microwave and resistive heating, therefore, mainly depends on the adsorbent's dielectric properties and electrical resistivity for microwave and resistive heating, respectively. Unlike carbonaceous adsorbents, however, most molecular sieves have relatively low dielectric properties and high resistivity. The range of these properties for molecular sieves, therefore, is the main limitation for effective use of microwave and resistive heating for their regeneration. Hence, molecular sieves should be modified if they were to be regenerated with microwave or resistive heating. Therefore, there is a need to understand dielectric and electric properties of molecular sieves for developing practical methods for their modification.

Although application of microwave and resistive heating has been proven efficient for regeneration of carbonaceous materials, there are challenges for their use for the regeneration of molecular sieves. Specifically, resistive heating of most of molecular sieves are not feasible due to their respective high resistivity. The proposed research will develop a method for modification

of molecular sieves to tune their dielectric and electric properties, which promote their adsorption and microwave/resistive heating regeneration as a fast and energy efficient air pollution control method.

1.1. Problem Statement and Hypothesis

1.1.1. Microwave Regeneration

As previously mentioned, performance of microwave heating for adsorbents regeneration mainly depends on their dielectric properties (dielectric constant, dielectric loss factor, and loss tangent). Low dielectric properties of the adsorbents could affect energy consumption and system heat loss during their microwave regeneration. Since most molecular sieves have relatively low dielectric properties, for an efficient use of microwave heating for their regeneration, they should be modified aiming for an enhancement in their dielectric properties.

Ion exchange and addition of microwave absorber (also known as lossy) species to molecular sieves are proposed as methods to tailor their dielectric properties in this research. These methods, while previously used for different purposes, have not been systematically evaluated for improving the performance of microwave heating for regeneration of molecular sieves.

Cations exchange is one of the techniques that are used for tuning the adsorption properties of molecular sieves. Exchanging the cation in the structure of the molecular sieves could result in significant changes to their adsorptive properties (Anson et al. 2008, Anson et al. 2009, Anson et al. 2010, Magnowski et al. 2011). Dielectric losses of molecular sieves can be described as the oscillations of their mobile cations in the microwave field. Mobility of the cations was shown to be dependent on the net charge of oxygen within the molecular sieve lattice, and can be highly

changed by its ion exchange (Roussy et al. 1984). Therefore, it is expected that ion exchange could affect molecular sieves' dielectric properties in addition to their adsorption properties.

Additionally, methods for the addition of carbon, a lossy specie, while individually well described in the literature, have been hardly considered to tune the dielectric properties of molecular sieves. Carbon coatings, for example, are the first step in preparation of zeolite-templated porous carbons (Song et al. 2012). Nanotubes grown from zeolite bases are used for catalytic reactions (Cao et al. 2013, Sano et al. 2013, Qi et al. 2015) and membrane separations (Liang et al. 2005, Sarno et al. 2013, Zhang et al. 2014). Mixed carbon/zeolite materials are applied in multi-pollutant control adsorption applications (Jha et al. 2008, Li and Chung 2008, Miyake et al. 2008). Implementation of these carbon addition methods, however, should be carefully done with respect to their effect on adsorption properties of the adsorbents.

1.1.1. Resistive Heating Regeneration

Resistive heating has been efficiently used for regeneration of carbonaceous adsorbents. As previously mentioned, most inorganic materials including most of molecular sieves, have relatively high resistivity and cannot be heated resistively. Addition of a conductive species to molecular sieves (as described in the previous section), therefore, is expected to reduce their electrical resistivity. Carbon addition is the most practical method for this purpose.

1.2. Goal and Objectives

The research goal is to tailor the dielectric and electric properties of a molecular sieve to enhance its microwave and resistive heating regeneration. Based on the research goal and the abovementioned hypotheses, the objectives of this research can be summarized as follows:

- ***Objective 1:*** Enhancing dielectric properties and microwave regeneration of molecular sieves
  - ✓ ***Objective 1.1:*** To investigate the effect of ion exchange on dielectric properties and microwave regeneration of a molecular sieve
  - ✓ ***Objective 1.2:*** To improve the dielectric properties of a molecular sieve for its microwave regeneration by carbon addition
- ***Objective 2:*** Enhancing the electrical resistivity of molecular sieves and allow for its resistive heating regeneration.
  1.1. ***Objective 2.1:*** To reduce the resistivity of a molecular sieve by different carbon addition methods, to make it suitable for resistive heating
  1.2. ***Objective 2.2:*** To optimize the best carbon addition method aiming for minimum change in adsorption properties while sufficiently reducing the resistivity of a molecular sieve
  1.3. ***Objective 2.3:*** To evaluate the performance of resistive heating regeneration of molecular sieve after modification compared to conventional conduction-convection heating methods

1.4. Research Significance

Project success will provide a notable advantage for gas purification and air pollution control in terms of reducing energy consumption and process duration. The proposed research will introduce an optimized method for modification of molecular sieves to tune their dielectric and electric properties with minimal change to their adsorption properties. This promotes adsorption and microwave/resistive heating regeneration of molecular sieves as a fast and energy efficient air pollution control method.

1.5. Thesis Outline

This dissertation consists of eight chapters. General overview of the potential application of molecular sieves and different methods for its regeneration, problem statement, research objectives and significance, and thesis outline are provided in Chapter 1. Chapter 2 presents a literature review of available methods for thermal regeneration of molecular sieves with specific focus on microwave and resistive heating as potential alternative to conventional heating methods, followed by different methods for molecular sieves modification that could tune their dielectric and electric properties. The experimental methodologies, and the results and discussion of this study are presented in Chapters 3 to 7.

Chapter 3 investigates the effect of ion-exchange of Engelhard Titanosilicate, ETS-10, (test molecular sieve), on its adsorption, dielectric, and microwave regeneration properties. Chapter 4 investigates the effect of different carbon addition methods (including physical mixing with powdered carbon, chemical vapor deposition of ethanol and benzene, carbon nanotube (CNT) addition through catalytic CH_4 decomposition, and thermal decomposition of polyvinyl alcohol) on the resistivity and adsorption properties of dealuminated zeolite Y which has high resistivity ($>10^7$ Ω.m). In Chapter 5, optimum condition for CNT deposition on dealuminated zeolite Y was investigated aiming for reduced effect on its adsorption properties while suitably reducing its resistivity.

Adsorption/resistive heating regeneration performance of modified zeolite with optimum CNT addition condition was investigated and compared to conventional conduction-convection thermal regeneration in Chapter 6. Chapter 7 investigated the dielectric properties of the sample modified through optimum CNT addition and compared its adsorption/microwave heating regeneration performance to microwave and conventional conduction-convection heating regeneration of

original zeolite. Finally, summary of findings, and recommendations for future work are presented in Chapter 8.

1.6. References

1. Al-Baghli, N. A. and Loughlin, K. F. (2005). "Adsorption of methane, ethane, and ethylene on titanosilicate ETS-10 zeolite." Journal of Chemical Engineering Data **50**(3): 843-848.

2. Ania, C. O., Parra, J. B., Menéndez, J. A. and Pis, J. J. (2005). "Effect of microwave and conventional regeneration on the microporous and mesoporous network and on the adsorptive capacity of activated carbons." Microporous and Mesoporous Materials **85**(1-2): 7-15.

3. Anson, A., Lin, C. C. H., Kuznicki, S. M. and Sawada, J. A. (2009). "Adsorption of carbon dioxide, ethane, and methane on titanosilicate type molecular sieves." Chemical Engineering Science **64**(16): 3683-3687.

4. Anson, A., Lin, C. C. H., Kuznicki, T. M. and Kuznicki, S. M. (2010). "Separation of ethylene/ethane mixtures by adsorption on small-pored titanosilicate molecular sieves." Chemical Engineering Science **65**(2): 807-811.

5. Anson, A., Wang, Y., Lin, C. C. H., Kuznicki, T. M. and Kuznicki, S. M. (2008). "Adsorption of ethane and ethylene on modified ETS-10." Chemical Engineering Science **63**(16): 4171-4175.

6. Cao, Y., Yu, H., Tan, J., Peng, F., Wang, H., Li, J., Zheng, W. and Wong, N. B. (2013). "Nitrogen-, phosphorous- and boron-doped carbon nanotubes as catalysts for the aerobic oxidation of cyclohexane." Carbon **57**: 433-442.

7. Cherbański, R., Komorowska-Durka, M., Stefanidis, G. D. and Stankiewicz, A. I. (2011). "Microwave swing regeneration Vs temperature swing regeneration - Comparison of desorption kinetics." Industrial & Engineering Chemistry Research **50**(14): 8632-8644.

8. Cherbański, R. and Molga, E. (2009). "Intensification of desorption processes by use of microwaves-An overview of possible applications and industrial perspectives." Chemical Engineering and Processing: Process Intensification **48**(1): 48-58.

9. Chowdhury, T., Shi, M., Hashisho, Z. and Kuznicki, S. M. (2013). "Indirect and direct microwave regeneration of Na-ETS-10." Chemical Engineering Science **95**: 27-32.

10. Chowdhury, T., Shi, M., Hashisho, Z., Sawada, J. A. and Kuznicki, S. M. (2012). "Regeneration of Na-ETS-10 using microwave and conductive heating." Chemical Engineering Science **75**: 282-288.

11. Fayaz, M., Shariaty, P., Atkinson, J. D., Hashisho, Z., Phillips, J. H., Anderson, J. E. and Nichols, M. (2015). "Using microwave heating to improve the desorption efficiency of high molecular weight VOC from beaded activated carbon." Environmental Science and Technology **49**(7): 4536-4542.

12. Jha, V. K., Matsuda, M. and Miyake, M. (2008). "Sorption properties of the activated carbon-zeolite composite prepared from coal fly ash for Ni2+, Cu2+, Cd2+ and Pb2+." Journal of Hazardous Materials **160**(1): 148-153.

13. Li, Y. and Chung, T. S. (2008). "Exploratory development of dual-layer carbon-zeolite nanocomposite hollow fiber membranes with high performance for oxygen enrichment and natural gas separation." Microporous and Mesoporous Materials **113**(1-3): 315-324.

14. Liang, Y., Zhang, H., Yi, B., Zhang, Z. and Tan, Z. (2005). "Preparation and characterization of multi-walled carbon nanotubes supported PtRu catalysts for proton exchange membrane fuel cells." Carbon **43**(15): 3144-3152.

15. Ling, J., Ntiamoah, A., Xiao, P., Webley, P. A. and Zhai, Y. (2015). "Effects of feed gas concentration, temperature and process parameters on vacuum swing adsorption performance for CO2 capture." Chemical Engineering Journal **265**: 47-57.

16. Luo, L., Ramirez, D., Rood, M. J., Grevillot, G., Hay, K. J. and Thurston, D. L. (2006). "Adsorption and electrothermal desorption of organic vapors using activated carbon adsorbents with novel morphologies." Carbon **44**(13): 2715-2723.

17. Magnowski, N. B. K., Avila, A. M., Lin, C. C. H., Shi, M. and Kuznicki, S. M. (2011). "Extraction of ethane from natural gas by adsorption on modified ETS-10." Chemical Engineering Science **66**(8): 1697-1701.

18. Miyake, M., Kimura, Y., Ohashi, T. and Matsuda, M. (2008). "Preparation of activated carbon-zeolite composite materials from coal fly ash." Microporous and Mesoporous Materials **112**(1-3): 170-177.

19. Nigar, H., Navascués, N., de la Iglesia, O., Mallada, R. and Santamaría, J. (2015). "Removal of VOCs at trace concentration levels from humid air by Microwave Swing Adsorption, kinetics and proper sorbent selection." Separation and Purification Technology **151**: 193-200.

20. Petkovska, M., Tondeur, D., Grevillot, G., Granger, J. and Mitrovic, M. (1991). "Temperature-swing gas separation with electrothermal desorption step." Separation Science and Technology **26**(3): 425-444.

21. Qi, J., Benipal, N., Chadderdon, D. J., Huo, J., Jiang, Y., Qiu, Y., Han, X., Hu, Y. H., Shanks, B. H. and Li, W. (2015). "Carbon nanotubes as catalysts for direct carbohydrazide fuel cells." Carbon **89**: 142-147.

22. Roussy, G., Zoulalian, A., Charreyre, M. and Thiebaut, J. M. (1984). "How microwaves dehydrate zeolites." Journal of physical Chemistry **88**(23): 5702-5708.

23. Russell, J. and Cohn, R. (2012). Joule Heating, Book on Demand.

24. Sano, N., Kodama, T. and Tamon, H. (2013). "Direct synthesis of carbon nanotubes on stainless steel electrode for enhanced catalyst efficiency in a glucose fuel cell." Carbon **55**: 365-368.

25. Sarno, M., Tamburrano, A., Arurault, L., Fontorbes, S., Pantani, R., Datas, L., Ciambelli, P. and Sarto, M. S. (2013). "Electrical conductivity of carbon nanotubes grown inside a mesoporous anodic aluminium oxide membrane." Carbon **55**: 10-22.

26. Shi, M., Lin, C. C. H., Kuznicki, T. M., Hashisho, Z. and Kuznicki, S. M. (2010). "Separation of a binary mixture of ethylene and ethane by adsorption on Na-ETS-10." Chemical Engineering Science **65**(11): 3494-3498.

27. Song, X. H., Teo, W. S. and Wang, K. (2012). "Synthesis and characterization of activated carbons prepared from benzene CVD on zeolite y." Journal of Porous Materials **19**(2): 211-215.

28. Zhang, L., Zhao, B., Wang, X., Liang, Y., Qiu, H., Zheng, G. and Yang, J. (2014). "Gas transport in vertically-aligned carbon nanotube/parylene composite membranes." Carbon **66**: 11-17.

Chapter 2. LITERATURE REVIEW

2.1. Adsorption and regeneration principles

Adsorption is a well-developed method in the industry for controlling greenhouse gas and gaseous pollutant emission. Activated carbon and molecular sieve adsorbents are most common materials for this purpose due to their unique structural properties. Activated carbon adsorbents have broad pore size distribution, and are suitable adsorbents for purification of gas streams containing impurities with different molecular size range (Bansal and Goyal 2005). Controlling volatile organic compounds (VOCs) emission is a widely used application of activated carbon. Molecular sieve adsorbents, however, have uniform pore size (Jacobs et al. 2001) and are more suitable for adsorptive separation purposes, such as natural gas separation (Nugent et al. 2013, Eyer et al. 2014).

Interaction of adsorbent and adsorbate or the affinity of adsorbent towards adsorbate is one of the key factors in the adsorption process that can be studied through "adsorption isotherms". Adsorption isotherms correlate the amount of adsorbate adsorbed on the surface of adsorbent and partial pressure of the adsorbate in gas stream at constant temperature (Donohue and Aranovich 1998). Based on IUPAC classification, adsorption isotherms for gas/solid are divided into six different types (Figure 2-1), each representing different adsorbent/adsorbate interaction (IUPAC-Recommendation 1994, Donohue and Aranovich 1998, Sing 1998). Adsorption on microporous adsorbents usually can be describe by type I isotherm, where the amount adsorbed approaches a constant value, representing strong adsorbate/adsorbent interactions. Type II and III describe adsorption on mesoporous adsorbents with strong and weak adsorbent/adsorbate interactions,

respectively. Mono- and multi-layer adsorption as well as capillary condensation can result in Types IV and V, and Type VI illustrates multistep adsorption.

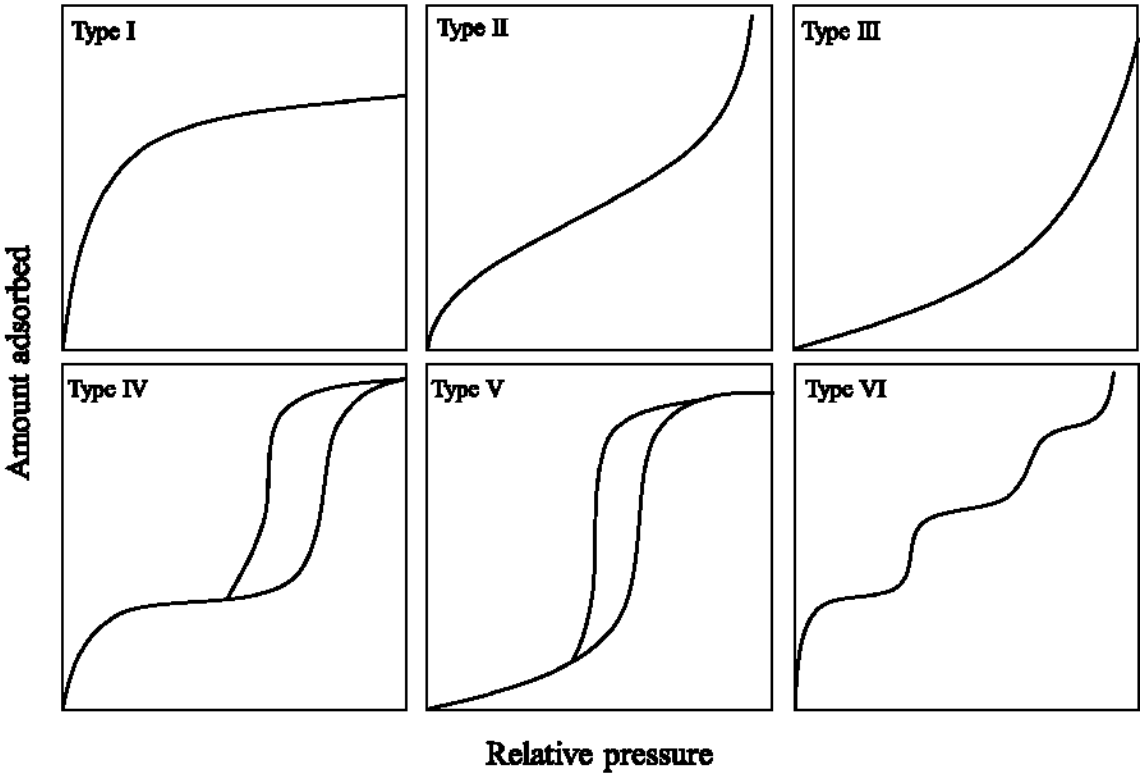

Figure 2-1. IUPAC Classification of Adsorption Isotherms for Gas–Solid Equilibria, adopted from Donohue and Aranovich (1998)

Following adsorption, an additional step, regeneration, is required to recover and reuse loaded adsorbents. During regeneration, the adsorbates are desorbed from the surface of the adsorbent to recover its adsorption capacity. Regeneration is typically done by increasing the temperature (temperature swing regeneration, TSR) or reducing the pressure (pressure swing regeneration, PSR) of loaded adsorbents. Conventional TSR and PSR techniques include steam, hot gas, conductive heating, and vacuum regeneration. Selection of the regeneration technique mainly depends on type of adsorbent and adsorbent/adsorbate interaction, which can be found from

adsorption isotherms as abovementioned. TSR is more favorable technique for strong adsorbent/adsorbate interaction (Type I isotherms), while PSR is more suitable for regeneration of adsorbents with weak adsorbent/adsorbate interaction (Type II and III isotherms) (Crittenden and Thomas 1998).

2.2. Microwave and Resistive Heating as an Alternative Thermal Regeneration Technique

Conventional PSR and TSR techniques have high energy consumption, are slow, and/or can alter the physical/chemical properties of the adsorbents and adsorbates (Al-Baghli and Loughlin 2005, Ania et al. 2005, Cherbański and Molga 2009, Cherbański et al. 2011, Chowdhury et al. 2012). Consequently, there is a need for alternative techniques to replace the conventional methods and overcome their drawbacks. Microwave and resistive heating are proposed as potential alternatives for conventional thermal regeneration methods. As further described in following sections, compared to conventional methods these techniques are faster, can have higher desorption efficiency, and require less energy to achieve a desired desorption efficiency. Performance of these methods, however, highly depends on dielectric and electric properties of the adsorbents as described below.

2.2.1. Microwave Heating

Microwaves are electromagnetic waves, which have a frequency and wavelength ranging from 0.3 GHz to 300 GHz and 1 mm to 1 m, respectively. The waves obey the laws of optics and so can be transmitted, absorbed, and reflected by a material (Jones et al. 2002, Bathen 2003, Yuen and Hameed 2009).

Depending on their ability to interact with microwaves, materials can be classified into three categories: conductors (reflect microwave), insulators (pass microwave without getting heated), and absorbers (pass and absorb microwave) (Jones et al. 2002).

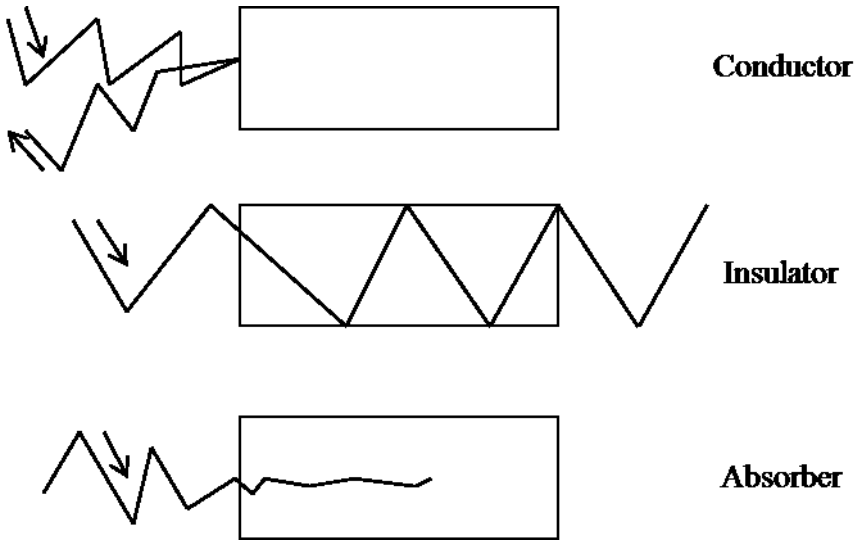

Figure 2-2. Materials with respect to their ability to be heated by microwave, adopted from Jones et al. (2002)

In principles, microwave energy dissipates in materials as thermal energy or heat according to their dielectric properties. Ionic conduction and dipole rotation/relaxation are the main heating mechanisms for solids (e.g., solid adsorbents) and polar molecules (e.g., H_2O), respectively (Rybakov et al. 2006, Polaert et al. 2010). Response of a material to microwave irradiation depends on its complex permittivity (ε^*), defined as follows:

$$\varepsilon^* = \varepsilon' - \varepsilon'' j \qquad \text{Eq. 1}$$

Dielectric constant ($\boldsymbol{\varepsilon'}$, real) is related to a material's ability to store energy. Dielectric loss factor ($\boldsymbol{\varepsilon''}$, imaginary) describes the dissipation of energy as heat. Loss tangent ($\tan\frac{\varepsilon''}{\varepsilon'}$) is also

commonly used to describe the losses within the material as a result of formation of the internal field within the affected medium by microwaves penetration, a consequence of which is volumetric heating (National Research Council 1994). Therefore, material's loss tangent could affect the volumetric power density ($P_{(z)avg.}, \frac{W}{m^3}$), which is the average microwave power converted into heat per unit volume:

$$P_{(z)_{ave.}} = 2\pi f \varepsilon_0 \varepsilon' \tan\delta \, E_{(z)}{}^2 \qquad \text{Eq. 2}$$

where f is wave frequency (1/s), ε_0 is free space permittivity (8.854×10^{-12} F/m), and $E_{(z)}$ is the internal electric field strength (V/m) in the material. Materials can be selectively heated with microwaves depending on their dielectric properties. A "lossy" material (high tan δ) can be heated more effectively than a low-loss (low tan δ) material (National Research Council 1994).

Microwave penetration into a material is another important parameter for implementation of microwave heating in industrial applications. Microwave penetration can be quantified using the Penetration Depth (d_E) which is defined as the characteristic length at which ~63% of the incident microwave power is dissipated (Metaxas and Meredith 1983):

$$d_E \approx \frac{\lambda_0}{2.\pi} \times \frac{\sqrt{\varepsilon'}}{\varepsilon''} \qquad \text{Eq. 3}$$

where λ_0 is wavelength in vacuum (m).

Very low (<1 cm) and very high (>100 cm) d_E values are not favorable for industrial applications of microwave heating. Low d_E would result in penetration of the microwaves into thin layer of the heating medium, while high d_E represents low microwave absorption by the heating medium and ineffective microwave heating (Bathen 2003).

Microwave regeneration of adsorbents was first reported in the 1980s (Roussy and Chenot 1981, Roussy et al. 1984). In a conventional thermal regeneration process, the thermal energy is delivered to material surface by radiation and/or convention heating, and then it is transferred to its bulk via conduction mechanism. In contrast, microwave heating can be considered as an energy conversion rather than heat transfer, whereby electromagnetic energy is converted to thermal energy through the molecular interaction of materials and the electromagnetic field (Das et al. 2009). During microwave heating, therefore, microwaves can penetrate the material and supply energy resulting in "volumetric heating" whereby heat generation is throughout the volume of the material (Das et al. 2009). Hence, the temperature gradient in a material during microwave heating is different than during conventional heating, which makes it possible to achieve rapid and uniform heating of thick materials.

The ease of microwave desorption, therefore, depends on adsorbent and adsorbate dielectric properties, which control the interaction of the electromagnetic waves and saturated adsorbents (i.e. microwave heating of saturated adsorbents) (Dechow 1989).

2.2.2. Resistive heating

Resistive (also known as ohmic, electrothermal, or Joule) heating is a heating technique, whereby electric current is passed through a material with sufficiently low resistivity and heat is generated by the Joule effect (Russell and Cohn 2012). The electric current (I) that can pass through a material is inversely related to its electrical resistance (R). As the electric current passes through the material, the electrical energy dissipates into heat due to its inherent electrical resistance. The power dissipated (P) is directly proportional to the square of electric current and electrical resistance of heated media ($P=I^2R$). If the electrical resistivity of all components in the material is the same, heat will be generated at the same rate throughout the volume of the heating

medium (also known as volumetric heating) (De Alwis and Fryer 1990, Varghese et al. 2012). Resistive heating regeneration allows for rapid adsorbent heating that is decoupled from the purge gas flow. Compared to conventional TSR heating methods, resistive heating regeneration is faster, can have higher desorption efficiency, and requires less energy to achieve a desired desorption efficiency (Sullivan et al. 2001, 2004). The performance of resistive heating, therefore, is highly dependent on the electrical resistivity of adsorbents (Subrenat et al. 2001, Luo et al. 2006, Park et al. 2007, Ribeiro et al. 2014).

Resistive heating is a well-established technique for regeneration of carbonaceous adsorbents (resistivity of 0.2-0.8 Ω.m (Johnsen et al. 2014)). Most inorganic adsorbents, including zeolites (resistivity of $>10^7$ Ω.m), however, are highly resistive (Álvaro et al. 2006) and cannot be heated resistively. The application of resistive heating, therefore, has been mainly studied for regeneration of carbon-based adsorbents, specifically activated carbon fiber cloth (ACFC) due to its unique form that can be readily incorporated into adsorption/resistive heating regeneration systems (Subrenat et al. 2001, Luo et al. 2006, Hashisho et al. 2008, Johnsen et al. 2011, Ramirez et al. 2011, Johnsen and Rood 2012, Johnsen et al. 2014).

2.3. Previous Works on Application of Microwave and Resistive Heating for Regeneration of adsorbents

2.3.1. Microwave heating regeneration

Carbon-based adsorbents are good candidates for regeneration with microwave heating due to their suitable dielectric properties. Microwave regeneration of carbon base adsorbents has been widely studied and compared to conventional thermal regeneration methods. Based on literature, in general, microwave regeneration resulted in higher regeneration rate, faster regeneration, and

more selective heating of the adsorbate and/or adsorbent (Mao et al. 2015, Palma and Meloni 2016, Li et al. 2017). Mao et al. (2015) reported that during regeneration of activated carbon saturated with organic vapors, desorption rate of constant power microwave heating was 20 and 40 times higher than constant temperature microwave and conductive heating, respectively. Conductive heating took 4 and 6 times longer duration than microwave heating with a constant temperature for toluene and acetone. Microwave heating for both constant power and constant temperature required 13.5 kJ/g (toluene) and 4.5 kJ/g (acetone), while conductive heating required 60.8 kJ/g (toluene) and 10.1 kJ/g (acetone). The humidity effect was found more pronounced for non-polar toluene than for polar acetone, suggesting the selective heating characteristic of microwave.

Since microwave heating directly heat the adsorbent/adsorbate, its performance is decoupled from the carrier gas flow and mainly depends on applied microwave energy and adsorbent/adsorbate dielectric properties. Performance of microwave regeneration of H_2S-saturated activated carbon adsorbent was investigated based on three different regeneration variables; microwave heating temperature (100–500 ^oC), N_2 flow rate (100–500 ml/min) and microwave heating time (5–25 min) (Mohamad Nor et al. 2016). Based on the experimental data, the regeneration of adsorbent was not effective at temperatures lower than 400 ^oC due to the insufficient microwave energy supplied to remove H_2S from adsorbent pore structures. However, increasing the microwave heating temperature to 400 ^oC provided adequate energy for the regeneration process, where the regeneration efficiency at 400 ^oC and 500 ^oC were increased by 3 and 6 folds, respectively. N_2 flow rate did not have significant influence on the regeneration efficiency (implying the direct microwave heating, which is decoupled from purge gas), while increases in microwave heating time resulted in increased regeneration efficiency. Based on obtained results, it was concluded that microwave heating duration should be properly selected

based on the dielectric properties of the heated medium. Very short microwave heating duration would result in insufficient microwave dissipation in the adsorbent, while very long duration would change the surface and porous structure of regenerated adsorbent.

Effects of microwave regeneration on structural properties of adsorbents after several adsorption/microwave regeneration cycles have also been evaluated in the literature. Depending on adsorbent and adsorbate properties and nature of adsorbent/adsorbate interaction, microwaves, in some cases, could change the structural properties of the adsorbent. This change, however, was reported to be less compared to using conventional heating methods. Microwave regeneration of activated carbon saturated with MEK, acetone, and trichloroethylene vapors was also studied after 20 adsorption/microwave heating regeneration cycles (Coss and Cha 2000). The results showed that the solvent was quickly desorbed and recovered from the inner pores of the adsorbent. Microwave regenerated adsorbent had similar adsorption capacity and surface area as the original activated carbon. Pan et al. (2016) studied microwave regeneration of two activated carbon with different structures (Arundo donax and waste fiberboard activated carbon) saturated with phenol. Waste fiberboard activated carbon maintained greater adsorption capacity (not complete) after 10 adsorption-microwave regeneration cycles compared to Arundo donax activated carbon due to its structural characteristics. Also, microwave regeneration found more efficient to regeneration activated carbon loaded with phenol compared to conventional regeneration methods. Since the adsorption of phenol on activated carbon assumed to be both physical and chemical, the chemically adsorbed part after increasing regeneration cycles decompose and the carbonaceous residue resulted in pore blockage.

Microwave heating has been also studied for regeneration of activate carbon saturated with ester contaminants (Zheng et al. 2016). The results indicated in a minimal change in adsorption

propertied due to the change in granular activated carbon textural properties, however, it was found that the ester contaminants can be easily remove from the adsorbent by microwave heating regeneration. Microwave regeneration performance was also investigated during adsorption/regeneration of functionalized carbon nanotubes (f-CNTs) in multiple cycles (Karimifard et al. 2016). The morphology, specific surface area, and pore volume of f-CNT samples were not significantly altered by microwave regeneration; however, the functional groups present on the f-CNTs' surface were gradually removed after successive cycles of regeneration/reuse. This resulted in sudden decrease (20%) in adsorption capacity. Comparing the amount desorbed over four adsorption/regeneration cycles, it was demonstrated that the microwave regeneration method can be utilized in consecutive cycles. However, after four cycles, the CNTs could not be considered as functionalized.

Although microwave heating of inorganic adsorbents is more challenging than carbonaceous adsorbents due to their relatively low dielectric properties, its performance was evaluated for regeneration of inorganic adsorbents such as molecular sieves. Previous investigations mostly proposed microwave heating for regeneration of saturated microwave transparent adsorbents with polar adsorbates. Reuß et al. (2002) showed that efficiency during microwave regeneration is related to the relative polarity of the adsorbate with respect to the adsorbent. Polar adsorbates were better desorbed from microwave transparent zeolites because; microwave energy was mainly dissipated in the adsorbate.

Witkiewicz and Nastaj (2014) studied microwave-assisted desorption of water and toluene from activated carbon and zeolite. They reported some drawbacks associated with microwave heating regeneration of zeolite, mainly included the large penetration depth of microwaves in adsorbents, plasma discharge, and problems with uniformity of the electric field strength. However, it was also

confirmed that using microwave heating in the desorption process has favorable effects, such as selective heating and restoration of the adsorption capacity of adsorbents. They also implied that microwave heating can be effective for the adsorption systems in which at least one component, adsorbent or adsorbate, is absorbing and dissipating microwave energy into heat. Consequently, the components having low dielectric loss factors can be desorbed by microwave heating only from adsorbents that are lossy dielectrics. It was also mentioned that high-silica zeolites can be used in the cyclic adsorption/microwave heating regeneration process where humid gas is applied. Pinchukova et al. (2015) studied zeolite-assisted ethanol dewatering with further microwave (MW) zeolite dehydration. Reduction of energy consumption by 1.7 times with 10-fold process time shortening was shown for lab-scale microwave heating zeolite dehydration, as compared to the corresponding conventional thermal method. Characterization of zeolite using XRD even after 20 regeneration cycles showed no effect on zeolite crystalline structure.

Since previous studies showed poor performance of microwave regeneration of adsorbents with low dielectric properties (such as inorganic adsorbents) saturated with nonpolar adsorbates, efforts were made to improve adsorbents dielectric properties. Nigar et al. (2016) worked on modification of an inorganic adsorbent (MCM-48) to enhance performance of CO_2 adsorption/microwave heating desorption system. It was found that, as the intensity of functionalization of MCM-48 with amino groups increased (from mono- to tri-amino silanes), both the CO_2 load and the dielectric response at microwave frequencies increased. The increase in the dielectric constant was reported to be related to higher density of N-H dipoles that can move freely in the grafted molecules. The incorporation of amino groups on otherwise low-interaction supports such as silica enabled polarization by the electromagnetic field and strongly enhanced response in the microwave frequency range. Comparing microwave regeneration of modified sample with conventional

heating method, shorter regeneration time (half of that in conventional heating) and faster heating (7 times) and desorption rate (3.5 times) were obtained. Hashisho et al. (2009) also reported modified dielectric properties of an activated carbon fiber cloth by changing its oxygen content through surface modification. Results showed increased dielectric properties (by ~50%) of hydrogen treated adsorbent (with ~72% decreased oxygen content). In contrary, acid treatment led to decreased dielectric properties (~89%) due to 677% increase in adsorbent's oxygen content.

2.3.2. Resistive heating regeneration

Resistive heating is another alternative to conventional thermal regeneration techniques. Performance of this technique has been widely evaluated for regeneration of carbonaceous adsorbents due to their suitable electric resistivity. Specifically, among all carbonaceous adsorbents several studies in the literature cover different aspects of resistive heating regeneration of activated carbon fiber cloth (ACFC), as it can be readily used in adsorption/resistive heating regeneration process due to its form.

Advantages of resistive heating over conventional heating methods for regeneration of carbonaceous adsorbents have been investigated in different studies. Sullivan et al. (2001) evaluated resistive heating regeneration of saturated ACFC with MEK. Results showed rapid desorption of MEK. No difference was observed in the ACFC properties after 40 adsorption-resistive heating desorption cycles, and adsorption capacity remained constant. Luo et al. (2006) studied resistive heating regeneration of different activated carbon adsorbents (including monolith (ACM), fiber cloth (ACFC), and beads (ACB)) after saturation with organic vapors. ACFC had 1–2 orders of magnitude lower electrical resistivity at 455 K, and was at least 5–10 times faster to be regenerated compared to ACB and ACM, respectively. ACFC's concentration factor was more than 22 times the concentration factor for ACM and ACB. Resistive heating regeneration of ACM,

ACB, and ACFC provided a wide range of readily controllable concentration factors at the outlet of all three systems. Such control of concentration factors was reported to be readily achievable because the energy applied to the adsorbent was controlled rapidly and decoupled from the carrier-gas flow rate during the resistive heating regeneration of the adsorbents. Performance of resistive heating for regeneration of carbon molecular sieve 3K saturated with water was also studied and compared with conventional thermal regeneration method (Ribeiro et al. 2011). The results showed higher heating rate and cooling rate of resistive heating compared to conventional thermal heating. It was also reported that resistive heating can be employed in separations where the feed stream is saturated with water with lower energy requirements than a TSR process. In large units, massive water condensation inside the column should be prevented to avoid contact of water with the lower electrode.

Some studies also showed some drawbacks associated with high heating rate of resistive heating regeneration towards some compounds that could lead to adsorbate decomposition and production of byproducts, which restrict adsorbent pores. Giraudet et al. (2014) investigated resistive heating regeneration of ACFC saturated with 5 different compounds including toluene, dichloromethane, isopropanol, siloxane D4, and ethyl mercaptan at 420 K. During the desorption tests, the temperature was shown to be homogeneously distributed over the entire ACFC implying uniform heating. The desorption was monitored by measuring the resistivity of ACFC during the regeneration step offering in measuring, in situ, and in controlled conditions using resistive heating regeneration. Two types of desorption behavior were clearly revealed. Among the five VOCs considered, toluene, dichloromethane, and isopropanol were shown to be completely removed at 420 K. On the contrary, siloxane D4 and ethyl mercaptan were more problematic because they were partially desorbed, and reduced adsorption capacities after regeneration were predicted,

mainly due to low regeneration temperature or deposition of byproduct in the ACFC, which could not be removed. The electric power required for the resistive heating desorption was also estimated at 1500 W/kg. Niknaddaf et al. (2016) also studied resistive heating regeneration of three activated carbon fiber cloths (ACFC10, ACFC15, and ACFC20, with increasing average pore widths and volumes) after cyclic adsorption/resistive heating regeneration using 1,2,4-trimethylbenzene (TMB). They reported that using resistive heating with high heating rate resulted in formation of carbon species by thermal degradation of TMB. Increased pore blockage was observed as the regeneration temperature was increased, confirming the thermal degradation of TMB to carbon species that cannot be thermally removed. Adsorption characteristics of propan-2-ol on Sorbonorit 4 activated carbon were also determined using the breakthrough curve tests in a cyclic adsorption/resistive heating desorption (Downarowicz 2015). Three samples of Sorbonorit 4 including virgin, direct resistively heated and regenerated through resistive heating after adsorption were used to assess the influence of resistive heating on the properties of the adsorbent. The structural characteristics of activated carbon showed that pure and resistively heated Sorbonorit 4 had a bimodal structure, formed by two micropore fractions, while regenerated Sorbonorit 4 contains only one fraction of micropores. It was found that regenerated Sorbonorit 4 had higher adsorption capacity than pure adsorbent while resistively heated Sorbonorit 4 depicted lower adsorption capacity.

Hu et al. (2017) also reported that adsorption/resistive heating regeneration system has the potential to be controlled with the electrical properties of the adsorbent. This was proven to be a replacement for gas and temperature sensors. 10 adsorption/resistive heating regeneration experiments with an air stream containing 2000 ppm_v isobutane and activated carbon fiber cloth (ACFC) were performed to evaluate regeneration energy consumption. It was reported that

resistive heating desorption energy efficiency can be improved through control of adsorbent heating, allowing for cost-effective separation and concentrating of organic gases for reuse. They provided a control logic based on temperature feedback achieved select temperature and power profiles during regeneration cycles while maintaining the ACFC's mean regeneration temperature (200 °C), which improves energy efficiency for separating and concentrating organic gases for post-desorption liquefaction of the organic gas for reuse. It was also proved that during adsorption/resistive heating regeneration, the temperature can be controlled by adsorbent resistance monitoring and control (Johnsen and Rood 2012).

Furthermore, many studies introduced resistive heating regeneration as an efficient method for recovery of organic vapors captured on ACFC, and its capability for scale up. Sullivan et al. (2004) studied resistive heating regeneration of ACFC saturated with Hazardous Air Pollutants and VOCs. It was found that resistive heating regeneration resulted in rapid condensation of the adsorbates on the adsorber walls. Results proved resistive heating as an efficient regeneration technique with unique characteristics, as rapid desorption at extremely low purge gas flow rate, rapid rate of ACFC heating, rapid mass transfer kinetics inherent to ACFC, and in-vessel condensation. In situ carbon resistive heating regeneration was also investigated as a means of decreasing the expense of methyl bromide recovery after its adsorption on activated carbon (Snyder and Leesch 2001). It was reported that Methyl bromide desorbed in this manner was easily condensed at moderate temperatures. Also, 12 successive adsorption/regeneration cycles were performed and compared with virgin samples, no change has been found in terms of adsorption equilibria and adsorption rate. A pilot-scale adsorption–resistive heating desorption cycles also performed to capture and recover organic vapor on activated carbon cloth, aiming for the influence of the desorption conditions on the desorbate quality (Subrenat and Le Cloirec 2004). It was

reported that the process led to desorbate effluent with high concentration and low flow rate with low energy cost and ease of implementation. Ramirez et al. (2011) developed the scale-up from the bench-scale to the pilot-scale of a novel adsorption-resistive heating system using ACFC. MEK was used as a test adsorbate. The bench-scale and pilot-scale systems achieved 91% and 68% liquid recovery efficiency, respectively. They reported that ACFC can be regeneration in bench and pilot-scale units less than 30 min, consuming electrical energy per unit recovered liquid MEK mass of 4.7 kJ/g and 18.3 kJ/g, respectively. Sullivan et al. (2004) also described an automated VOCs adsorption/resistive heating desorption bench-scale system with ACFC. The desorbed adsorbate condensed onto the inner walls of the adsorber and was collected at the bottom of the vessel without the use of ancillary cooling. Seventy percent of the adsorbate was collected per cycle as condensate, with the balance being retained in the regenerated adsorber or recycled to the second adsorber. Resistive heating desorption with in-vessel condensation results in minimal N_2 consumption and short regeneration cycle times allowing the process to be cost competitive with conventional adsorption processes. Another bench-scale study on adsorption/resistive heating regeneration for capture and recovery of organic vapors from air on ACFC reported that the electrical energy consumed during regeneration per mole of liquid organic compound recovered decreased with increasing relative pressure of the inlet gas stream, ranging from 4698 kJ/mol to 327 kJ/mol (Dombrowski et al. 2004).

The performance of resistive heating was also investigated after modification of the adsorbent, resulting in a change in its electrical resistivity (the key parameter in resistive heating). Emamipour et al. (2015) performed adsorption and resistive heating regeneration for capture of toxic industrial chemicals using ACFC modified with silica nanoparticles. It was found that although the resistivity of the modified sample was twice of that for original ACFC, the resistivity was still suitable for

complete regeneration of the modified ACFC with resistive heating. Hashisho et al. (2009) also changed ACFC resistivity by changing its oxygen content through surface modification. 72% decrease and 677% increase was obtained in oxygen content by hydrogen and acid treatment, respectively. Based on their observations, ACFC resistivity increased (3200%) by increasing the oxygen content of the adsorbent and decreased (63%) by decreasing the oxygen content. Graphitized carbon with mesoporous and microporous structures were also synthesized and tested for adsorption/resistive heating regeneration of benzene (Li et al. 2012). Due to the high electrical conductivities associated with the graphitized structures, a resistive heating desorption technique was employed to regenerate the saturated adsorbents and produce enriched benzene vapors. In comparison to microporous activated carbon, the porous graphitized carbon was found to afford much quicker and more efficient regeneration by resistive heating desorption due to their enhanced conductivity and larger pore sizes. In addition, the concentration of the desorbed organics was reported to be controlled by adjusting the applied voltages, which might be interesting for practical secondary treatment.

2.4. Molecular sieve adsorbents

A class of materials with three-dimensional framework structure that forms uniformly sized pores of molecular dimensions that exhibited selective adsorption properties, and separate components of a mixture based on molecular size and shape differences. As the pores preferentially adsorb molecules that fit inside the pores and exclude molecules that are too large, they act as sieves on a molecular scale, also known as molecular sieve effect. They were initially known as zeolite (named by Swedish geologist Axel Cronstedt in 1756, which literally means “boiling stone”) and certain microporous charcoals. Since molecular sieves now consist of different classes

of materials, the classical name, zeolite, nowadays is just carried by aluminosilicates molecular sieves (Jacobs et al. 2001, Auerbach et al. 2003, Cejka et al. 2010).

Classical zeolite is a crystalline aluminosilicate consist of robust, crystalline silica (SiO_2) frameworks, where Al^{3+} has replaced Si^{4+} at some places in the framework resulted in a negative charge. It also contains loosely held cations within its cavities preserving electroneutrality of zeolite, which are amenable to exchange with other cations. These cations result in higher affinity of these materials to adsorb polar molecules. There are other materials (mostly inorganic) follow the same principles forming different categories of molecular sieve adsorbents. Each category shows unique performance due to its structural properties (Jacobs et al. 2001, Auerbach et al. 2003, Cejka et al. 2010).

Application of molecular sieves is well known in adsorption process-as an air pollution control technique. Specifically, they demonstrate substantial selectivity and adsorption capacity for adsorptive separation of hydrocarbons and purification/speciation of natural gas, which could result in less greenhouse gas and VOCs emissions. Different molecular sieves have been conventionally used for different abatement systems. Zeolite 13x is a conventional adsorbent used in CO_2 capture and storage process (CCS) (Ben-Mansour et al. 2016), zeolite Y is used in VOCs abatement systems (Kim and Ahn 2012), zeolite 5A is typically used for natural gas purification (Nugent et al. 2013, Eyer et al. 2014), and natural zeolite and mixed coordination molecular sieves (ETS-10, ETS-2) are good adsorbents for natural gas speciation and gas drying applications (Anson et al. 2009, Avila et al. 2011, Chowdhury et al. 2012, Shariaty et al. 2017). They are also suitable materials for gas sensing applications due to their unique physical/chemical properties (Zarifi et al. 2017). Similar to other adsorbents, saturated molecular sieves should be regenerated for reuse in following adsorption cycles and avoid additional cost due to their replacement.

2.5. Backgrounds on methods for modification of molecular sieves' properties

2.5.1. Ion exchange

Cation exchange is one of the techniques that mainly used for tuning the adsorption properties of molecular sieves. Exchanging the cation in the structure of the molecular sieves could result in significant changes in their adsorptive properties (Anson et al. 2008, Anson et al. 2009, Anson et al. 2010, Magnowski et al. 2011). The substitution of extra framework cations inside the structure of molecular sieves can affect their adsorption properties, such as BET surface area, pore volume, and pore width. Besides, enhanced selectivity of the molecular sieves could be achieved due to changes in their affinity towards adsorbates as a result of cation replacement (Anson et al. 2009, Park et al. 2010). The type of the substituted cations could also affect the electric field inside adsorbent pores (Park et al. 2010), and its basicity (Waghmode et al. 2003).

Additionally, few studies investigated the effect of ion exchange on dielectric properties of adsorbents. Khachatryan and Gevorgyan (2010) measured changes in the dielectric constant and loss factor for natural zeolites by displacing their cations. Cation exchange resulted in reduced dielectric constant and loss factor due to the change in hindered ionic conduction or ionic relaxation, which are responsible for the dielectric response. Roussy et al. (1984) also defined dielectric losses of the zeolites as the oscillations of their mobile cations in the microwave field. Mobility of the cations was shown to be dependent on the net charge of oxygen within the molecular sieve lattice. Mobility of the cations is a stronger factor in determining the ionic conductivity and dielectric properties of molecular sieve adsorbents, and can be highly changed by its ion exchange. Legras et al. (2012) studied changes in dielectric properties of two different zeolite faujasite structure (zeolite X and Y) by ion exchange with alkaline cations including Li^+, Na^+, and K^+. They reported three major phenomena for original Na-FAU and exchanged zeolites

with Li and K cations including ionic conductivity, interfacial polarization, and rotational polarization of water molecules adsorbed, which affect zeolite polarization in microwave field. Ion exchange with both cations resulted in reduction in dielectric properties of zeolites. Li cations were reported to be more strongly linked to the framework than K^+ and Na^+ and induce a lower ionic conductivity, resulted in its lowest dielectric properties obtained.

2.5.2. Carbon addition

Different forms of carbon addition have been previously used for improving electrical conductivity, dielectric properties, and mechanical strength of polymers, ceramic matrices, and elastomers. Specifically, application of black fillers including carbon nanotube for improved properties have been reported (Wang and Dang 2005, Bokobza 2007, Shin and Hong 2012, Qing et al. 2014, Wu et al. 2016, Zhao et al. 2016, He et al. 2017). Shin and Hong (2012) showed enhanced electrical properties of ceramic matrix by physically dispersing single wall carbon nanotube (SWCNT) using sonicator into ceramic initial solution. It was found that the electrical resistivity of ceramic drastically decreased from 10^{12} Ω.cm to 0.3 Ω.cm after 1wt% SWCNT addition. Bokobza (2007) also reported that addition of black fillers (carbon black or carbon nanotubes) impart conductivity to low resistivity elastomeric matrices. These results indicated that electrical properties are strongly affected by the filler concentration, morphology (e.g. particle size), and structure as well as filler-filler and filler-matrix interactions which determine the state of dispersion (Bokobza 2007). Also, in case of carbon nanotubes, their orientation inside the matrix was reported as an important parameter in changing the resistivity of the polymer. For instance, the resistivity of styrene butadiene rubber composites was reduced from $\sim 6\times10^{13}$ to $\sim 5\times10^{3}$ and $\sim 5\times10^{4}$ Ω.cm by addition of carbon nanotube and carbon black, respectively (Bokobza 2007).

The effect of physical blending of carbon-nanotube/poly(vinylidene fluoride) (MWCNT/PVDF) on the dielectric and electric properties of the composite were investigated (Wang and Dang 2005). The dielectric properties and electrical conductivity of the composite increased by more than one order of magnitude compared to the PVDF sample without any CNT. Qing et al. (2014) completed a study by physically mixing CNT with starting solution for ceramic composite. The modification resulted in an enhancement in electrical conductivity and dielectric properties of the composite, which ultimately increased its microwave absorption. It was also mentioned that these properties are highly dependent on how CNT is distributed throughout the ceramic matrix with better distribution resulted in more improvement in dielectric and electric properties. Zhao et al. (2016) investigated the effect of CNT addition, ranging from 0 to 0.9 vol%, on dielectric properties of a cement–sand-based piezoelectric composite. Results demonstrated an increase in dielectric properties of the composite with optimal CNT content of 0.6 vol%. It was also demonstrated that dispersion of graphene oxide as conductive filler in polymer matrix led to improved dielectric constant with minimal change in dielectric loss factor (Wu et al. 2016).

Considering the previous reports on the effect of carbon filler on dielectric and properties of polymers, ceramic matrices, and elastomers, the same principles could be used for molecular sieves modification. However, in this case, the carbon addition can be readily completed through post synthesis modification process. Carbon can be added to solid substrates by chemical vapor deposition (CVD) (Kim et al. 1999, Lu et al. 2004, Song et al. 2012), thermal degradation of polymers (Nath and Sahajwalla 2011, Nath and Sahajwalla 2011, Yang et al. 2012, Uda et al. 2013), and physical mixing (Bueche 1973, Park et al. 2007, Park et al. 2009). Depending on method, carbon may be added to the substrate as (1) individual particles (Fan et al. 2014, Jiang et al. 2014), (2) monolayer or multilayer surface coverage (Kim et al. 1999, Song et al. 2012), or (3)

carbon nanotubes (CNT) grown from catalyst roots on the substrate's surface (Kumar and Ando 2005, Khatri et al. 2010, Nath and Sahajwalla 2011, Nath and Sahajwalla 2011, Janas and Koziol 2014). If added carbon is periodic (i.e., structured carbon), no electrons will be scattered. Electrons have greater probability of scattering if the structure is imperfect (i.e., amorphous carbon). Less scattered electrons (i.e., structured carbon) will result in lower electrical resistivity, improving resistive heating potential (Jullien 1989, Singleton 2001). These carbon-addition methods, while individually well described in the literature, have been hardly considered as techniques to tune the properties of molecular sieves. Carbon coatings, for example, are the first step in preparation of zeolite-templated porous carbons (Song et al. 2012). Nanotubes grown from zeolite bases are used for catalytic reactions (Cao et al. 2013, Sano et al. 2013, Qi et al. 2015) and membrane separations (Liang et al. 2005, Sarno et al. 2013, Zhang et al. 2014). Mixed carbon/zeolite materials are applied in multi-pollutant control adsorption applications (Jha et al. 2008, Li and Chung 2008, Miyake et al. 2008).

2.6. References

1. Al-Baghli, N. A. and Loughlin, K. F. (2005). "Adsorption of methane, ethane, and ethylene on titanosilicate ETS-10 zeolite." Journal of Chemical Engineering Data **50**(3): 843-848.

2. Álvaro, M., Cabeza, J. F., Fabuel, D., García, H., Guijarro, E. and De Juan, J. L. M. (2006). "Electrical conductivity of zeolite films: Influence of charge balancing cations and crystal structure." Chemistry of Materials **18**(1): 26-33.

3. Ania, C. O., Parra, J. B., Menéndez, J. A. and Pis, J. J. (2005). "Effect of microwave and conventional regeneration on the microporous and mesoporous network and on the adsorptive capacity of activated carbons." Microporous and Mesoporous Materials **85**(1-2): 7-15.

4. Anson, A., Lin, C. C. H., Kuznicki, S. M. and Sawada, J. A. (2009). "Adsorption of carbon dioxide, ethane, and methane on titanosilicate type molecular sieves." Chemical Engineering Science **64**(16): 3683-3687.

5. Anson, A., Lin, C. C. H., Kuznicki, T. M. and Kuznicki, S. M. (2010). "Separation of ethylene/ethane mixtures by adsorption on small-pored titanosilicate molecular sieves." Chemical Engineering Science **65**(2): 807-811.

6. Anson, A., Wang, Y., Lin, C. C. H., Kuznicki, T. M. and Kuznicki, S. M. (2008). "Adsorption of ethane and ethylene on modified ETS-10." Chemical Engineering Science **63**(16): 4171-4175.

7. Auerbach, S. M., Carrado, K. A. and Dutta, P. K. (2003). Handbook of Zeolite Science and Technology, CRC Press.

8. Avila, A. M., Yang, F., Shi, M. and Kuznicki, S. M. (2011). "Extraction of ethane from natural gas at high pressure by adsorption on Na-ETS-10." Chemical Engineering Science **66**(13): 2991-2996.

9. Bansal, R. C. and Goyal, M. (2005). Activated Carbon Adsorption, CRC Press.

10. Bathen, D. (2003). "Physical waves in adsorption technology - An overview." Separation and Purification Technology **33**(2): 163-177.

11. Ben-Mansour, R., Habib, M. A., Bamidele, O. E., Basha, M., Qasem, N. A. A., Peedikakkal, A., Laoui, T. and Ali, M. (2016). "Carbon capture by physical adsorption: Materials, experimental investigations and numerical modeling and simulations - A review." Applied Energy **161**: 225-255.

12. Bokobza, L. (2007). "Multiwall carbon nanotube elastomeric composites: A review." Polymer **48**(17): 4907-4920.

13. Bueche, F. (1973). "A new class of switching materials." Journal of Applied Physics **44**(1): 532-533.

14. Cao, Y., Yu, H., Tan, J., Peng, F., Wang, H., Li, J., Zheng, W. and Wong, N. B. (2013). "Nitrogen-, phosphorous- and boron-doped carbon nanotubes as catalysts for the aerobic oxidation of cyclohexane." Carbon **57**: 433-442.

15. Cejka, J., Corma, A. and Zones, S. (2010). Zeolites and Catalysis: Synthesis, Reactions and Applications, Wiley.

16. Cherbański, R., Komorowska-Durka, M., Stefanidis, G. D. and Stankiewicz, A. I. (2011). "Microwave swing regeneration Vs temperature swing regeneration - Comparison of desorption kinetics." Industrial & Engineering Chemistry Research **50**(14): 8632-8644.

17. Cherbański, R. and Molga, E. (2009). "Intensification of desorption processes by use of microwaves-An overview of possible applications and industrial perspectives." Chemical Engineering and Processing: Process Intensification **48**(1): 48-58.

18. Chowdhury, T., Shi, M., Hashisho, Z., Sawada, J. A. and Kuznicki, S. M. (2012). "Regeneration of Na-ETS-10 using microwave and conductive heating." Chemical Engineering Science **75**: 282-288.

19. Coss, P. M. and Cha, C. Y. (2000). "Microwave regeneration of activated carbon used for removal of solvents from vented air." Journal of the Air and Waste Management Association **50**(4): 529-535.

20. Crittenden, B. and Thomas, W. J. (1998). Adsorption Technology and Design, Elsevier Science.

21. Das, S., Mukhopadhyay, A. K., Datta, S. and Basu, D. (2009). "Prospects of microwave processing: An overview." Bulletin of Materials Science **32**(1): 1-13.

22. De Alwis, A. A. P. and Fryer, P. J. (1990). "The use of direct resistance heating in the food industry." Journal of Food Engineering **11**(1): 3-27.

23. Dechow, F. J. (1989). Separation and purification techniques in biotechnology, Noyes Publications.

24. Dombrowski, K. D., Lehmann, C. M. B., Sullivan, P. D., Ramirez, D., Rood, M. J. and Hay, K. J. (2004). "Organic vapor recovery and energy efficiency during electric regeneration of an activated carbon fiber cloth adsorber." Journal of Environmental Engineering **130**(3): 268-275.

25. Donohue, M. D. and Aranovich, G. L. (1998). "Classification of Gibbs adsorption isotherms." Advances in Colloid and Interface Science **76**: 137-152.

26. Downarowicz, D. (2015). "Adsorption characteristics of propan-2-ol vapours on activated carbon Sorbonorit 4 in electrothermal temperature swing adsorption process." Adsorption **21**(1-2): 87-98.

27. Emamipour, H., Johnsen, D. L., Rood, M. J., Jain, M. and Skandan, G. (2015). "Novel activated carbon fiber cloth filter with functionalized silica nanoparticles for adsorption of toxic industrial chemicals." Adsorption **21**(4): 265-272.

28. Eyer, S., Stadie, N. P., Borgschulte, A., Emmenegger, L. and Mohn, J. (2014). "Methane preconcentration by adsorption: A methodology for materials and conditions selection." Adsorption **20**(5-6): 657-666.

29. Fan, R. J., Sun, Q., Zhang, L., Zhang, Y. and Lu, A. H. (2014). "Photoluminescent carbon dots directly derived from polyethylene glycol and their application for cellular imaging." Carbon **71**: 87-93.

30. Giraudet, S., Boulinguiez, B. and Le Cloirec, P. (2014). "Adsorption and electrothermal desorption of volatile organic compounds and siloxanes onto an activated carbon fiber cloth for biogas purification." Energy and Fuels **28**(6): 3924-3932.

31. Hashisho, Z., Emamipour, H., Rood, M. J., Hay, K. J., Kim, B. J. and Thurston, D. (2008). "Concomitant adsorption and desorption of organic vapor in dry and humid air streams using microwave and direct electrothermal swing adsorption." Environmental Science and Technology **42**(24): 9317-9322.

32. Hashisho, Z., Rood, M. J., Barot, S. and Bernhard, J. (2009). "Role of functional groups on the microwave attenuation and electric resistivity of activated carbon fiber cloth." Carbon **47**(7): 1814-1823.

33. He, Y., Gao, J., Gong, X. and Xu, J. (2017). "The role of carbon nanotubes in promoting the properties of carbon black-filled natural rubber/butadiene rubber composites." Results in Physics.

34. Hu, M. M., Emamipour, H., Johnsen, D. L., Rood, M. J., Song, L. and Zhang, Z. (2017). "Monitoring and Control of an Adsorption System Using Electrical Properties of the Adsorbent for Organic Compound Abatement." Environmental Science and Technology **51**(13): 7581-7589.

35. IUPAC-Recommendation (1994). "Recommendations for the characterization of porous solids (Technical Report)." Pure and Applied Chemistry **66**(8): 1739-1758.

36. Jacobs, P. A., Flanigen, E. M., Jansen, J. C. and van Bekkum, H. (2001). Introduction to Zeolite Science and Practice, Elsevier Science.

37. Janas, D. and Koziol, K. K. (2014). "A review of production methods of carbon nanotube and graphene thin films for electrothermal applications." Nanoscale **6**(6): 3037-3045.

38. Jha, V. K., Matsuda, M. and Miyake, M. (2008). "Sorption properties of the activated carbon-zeolite composite prepared from coal fly ash for Ni2+, Cu2+, Cd2+ and Pb2+." Journal of Hazardous Materials **160**(1): 148-153.

39. Jiang, Z., Nolan, A., Walton, J. G. A., Lilienkampf, A., Zhang, R. and Bradley, M. (2014). "Photoluminescent carbon dots from 1,4-addition polymers." Chemistry - A European Journal **20**(35): 10926-10931.

40. Johnsen, D. L., Mallouk, K. E. and Rood, M. J. (2011). "Control of electrothermal heating during regeneration of activated carbon fiber cloth." Environmental Science and Technology **45**(2): 738-743.

41. Johnsen, D. L. and Rood, M. J. (2012). "Temperature control during regeneration of activated carbon fiber cloth with resistance-feedback." Environmental Science and Technology **46**(20): 11305-11312.

42. Johnsen, D. L., Zhang, Z., Emamipour, H., Yan, Z. and Rood, M. J. (2014). "Effect of isobutane adsorption on the electrical resistivity of activated carbon fiber cloth with select physical and chemical properties." Carbon **76**(0): 435-445.

43. Johnsen, D. L., Zhang, Z., Emamipour, H., Yan, Z. and Rood, M. J. (2014). "Effect of isobutane adsorption on the electrical resistivity of activated carbon fiber cloth with select physical and chemical properties." Carbon **76**: 435-445.

44. Jones, D. A., Lelyveld, T. P., Mavrofidis, S. D., Kingman, S. W. and Miles, N. J. (2002). "Microwave heating applications in environmental engineering - A review." Resources, Conservation and Recycling **34**(2): 75-90.

45. Jullien, A. G. a. R. (1989). The Solid State: From Superconductors to Superalloys. New York, Oxford Science Publications.

46. Karimifard, S., Reza, M. and Moghaddam, A. (2016). "The effects of microwave regeneration on adsorptive performance of functionalized carbon nanotubes." Water Science and Technology **73**(11): 2638-2643.

47. Khachatryan, S. V. and Gevorgyan, T. A. (2010). "Dielectric properties of natural, modified, and irradiated zeolites." Technical Physics **55**(5): 732-734.

48. Khatri, I., Kishi, N., Zhang, J., Soga, T., Jimbo, T., Adhikari, S., Aryal, H. R. and Umeno, M. (2010). "Synthesis and characterization of carbon nanotubes via ultrasonic spray pyrolysis method on zeolite." Thin Solid Films **518**(23): 6756-6760.

49. Kim, J. H., Ikoma, Y. and Niwa, M. (1999). "Control of the pore-opening size of HY zeolite by CVD of silicon alkoxide." Microporous and Mesoporous Materials **32**(1-2): 37-44.

50. Kim, K. J. and Ahn, H. G. (2012). "The effect of pore structure of zeolite on the adsorption of VOCs and their desorption properties by microwave heating." Microporous and Mesoporous Materials **152**: 78-83.

51. Kumar, M. and Ando, Y. (2005). "Controlling the diameter distribution of carbon nanotubes grown from camphor on a zeolite support." Carbon **43**(3): 533-540.

52. Legras, B., Polaert, I., Estel, L. and Thomas, M. (2012). "Effect of alcaline cations in zeolites on their dielectric properties." Journal of Microwave Power and Electromagnetic Energy **46**(1): 5-11.

53. Li, C., Zhang, L., Xia, H., Peng, J., Cheng, S., Shu, J., Zhang, Q. and Jiang, X. (2017). "Analysis of devitalization mechanism and chemical constituents for fast and efficient regeneration of spent carbon by means of ultrasound and microwaves." Journal of Analytical and Applied Pyrolysis **124**: 42-50.

54. Li, J., Lu, R., Dou, B., Ma, C., Hu, Q., Liang, Y., Wu, F., Qiao, S. and Hao, Z. (2012). "Porous graphitized carbon for adsorptive removal of benzene and the electrothermal regeneration." Environmental Science and Technology **46**(22): 12648-12654.

55. Li, Y. and Chung, T. S. (2008). "Exploratory development of dual-layer carbon-zeolite nanocomposite hollow fiber membranes with high performance for oxygen enrichment and natural gas separation." Microporous and Mesoporous Materials **113**(1-3): 315-324.

56. Liang, Y., Zhang, H., Yi, B., Zhang, Z. and Tan, Z. (2005). "Preparation and characterization of multi-walled carbon nanotubes supported PtRu catalysts for proton exchange membrane fuel cells." Carbon **43**(15): 3144-3152.

57. Lu, D., Kondo, J. N., Domen, K., Begum, H. A. and Niwa, M. (2004). "Ultra-fine tuning of microporous opening size in zeolite by CVD." Journal of Physical Chemistry B **108**(7): 2295-2299.

58. Luo, L., Ramirez, D., Rood, M. J., Grevillot, G., Hay, K. J. and Thurston, D. L. (2006). "Adsorption and electrothermal desorption of organic vapors using activated carbon adsorbents with novel morphologies." Carbon **44**(13): 2715-2723.

59. Magnowski, N. B. K., Avila, A. M., Lin, C. C. H., Shi, M. and Kuznicki, S. M. (2011). "Extraction of ethane from natural gas by adsorption on modified ETS-10." Chemical Engineering Science **66**(8): 1697-1701.

60. Mao, H., Zhou, D., Hashisho, Z., Wang, S., Chen, H. and Wang, H. H. (2015). "Constant power and constant temperature microwave regeneration of toluene and acetone loaded on microporous activated carbon from agricultural residue." Journal of Industrial and Engineering Chemistry **21**: 516-525.

61. Metaxas, A. C. and Meredith, R. J. (1983). Industrial Microwave Heating, P. Peregrinus.

62. Miyake, M., Kimura, Y., Ohashi, T. and Matsuda, M. (2008). "Preparation of activated carbon-zeolite composite materials from coal fly ash." Microporous and Mesoporous Materials **112**(1-3): 170-177.

63. Mohamad Nor, N., Sukri, M. F. F. and Mohamed, A. R. (2016). "Development of high porosity structures of activated carbon via microwave-assisted regeneration for H2S removal." Journal of Environmental Chemical Engineering **4**(4): 4839-4845.

64. Nath, D. C. D. and Sahajwalla, V. (2011). "Application of fly ash as a catalyst for synthesis of carbon nanotube ribbons." Journal of Hazardous Materials **192**(2): 691-697.

65. Nath, D. C. D. and Sahajwalla, V. (2011). "Growth mechanism of carbon nanotubes produced by pyrolysis of a composite film of poly (vinyl alcohol) and fly ash." Applied Physics A: Materials Science and Processing **104**(2): 539-544.

66. National Research Council (1994). Microwave processing of materials, The National Academies Press.

67. Nigar, H., Garcia-Baños, B., Peñaranda-Foix, F. L., Catalá-Civera, J. M., Mallada, R. and Santamaría, J. (2016). "Amine-functionalized mesoporous silica: A material capable of CO2 adsorption and fast regeneration by microwave heating." AIChE Journal **62**(2): 547-555.

68. Niknaddaf, S., Atkinson, J. D., Shariaty, P., Jahandar Lashaki, M., Hashisho, Z., Phillips, J. H., Anderson, J. E. and Nichols, M. (2016). "Heel formation during volatile organic compound desorption from activated carbon fiber cloth." Carbon **96**: 131-138.

69. Nugent, P., Giannopoulou, E. G., Burd, S. D., Elemento, O., Giannopoulou, E. G., Forrest, K., Pham, T., Ma, S., Space, B., Wojtas, L., Eddaoudi, M. and Zaworotko, M. J. (2013). "Porous materials with optimal adsorption thermodynamics and kinetics for co2 separation." Nature **495**(7439): 80-84.

70. Palma, V. and Meloni, E. (2016). "Microwave assisted regeneration of a catalytic diesel soot trap." Fuel **181**: 421-429.

71. Pan, R. R., Fan, F. L., Li, Y. and Jin, X. J. (2016). "Microwave regeneration of phenol-loaded activated carbons obtained from: Arundo donax and waste fiberboard." RSC Advances **6**(39): 32960-32966.

72. Park, S., Kwon, Y. P., Kwon, H. C., Lee, J. H., Lee, H. W. and Lee, J. C. (2007). "Electrothermal properties of porous ceramic fiber media containing carbon materials." Journal of Nanoscience and Nanotechnology **7**(11): 3776-3779.

73. Park, S., Kwon, Y. P., Kwon, H. C., Lee, J. H., Lee, H. W. and Lee, J. C. (2009). "Electrothermal properties of regenerable carbon contained porous ceramic fiber media." Journal of Electroceramics **22**(1-3): 315-318.

74. Park, S. W., Yun, Y. H., Kim, S. D., Yang, S. T., Ahn, W. S., Seo, G. and Kim, W. J. (2010). "CO2 retention ability on alkali cation exchanged titanium silicate, ETS-10." Journal of Porous Materials **17**(5): 589-595.

75. Pinchukova, N. A., Voloshko, A. Y., Baumer, V. N., Shishkin, O. V. and Chebanov, V. A. (2015). "The use of microwave irradiation for zeolite regeneration in a continuous ethanol dewatering process." Chemical Engineering and Processing: Process Intensification **95**: 151-158.

76. Polaert, I., Estel, L., Huyghe, R. and Thomas, M. (2010). "Adsorbents regeneration under microwave irradiation for dehydration and volatile organic compounds gas treatment." Chemical Engineering Journal **162**(3): 941-948.

77. Qi, J., Benipal, N., Chadderdon, D. J., Huo, J., Jiang, Y., Qiu, Y., Han, X., Hu, Y. H., Shanks, B. H. and Li, W. (2015). "Carbon nanotubes as catalysts for direct carbohydrazide fuel cells." Carbon **89**: 142-147.

78. Qing, Y., Wang, X., Zhou, Y., Huang, Z., Luo, F. and Zhou, W. (2014). "Enhanced microwave absorption of multi-walled carbon nanotubes/epoxy composites incorporated with ceramic particles." Composites Science and Technology **102**: 161-168.

79. Ramirez, D., Emamipour, H., Vidal, E. X., Rood, M. J. and Hay, K. J. (2011). "Capture and recovery of methyl ethyl ketone with electrothermal-swing adsorption systems." Journal of Environmental Engineering **137**(9): 826-832.

80. Reuß, J., Bathen, D. and Schmidt-Traub, H. (2002). "Desorption by microwaves: Mechanisms of multicomponent mixtures." Chemical engineering and Technology **25**(4): 381-384.

81. Ribeiro, R. P. P. L., Grande, C. A. and Rodrigues, A. E. (2011). "Adsorption of water vapor on carbon molecular sieve: Thermal and electrothermal regeneration study." Industrial and Engineering Chemistry Research **50**(4): 2144-2156.

82. Ribeiro, R. P. P. L., Grande, C. A. and Rodrigues, A. E. (2014). "Electric Swing Adsorption for Gas Separation and Purification: A Review." Separation Science and Technology (Philadelphia) **49**(13): 1985-2002.

83. Roussy, G. and Chenot, P. (1981). Selective Energy Supply to Adsorbed Water and Non Classical Thermal Process During Microwave Dehydration of Zeolite. 16th Annual Symposium on Microwave Power., Toronto, Canada.

84. Roussy, G., Zoulalian, A., Charreyre, M. and Thiebaut, J. M. (1984). "How microwaves dehydrate zeolites." The Journal of Physical Chemistry **88**(23): 5702-5708.

85. Roussy, G., Zoulalian, A., Charreyre, M. and Thiebaut, J. M. (1984). "How microwaves dehydrate zeolites." Journal of physical Chemistry **88**(23): 5702-5708.

86. Russell, J. and Cohn, R. (2012). Joule Heating, Book on Demand.

87. Rybakov, K. I., Semenov, V. E., Egorov, S. V., Eremeev, A. G., Plotnikov, I. V. and Bykov, Y. V. (2006). "Microwave heating of conductive powder materials." Journal of Applied Physics **99**(2).

88. Sano, N., Kodama, T. and Tamon, H. (2013). "Direct synthesis of carbon nanotubes on stainless steel electrode for enhanced catalyst efficiency in a glucose fuel cell." Carbon **55**: 365-368.

89. Sarno, M., Tamburrano, A., Arurault, L., Fontorbes, S., Pantani, R., Datas, L., Ciambelli, P. and Sarto, M. S. (2013). "Electrical conductivity of carbon nanotubes grown inside a mesoporous anodic aluminium oxide membrane." Carbon **55**: 10-22.

90. Shariaty, P., Jahandar Lashaki, M., Hashisho, Z., Sawada, J., Kuznicki, S. and Hutcheon, R. (2017). "Effect of ETS-10 ion exchange on its dielectric properties and adsorption/microwave regeneration." Separation and Purification Technology **179**: 420-427.

91. Shin, J. H. and Hong, S. H. (2012). "Microstructure and mechanical properties of single wall carbon nanotube reinforced yttria stabilized zircona ceramics." Materials Science and Engineering A **556**: 382-387.

92. Sing, K. S. W. (1998). "Adsorption methods for the characterization of porous materials." Advances in Colloid and Interface Science **76**: 3-11.

93. Singleton, J. (2001). Band Theory and Electronic Properties of Solids. New York, Oxford University Press.

94. Snyder, J. D. and Leesch, J. G. (2001). "Methyl bromide recovery on activated carbon with repeated adsorption and electrothermal regeneration." Industrial and Engineering Chemistry Research **40**(13): 2925-2933.

95. Song, X. H., Teo, W. S. and Wang, K. (2012). "Synthesis and characterization of activated carbons prepared from benzene CVD on zeolite y." Journal of Porous Materials **19**(2): 211-215.

96. Subrenat, A., Baléo, J. N., Le Cloirec, P. and Blanc, P. E. (2001). "Electrical behaviour of activated carbon cloth heated by the joule effect: Desorption application." Carbon **39**(5): 707-716.

97. Subrenat, A. and Le Cloirec, P. (2004). "Adsorption onto activated carbon cloths an electrothermal regeneration: Its potential industrial applications." Journal of Environmental Engineering **130**(3): 249-257.

98. Sullivan, P. D., Rood, M. J., Dombrowski, K. D. and Hay, K. J. (2004). "Capture of organic vapors using adsorption and electrothermal regeneration." Journal of Environmental Engineering **130**(3): 258-267.

99. Sullivan, P. D., Rood, M. J., Grevillot, G., Wander, J. D. and Hay, K. J. (2004). "Activated carbon fiber cloth electrothermal swing adsorption system." Environmental Science and Technology **38**(18): 4865-4877.

100. Sullivan, P. D., Rood, M. J., Hay, K. J. and Qi, S. (2001). "Adsorption and electrothermal desorption of hazardous organic vapors." Journal of Environmental Engineering **127**(3): 217-223.

101. Uda, A., Morita, S. and Ozaki, Y. (2013). "Thermal degradation of a poly(vinyl alcohol) film studied by multivariate curve resolution analysis." Polymer (United Kingdom) **54**(8): 2130-2137.

102. Varghese, K. S., Pandey, M. C., Radhakrishna, K. and Bawa, A. S. (2012). "Technology, applications and modelling of ohmic heating: a review." Journal of Food Science and Technology **51**(10): 2304-2317.

103. Waghmode, S. B., Vetrivel, R., Hegde, S. G., Gopinath, C. S. and Sivasanker, S. (2003). "Physicochemical investigations of the basicity of the cation exchanged ETS-10 molecular sieves." Journal of Physical Chemistry B **107**(33): 8517-8523.

104. Wang, L. and Dang, Z. M. (2005). "Carbon nanotube composites with high dielectric constant at low percolation threshold." Applied Physics Letters **87**(4).

105. Witkiewicz, K. and Nastaj, J. (2014). "Modeling of Microwave-Assisted Regeneration of Selected Adsorbents Loaded with Water or Toluene." Drying Technology **32**(11): 1369-1385.

106. Wu, K., Lei, C., Yang, W., Chai, S., Chen, F. and Fu, Q. (2016). "Surface modification of boron nitride by reduced graphene oxide for preparation of dielectric material with enhanced dielectric constant and well-suppressed dielectric loss." Composites Science and Technology **134**: 191-200.

107. Yang, H., Xu, S., Jiang, L. and Dan, Y. (2012). "Thermal decomposition behavior of poly (vinyl alcohol) with different hydroxyl content." Journal of Macromolecular Science, Part B: Physics **51**(3): 464-480.

108. Yuen, F. K. and Hameed, B. H. (2009). "Recent developments in the preparation and regeneration of activated carbons by microwaves." Advances in Colloid and Interface Science **149**(1): 19-27.

109. Zarifi, M. H., Shariaty, P., Hashisho, Z. and Daneshmand, M. (2017). "A non-contact microwave sensor for monitoring the interaction of zeolite 13X with CO2 and CH4 in gaseous streams." Sensors and Actuators, B: Chemical **238**: 1240-1247.

110. Zhang, L., Zhao, B., Wang, X., Liang, Y., Qiu, H., Zheng, G. and Yang, J. (2014). "Gas transport in vertically-aligned carbon nanotube/parylene composite membranes." Carbon **66**: 11-17.

111. Zhao, P., Wang, S., Kadlec, A., Li, Z. and Wang, X. (2016). "Properties of cement-sand-based piezoelectric composites with carbon nanotubes modification." Ceramics International.

112. Zheng, T., Wang, Q., Shi, Z., Zhang, Z. and Ma, Y. (2016). "Microwave regeneration of spent activated carbon for the treatment of ester-containing wastewater." RSC Advances **6**(65): 60815-60825.

Chapter 3. EFFECT OF ETS-10 ION EXCHANGE ON ITS DIELECTRIC PROPERTIES AND ADSORPTION/MICROWAVE REGENERATION

3.1. Chapter Overview

This chapter summarizes the information related to the effect of ion exchange on dielectric properties of Engelhard Titanosilicate Molecular Sieve, ETS-10. Since ion exchange is a common process for modification of molecular sieve adsorbents, it was selected as the first modification method. The modification was evaluated based on its effect on adsorbents properties with the main focus on dielectric properties. EST-10 was selected as a representative of molecular sieve adsorbents due to recent interests towards its application for different adsorptive separation processes.

Note: Since ion exchanged samples had minimal effect on electric properties of ETS-10, we just focused on the impact on dielectric properties.

3.2. Introduction

ETS-10 is a large-pored, mixed octahedral/tetrahedral titaniumsilicate molecular sieve with a three dimensional 12-ring pore network of interconnecting 7.6 Å × 4.9 Å channels (Kuznicki 1991, Anderson et al. 1994, Ohsuna et al. 1994). These structural characteristics (Rocha and Anderson 2000) make it suitable for adsorptive separation (Shi et al. 2011), catalysis (Uma et al. 2004), and ion exchange (Choi et al. 2006) applications.

Conventional temperature and pressure swing regeneration (TSR and PSR) are well established techniques for regenerating adsorbents. These techniques, however, have high energy consumption, long regeneration duration, and can cause adsorbent (and adsorbate) destruction (Al-Baghli and Loughlin 2005, Ania et al. 2005, Cherbański and Molga 2009, Cherbański et al. 2011, Chowdhury et al. 2012). Regeneration by microwave heating is an alternative, particularly for adsorbents saturated with polar (microwave-absorbing) adsorbates. For regeneration of ETS-10 saturated with hydrocarbons, microwave heating has low energy consumption, high desorption rate, and short desorption time (Shi et al. 2010, Chowdhury et al. 2012, 2013) – further improvements with a polar adsorbate, such as water, can be expected. Direct adsorbent and adsorbate heating minimizes heat losses (Ania et al. 2005, Hashisho et al. 2005, Kim and Ahn 2012).

Microwave energy dissipates in an adsorbent and/or adsorbate as thermal energy or heat according to its dielectric properties. Ionic conduction and dipole rotation/relaxation are the main heating mechanisms for solid powders (e.g., ETS-10) and polar molecules (e.g., H_2O), respectively (Rybakov et al. 2006, Polaert et al. 2010). The response of a material to microwave irradiation depends on its complex permittivity (ε^*), defined as follows:

$$\varepsilon^* = \varepsilon' - \varepsilon'' j \qquad \text{Eq. 4}$$

The dielectric constant (ε', real) is related to a material's ability to store energy. The dielectric loss factor (ε'', imaginary) describes the dissipation of energy as heat. The loss tangent ($\tan\frac{\varepsilon''}{\varepsilon'}$) is also commonly used to describe the losses within the material as a result of formation of the internal field within the affected medium by microwaves penetration, a consequence of which is

volumetric heating. Therefore, material's loss tangent could affect the volumetric power density ($P_{(z)avg.}, \frac{W}{m^3}$), which is the average microwave power converted into heat per unit volume:

$$P_{(z)_{ave.}} = 2\pi f \varepsilon_0 \varepsilon' \tan\delta \, E_{(z)}^{\ 2} \qquad \text{Eq. 5}$$

where f is wave frequency (1/s), ε_0 is free space permittivity (8.854×10^{-12} F/m), and $E_{(z)}$ is the internal electric field strength (V/m) in the material. Materials can be selectively heated with microwaves depending on their dielectric properties. A "lossy" material (high tan δ) can be heated more effectively than a low-loss (low tan δ) material (National Research Council 1994).

Microwave penetration into an adsorbent material is another important parameter for implementation of microwave regeneration in industrial applications. Microwave penetration can be quantified using the Penetration Depth (d_E) which is defined as the characteristic length at which ~63% of the incident microwave power is dissipated (Bathen 2003):

$$d_E \approx \frac{\lambda_0}{2.\pi} \times \frac{\sqrt{\varepsilon'}}{\varepsilon''} \qquad \text{Eq. 6}$$

where λ_0 is wavelength in vacuum (m).

Very low (<1cm) and very high (>100cm) d_E values are not favorable for industrials applications. Low d_E would result in penetration of the microwave into thin layer of the adsorbent bed, while high d_E means low microwave absorption by the adsorbent bed and ineffective microwave heating (Bathen 2003).

Reuß et al. (2002) showed that efficiency during microwave regeneration is related to the relative polarity of the adsorbate with respect to the adsorbent. Polar adsorbates were better desorbed from microwave transparent zeolites because, in microwave absorbing zeolites, microwave energy was dissipated in the adsorbent (Reuß et al. 2002). Decreased dielectric

properties for an adsorbent, therefore, can improve regeneration efficiency if polar adsorbates are considered, justifying adsorbent tailoring to increase its adsorption capacity at the expense of its dielectric properties. These focused adsorbent modifications have not yet been reported in the literature.

Cation exchange impacts ETS-10 adsorption properties by varying the material's selectivity, basicity, and physical/chemical properties (Waghmode et al. 2003, Anson et al. 2008, Anson et al. 2009, Anson et al. 2010, Park et al. 2010, Magnowski et al. 2011). Specifically, for water adsorption, displacing Na^+ with Ca^{2+}, which is larger and more electronegative, increased water adsorption capacity by as much as 75% (Tanchuk et al. 2013). The impact of this ion exchange on the dielectric properties and microwave regeneration of the saturated adsorbents, however, was not discussed and similar studies are not available elsewhere.

This work provides a systematic investigation of the impacts of ion exchange on the dielectric properties and microwave regeneration of ETS-10. This work strives to introduce a method to modify ETS-10, in which its microwave regeneration in different adsorption applications results in less frequent adsorbent replacement (higher desorption efficiency) and lower overall energy consumption than conventional regeneration systems. The expectation is that substituted cations will alter the physical/chemical/adsorption properties of ETS-10. Since strong adsorbate-adsorbent interaction could decrease the efficiency and increase energy consumption during regeneration, the effect of ion exchange was specifically studied on regeneration of water (polar adsorbate) loaded ETS-10. Ion exchange was completed using monovalent and divalent cations (Na^+, Li^+, K^+, Ca^{2+}, Cu^{2+}, and Ba^{2+}). The samples were characterized in terms of elemental composition, pore volume, water adsorption capacity, dielectric properties, and pH of the point of zero charge (pH_{PZC}). The microwave regeneration behaviors of all ion exchanged samples were compared to

that of untreated ETS-10 in terms of temperature profile, microwave absorbance, regeneration efficiency, and energy consumption during microwave regeneration.

3.3. Materials and Methods

3.3.1. Adsorbents Preparation

ETS-10 was synthesized using the hydrothermal technique, as described elsewhere (Kuznicki 1991, Anson et al. 2009). As-prepared ETS-10 was ion exchanged through exposure to a solution containing an excess of the salt of the target ion (Anson et al. 2008). The following salts were dissolved in deionized water (10 g water / g ETS-10) with the described weight ratios with respect to ETS-10: NaCl (1.05 g/g ETS-10), KCl (1.34 g/g), LiCl (0.76 g/g), $CaCl_2$ (2.65 g/g), $BaCl_2$ (4.40 g/g), and $CuSO_4$ (4.49 g/g). ETS-10 was then added to the mixture, creating slurry. The slurry was placed in an oven at 80 °C for 24 h. After, exchanged samples were filtered and washed with deionized water (1L/10g ETS-10) and then dried at 100 °C overnight. This procedure was repeated three times to achieve complete ion exchange.

Prepared samples were pelletized and sieved before characterization and use in adsorption/microwave regeneration tests. Samples were pressed at 5 kPSI and the cake was then crushed and sieved to 20 – 50 mesh.

3.3.2. Adsorbent Characterization

Elemental composition*:* Prepared samples were analyzed using scanning electron microscopy (SEM) (Vega-3, Tescan) equipped with energy dispersive x-ray spectroscopy (EDX) (Oxford Instruments) to determine their elemental composition and extent of cation exchange. Samples were coated with carbon and then analyzed under high vacuum ($< 3\times10^{-3}$ Pa) from 0.2 to 6 keV.

Micropore surface analysis: Samples were characterized using micropore surface analysis (iQ2MP, Quantachrome) with nitrogen as the probe gas at 77 K with relative pressures from 10^{-7} to 1. 60 – 70 mg of sample was activated at 200 °C for 12 h to remove moisture. Brunauer-Emmett-Teller (BET) surface area and pore volume were obtained from relative pressure ranges of 0.01 − 0.07 and at P/P_0=0.95 using the BET equation and DFT method (Olivier 1998), respectively. BET area and pore volume for all samples are normalized per gram of the original ETS-10.

pH_{PZC}: pH_{PZC} was measured for all cation exchanged samples, as described elsewhere (Atkinson et al. 2013). 200 mg of sample was added to a beaker with 10 g of deionized water and the mixtures were stirred for 24 h. After the suspension settled, the pH of the solution was measured using a pH meter (Oakton, model pH-700) in triplicates and the average was taken as the pH_{PZC} of the sample.

Dielectric properties*:* The dielectric properties of the samples were measured using the TM_0n_0 Multimode Cavity Dielectric Properties Measurement System at Microwave Properties North (Ontario, Canada). Detailed information about this method is given in Adams et al. (1992) and Hutcheon et al. (1992). Each powdered sample was uniaxially pressed at ~35 kPSI to make three cylindrical pellets that were stacked to form each measurement sample (3.66 ± 0.05 mm diameter and totaling 12.43 ± 0.05 mm length). Each pellet stack was inserted into a thin-walled silica glass sample holder and placed in the dielectric properties measurement system. 10 mL/min of argon was directed towards the interior of the holder to remove evolved gases from the measurement volume. Each sample was dried at 130 °C for 2 h before cooling the furnace to room temperature and measuring the dielectric properties in steps from 25 °C to 200 °C at 397, 912, 1499, 1977, 2466, and 2986 MHz.

Water adsorption capacity*:* The adsorption setup (Figure 3-1) consisted of a reactor, an adsorbate generation system, and a relative humidity (RH) meter. The reactor was a double-ended,

cylindrical, vertically-oriented quartz tube (2.14 cm inner diameter, 20 cm long) containing 9.9 ± 0.1 g of adsorbent (3.5 ± 0.3 cm in height). The adsorbate generation system included a syringe pump (KD Scientific, KDS-220) to inject water into 4 L/min of CO_2, controlled by a mass flow controller (Alicat Scientific). The injection rate was calculated based on the ideal gas law using the molecular weight and density of water. A relative humidity meter (OMEGAETTE® HH311 RS-232) continuously monitored the effluent RH.

Adsorption proceeded until full saturation of the adsorbent, as indicated by the effluent RH. An influent RH of 70% (28,450 ppm_v at 25 °C) was used for all tests. Adsorption capacity was calculated gravimetrically for each adsorbent and normalized based on the weight of the original ETS-10 used for ion exchange, because ion exchange changed the sample's bulk density (Eq. 3).

$$Adsorption\ capacity = \frac{Mass\ of\ adsorbed\ water\ (g) * Bulk\ density\ of\ the\ adsorbent\ (\frac{g}{cm^3})}{Mass\ of\ the\ adsorbent\ (g) * Bulk\ density\ of\ ETS{-}10\ (\frac{g}{cm^3})} \quad \text{Eq. 7}$$

The normalization based on the weight of the original ETS-10 makes the comparison of gravimetric adsorption capacities for all samples more accurate since different cations (lighter and heavier than ETS-10 original cations) are used for ion exchange. This would account for bias in the adsorption capacity due to the difference in densities of the adsorbents. Hence, the normalization shows that for starting with 1 gram of ETS-10, how cation exchange with different cations affects ETS-10 adsorption capacity. Bulk densities of all samples were calculated using the mass and volume of the prepared pellet during dielectric properties measurements.

3.3.3. Microwave Regeneration Setup and Method

The regeneration setup (Figure 3-1) is described in detail in Chowdhury, et al. (Chowdhury et al. 2012), and briefly described here for clarity. It consisted of a 2 kW power supply (SM745G.1, Alter), a 2 kW variable output microwave generator (MH2.0W S, National Electronics) equipped

with a 2.45 GHz magnetron, an isolator (National Electronics), a three-stub tuner (National Electronics), and a waveguide applicator connected to a sliding short (IBF Electronic GmbH & Co. KG). A dual channel microwave power meter (E4419B, Agilent), two power sensors (8481 A, Agilent), and a dual directional coupler with 60 db attenuation (Mega Industries) were used to measure forward and reverse power during regeneration. A fiber optic sensor with a signal conditioner (Reflex, Neoptix) measured the temperature. A data acquisition and control (DAC) system (Compact DAC, National Instruments) equipped with LabVIEW (National Instruments) recorded temperature and power during heating, and controlled the power supply's output to maintain the set-point temperature.

Following adsorption, loaded adsorbents were regenerated for 20 min with microwave heating at 130 °C using 4 – 60 W of power. During regeneration, the adsorbent bed was continuously purged with 0.3 L/min nitrogen. Regeneration efficiency was calculated using a mass balance (weight difference before adsorption and after regeneration). Power absorbance was calculated (Eq. 4) to determine the effect of ion exchange on the response of the samples to microwave heating.

$$Power\ Absorbance = \frac{Applied\ power - Reverse\ power}{Applied\ power} \quad \text{Eq. 8}$$

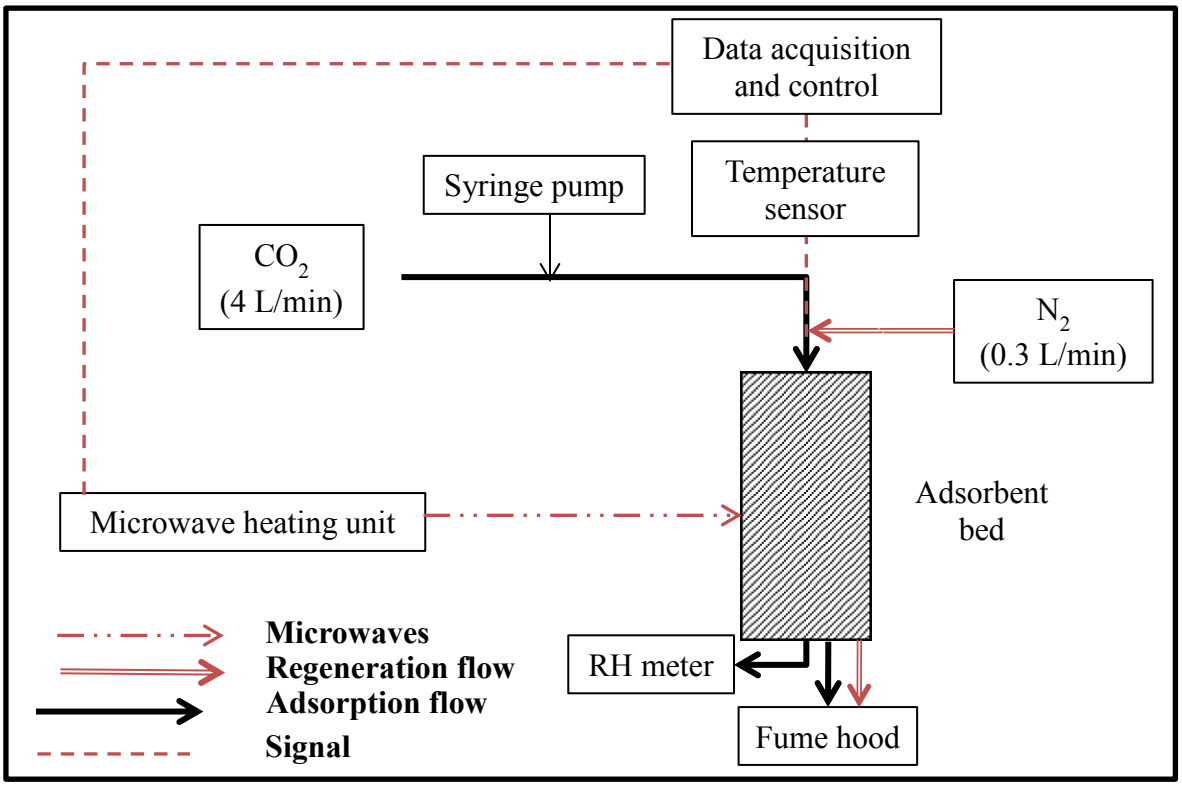

Figure 3-1. Adsorption/Microwave regeneration set-up

3.4. Results and Discussion

3.4.1. Characterization Tests

The composition of the three main elements in the structure of ETS-10, obtained using EDX, for all prepared samples are presented in Table 3-1. Composition is expressed as the atomic ratio of Si, Na, or K to titanium (Ti), which was considered to be constant in all samples (Waghmode et al. 2003, Park et al. 2010). This method was used because Li cannot be detected with EDX, preventing direct quantification of all exchanged cations. Exchanged cations primarily displaced Na^+. This is consistent with Anderson, et al. (1994), who proposed that unlike Na^+, a portion of K^+ is locked within ETS-10 cage structure and, therefore, unavailable for exchange. Cation displacement was more significant for divalent cations compared to monovalent cations, which is also consistent with the literature (Lv et al. 2004, Camarinha et al. 2009, Nak et al. 2009).

Table 3-1.Elemental composition and pH_{pzc} of original and modified ETS-10

Samples	Atomic Ratio			pH_{pzc}
	Si:Ti	Na:Ti	K:Ti	
ETS-10	4.57	1.21	0.26	10.45
Na-ETS-10	4.68	1.22	0.26	10.41
K-ETS-10	4.48	0.53	1.05	10.35
Li-ETS-10	4.76	0.61	0.25	10.03
Ca-ETS-10	4.63	0.20	0.27	9.87
Ba-ETS-10	4.71	0.65	0.26	9.54
Cu-ETS-10	4.69	0.00	0.07	5.26

For all samples except Ba and Cu-ETS-10, surface area and pore volume changed minimally (Figure 3-2). K and Ca are slightly larger than Na, so their proportional addition caused only small

changes (< 6%) in surface area and pore volume. Li is smaller than Na, so this exchange caused small increases (< 5%) in surface area and pore volume. Exchange of Na with Ba, the largest atom considered, necessarily resulted in additional surface coverage and pore blockage. Cu, while smaller than Na, Ca, and K, was added to such a large extent (replacing both Na and K) that additional pore blockage, possibly due to surface deposition in addition to ion exchange, may explain the notably lower surface area and pore volume. Changes in physical properties of the ion exchanged materials may also be attributed to the location of the exchange within the ETS-10 framework. Anderson, et al. (1994) showed five ion exchange sites inside ETS-10, two of which are located in the 12-ring pore. If exchange occurs in these pores, bonding strength (especially when exchanging Na^+ with divalent cations) may also change, impacting the pore dimensions and overall surface area and pore volume of the material.

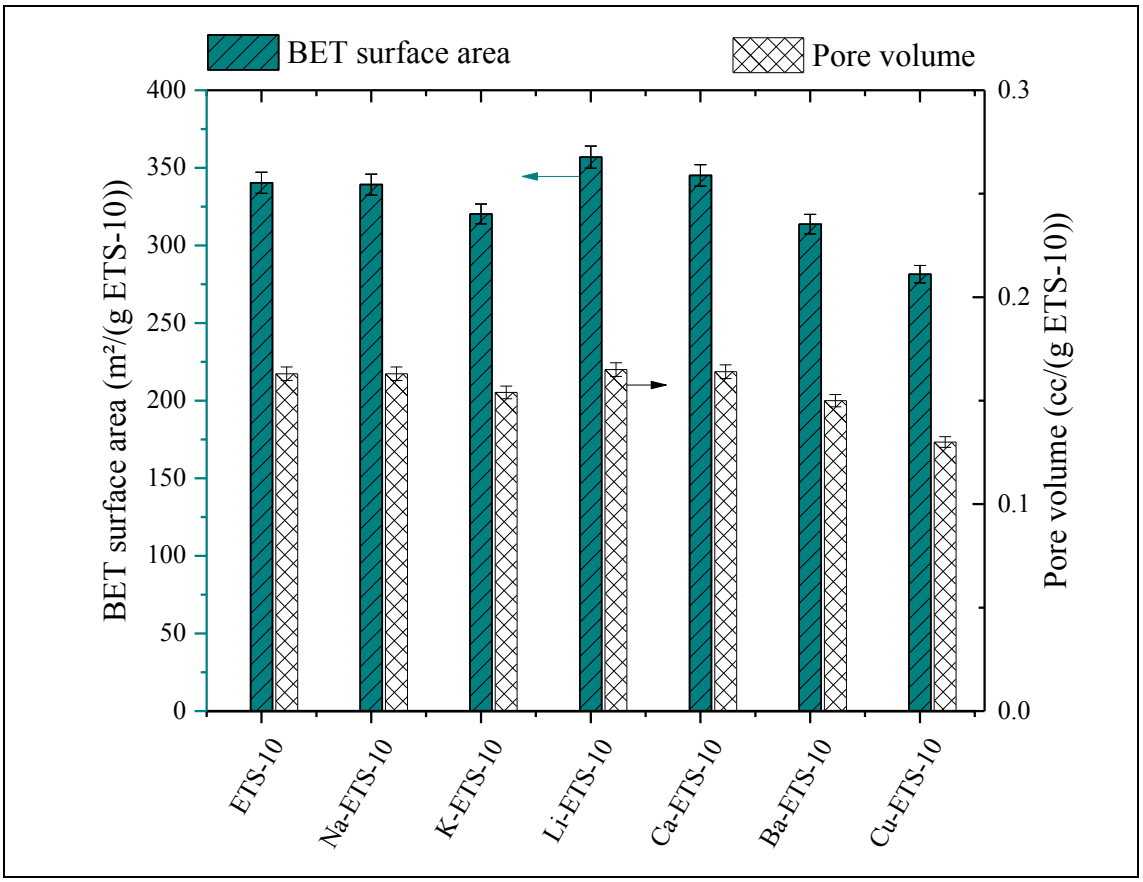

Figure 3-2. Micropore surface analysis of as synthesized and modified ETS-10. Values are an average of triplicates ± standard deviation

Cations with different electronegativity impact the surface charge of ETS-10, potentially altering the material's dielectric properties. Using pH_{PZC} as an indicator, the basicity of ion exchanged ETS-10 was found to be higher for samples exchanged with monovalent cations compared to divalent cations (Table 3-1). All samples, however, are less basic than the ETS-10 starting material. Waghmode, et al. (Waghmode et al. 2003) showed that the change in basicity of ETS-10 exchanged with Li^+, K^+, Na^+, and Ba^{2+} could result from a change in the net oxygen charge in the ETS-10 lattice and its average intermediate electronegativity. The higher the charge (more negative) on the oxygen in the ETS-10 lattice, the higher the basicity of the material.

The dielectric constant, loss factor, and loss tangent of ETS-10 decreased after ion exchange, with larger decreases after exchange with divalent cations (Figure 3-3). Khachatryan and Gevorgyan [32] measured decreases in dielectric constants and loss factors of natural zeolites with displaced cations, attributing the results to changes in hindered ionic conduction or ionic relaxation, which are responsible for the dielectric response of a solid material. Dielectric losses in zeolites can be described as oscillations of their mobiles cations in the microwave field[33]. The mobility of the cations depends on the net charge of the ETS-10 lattice oxygen[1]. The mobility of the cations is a stronger factor in determining the ionic conductivity and dielectric properties of the material. Since dielectric properties decreased for all ion exchanged materials studied in this work, it is expected that the exchanged cations have less mobility and that the corresponding charge of the ETS-10 lattice oxygen is lower. This lower oxygen charge is confirmed by decreasing basicity (decreasing pH_{pzc} values) of the ion exchanged ETS-10 samples (Table 3-1).

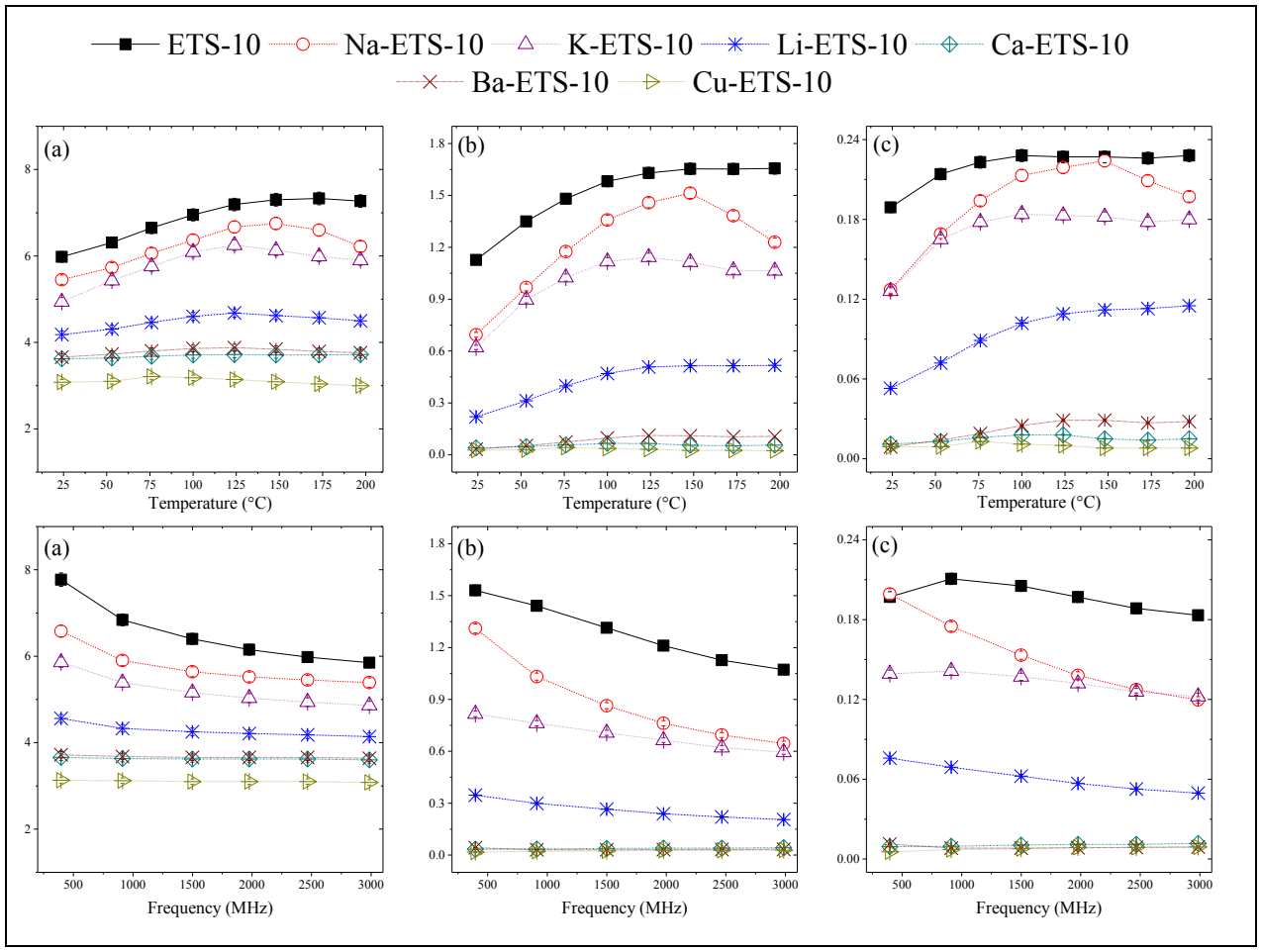

Figure 3-3. Dielectric constant (a), dielectric loss factor (b), and loss tangent (c) of as synthesized and modified ETS-10 at constant temperature of 25°C (bottom row) and constant frequency of 2.45 GHz (top row). Values are an average of triplicates ± standard deviation

Additionally, penetration depth (dE) at 25 ºC and 2.45 GHz was calculated for each sample (Figure 3-4) using Eq.3, the obtained dielectric properties and λ_0 of 12.24 cm at 2.45 GHz (Bathen 2003). It was found that ion exchange resulted in an increase in penetration depth, while the changes for divalent cations were more significant.

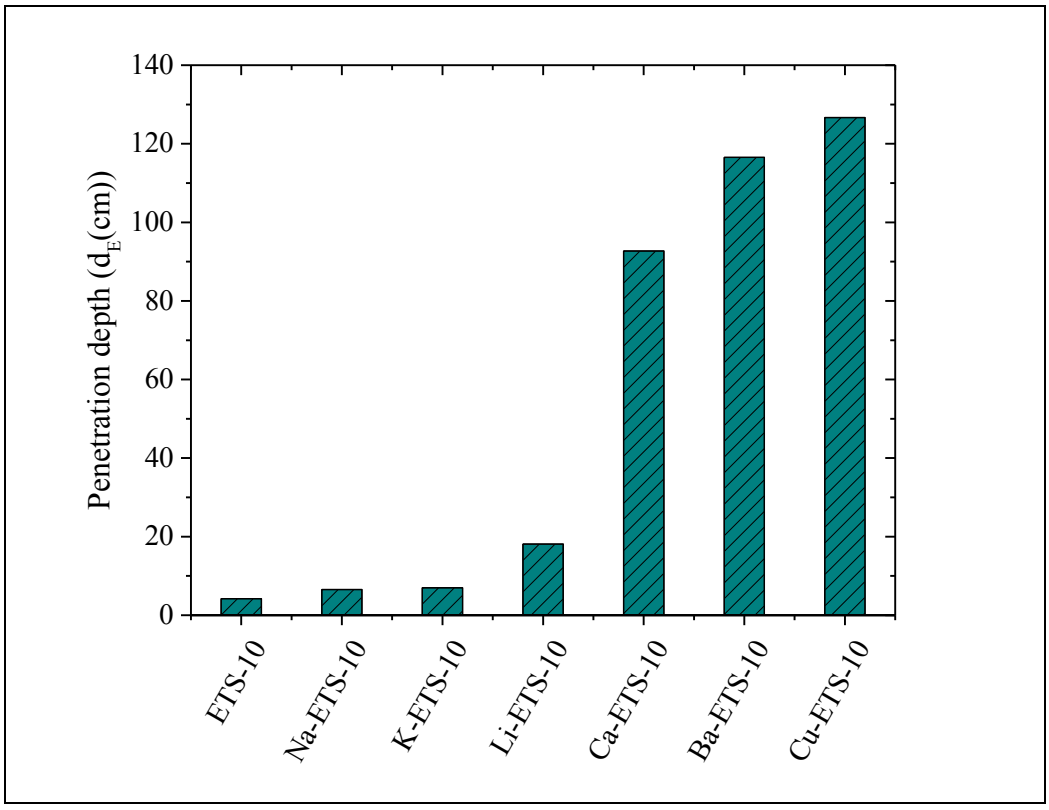

Figure 3-4. Penetration depth (d_E) for all samples calculated at 25 °C and 2.45 GHz.

To summarize, characterization results indicate that, compared to untreated ETS-10, ion-exchanged samples have similar physical properties, and decreased dielectric properties due to decreased ion mobility. Based on the literature, such samples may be preferred materials for microwave regeneration when loaded with polar material (Reuß et al. 2002).

3.4.2. Adsorption/Microwave Regeneration Tests

Water adsorption capacities for all samples are shown in Figure 3-5. The increases in water adsorption capacities were most significant for Li-ETS-10, Ca-ETS-10, and Ba-ETS-10 (Figure 3-5). Changes in adsorption capacity could be attributed to changes in the size, the electronegativity of exchanged cations, as well as the affinity of the cations towards water, which may change the adsorbent-adsorbate interaction and the available pore volume for adsorption.

Jänchen et al. (2004) found stronger bonds between water and an ion exchanged zeolite with higher charge density cations. This is consistent with the results presented here, as Li, Ca, and Ba have the highest charge density of the considered elements (Nakada and Ishii 2011) and Li-ETS-10, Ca-ETS-10, and Ba-ETS-10 have the highest water adsorption capacities. Figure 3-5 also includes regeneration efficiencies based on gravimetric measurements. All regeneration efficiencies are higher for ion-exchanged samples compared to the original ETS-10. Further discussion of these results is presented in the context of power absorption.

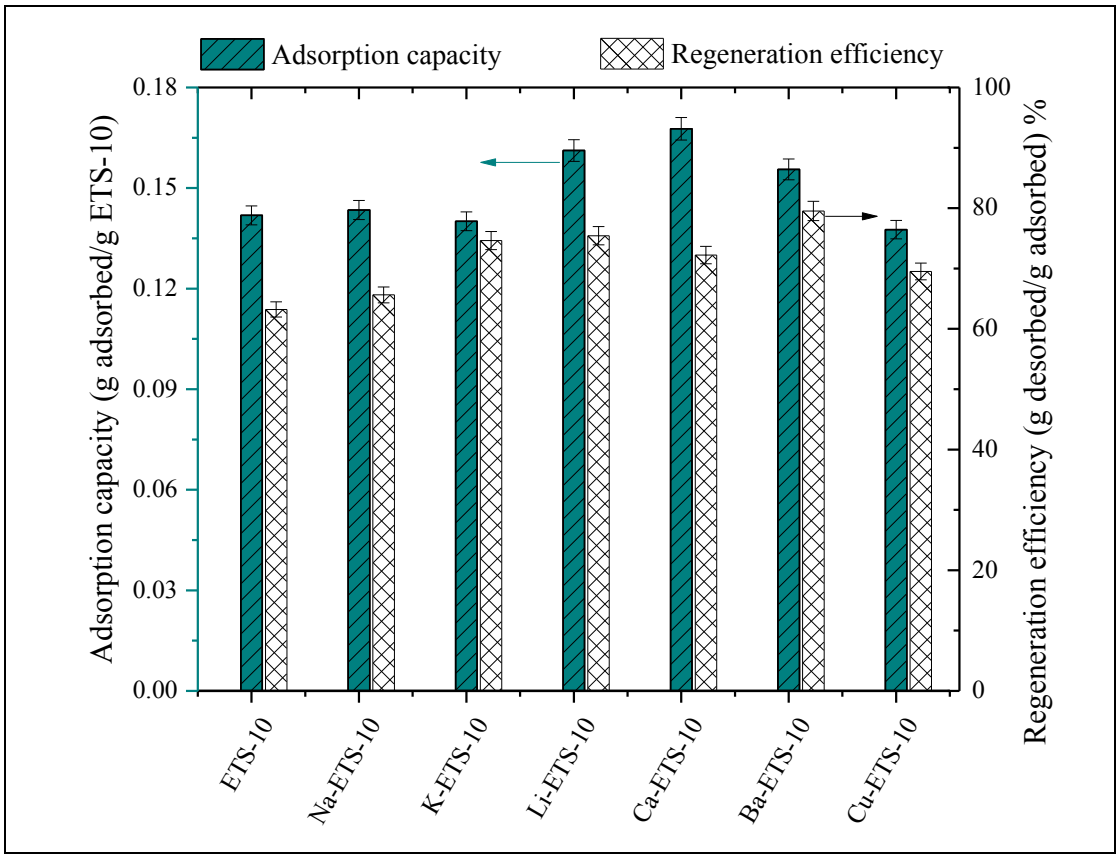

Figure 3-5. Adsorption capacity and microwave regeneration efficiency for all samples. Values are an average of triplicates ± standard deviation

Energy dissipated in the samples as heat during microwave regeneration is related to the sample's loss tangent (Eq. 2). Decreases in loss tangent after ion exchange are expected to decrease

microwave power absorbance, but the increased amount of microwave-absorbing adsorbate may counter these effects. Figure 3-6.a describes the temperature profiles of non-loaded samples during microwave heating. Since loss tangent decreased after ion exchange, it is harder to heat the prepared materials (Figure 3-3 and Figure 3-6.a). This is especially true for those samples exchanged with divalent cations. Since power dissipated in a material depends on its loss tangent, decreases in power absorbance (Figure 3-3 and Figure 3-6.b) can also be attributed to changes in loss tangent associated with ion exchange. Dielectric losses in zeolites are mainly due to electronic conduction, which is related to the migration of exchangeable cations along the channels and cavities inside the zeolite framework due to an ion-hopping mechanism (Kurzweil et al. 1995, Rybakov et al. 2006). Microwave energy absorbance in zeolites is also related to cation mobility(Ohgushi et al. 2009). The obtained values for these parameters (Figure 3-6.a and Figure 3-6.b) confirm that exchanging cations inside the ETS-10 structure changes the mobility of the cations due to charge and size differences, consequently, changing its loss factor and impacting power absorbance.

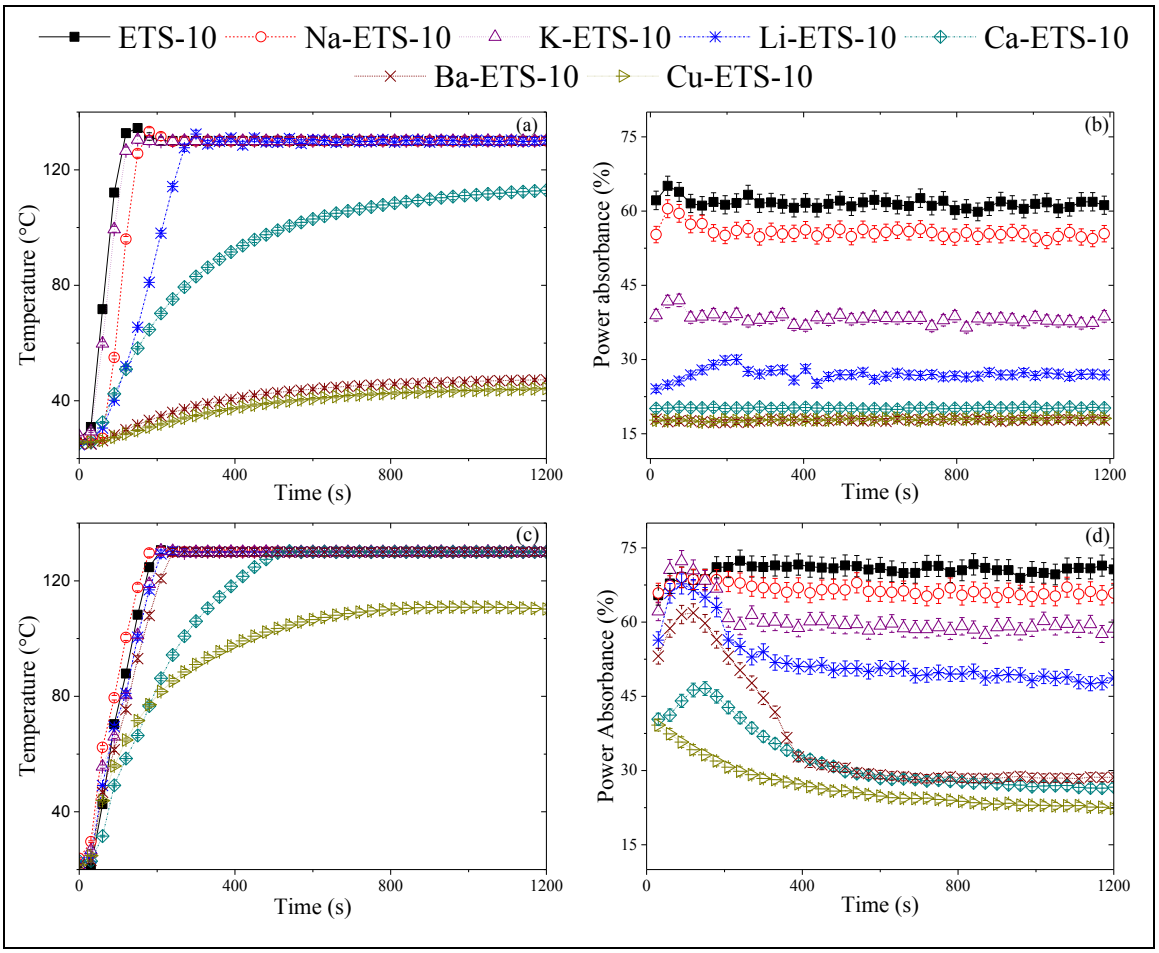

Figure 3-6. Temperature profile and power absorbance obtained from non-loaded (a and b) and loaded samples (c and d) during microwave heating. Values are an average of triplicates ± standard deviation.

Figure 3-6.c and Figure 3-6.d show that temperature profile and power absorbance change after loading the adsorbents with water. Roussy et al. (1984), Kraus et al. (2011), and Bellat et al. (2009) explained that for faujasite zeolites with low microwave absorbance, water desorption occurs mainly due to interactions between adsorbate and the applied electromagnetic field, because water is polar and has dielectric properties that favor microwave absorbance. In this work, decreasing the microwave absorbance of the ion exchanged materials favors direct heating of adsorbed water,

possibly increasing regeneration efficiencies. Power absorbance directly attributed to water adsorbed on ETS-10 can be quantified from the difference in power absorbance before and after water loading (Figure 3-7). Large differences (> 1 order of magnitude) between the dielectric properties of the ion exchanged samples (Figure 3-3) and water ($\varepsilon' = 79$ and $\varepsilon'' = 11$ at T=20 °C and f=2.45 GHz (Polaert et al. 2010)) may explain the improved power absorbance of the loaded samples compared to the non-loaded ones. Selective heating of the adsorbate is likely to occur in this scenario, whereby the component with the higher dielectric loss factor absorbs most of the input microwave energy (Reuß et al. 2002). This is accentuated at the beginning of the tests, when the adsorbent is still saturated with water. Abrioux et al. (2008), Bellat, et al. (2009), and Kraus, et al. (2011), however, described that water adsorption on faujasite zeolites (NaX and NaY) may also cause additional cation migration. Therefore, selective heating and cation migration, both attributed to water adsorption, are likely contributors to the observed changes in power absorbance. The change in power absorbance during regeneration was most significant for samples with a smaller dielectric loss tangent (e.g., Ba-ETS-10), where microwave energy can heat water more selectively. For ETS-10 ion exchanged with monovalent cations, the difference between power absorbance at the beginning and end of regeneration was lower compared to ETS-10 exchanged with divalent cations (Figure 3-6.d). This is attributed to the low power absorbance of the non-loaded, divalent cation exchanged samples (Figure 3-6.b). Hence, low power absorbance and ability of the material to convert the absorbed power to heat due to its loss tangent caused a low heating rate, preventing the material from reaching the target temperature (Figure 3-6.a).

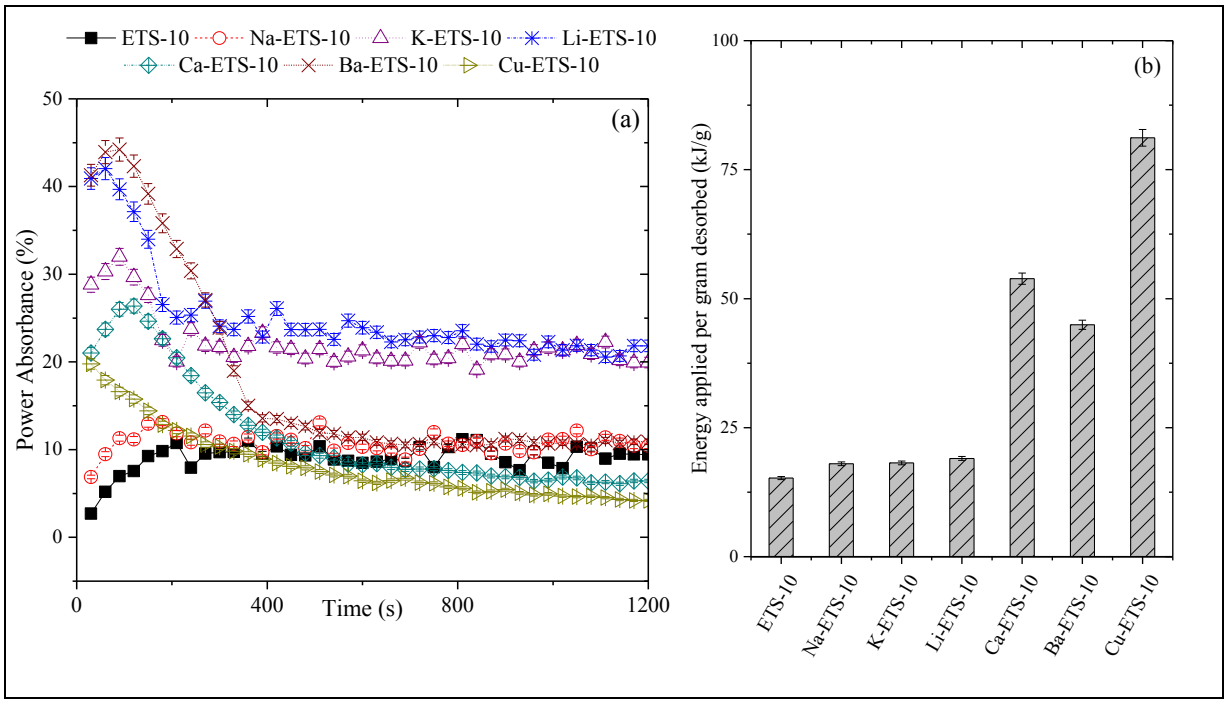

Figure 3-7. The difference between the power absorbance of the loaded and non-loaded samples during the microwave irradiation (a), and energy consumed during microwave regeneration (b). Values are an average of triplicates ± standard deviation

Based on Figure 3-7.a, trends for the differences in initial power absorbance of loaded and non-loaded samples match trends for regeneration efficiency (Figure 3-5) – a higher difference in power absorbance at the beginning of the regeneration corresponds to higher regeneration efficiency. Improvements in regeneration efficiency show that regeneration depends on how selectively the electromagnetic field transfers energy to adsorbed water or to mobile cations inside the adsorbents. A similar conclusion was made by Roussy and Chenot (1981) when desorbing water from other zeolites with microwave heating. The more energy that is transferred to the adsorbed water, the higher the obtained regeneration efficiency (Figure 3-5 and Figure 3-7.a).

Energy consumed during regeneration was calculated by integrating the applied power over the regeneration duration. The calculated values were then normalized by the amount of water

desorbed (Figure 3-7.b). Energy required for regeneration of samples with divalent cations was higher (> 62%) than for samples with monovalent cations mainly due to their significantly lower loss tangent (> 1 order of magnitude, Figure 3-3). This might also imply that the heat of adsorption of the water molecules is higher in samples with divalent cations than in samples with monovalent cations due to their stronger interaction. All modified samples required more energy compared to the original ETS-10. This difference is attributed to heating inefficiencies for the samples with lower power absorbance, which results in more energy consumption to maintain the temperature at 130 °C during regeneration.

To summarize, adsorption/microwave regeneration results indicate that Li-ETS-10 and Ba-ETS-10 are strong candidates for microwave regeneration when loaded with water due to their higher adsorption capacity and regeneration efficiency. However, when approaching for complete regeneration, Li-ETS-10 is more favored adsorbent due to its lower energy consumption, which allows for more effective microwave heating.

3.5. Conclusion

All ion exchanged ETS-10 samples showed increased water adsorption capacity and regeneration efficiency compared to untreated ETS-10. Exchanging ETS-10 cations also resulted in a decrease in its cation mobility, basicity, and the dielectric properties. This led to widening of the gap between the dielectric properties of adsorbent and polar adsorbate (e.g. water), resulting in better microwave regeneration efficiency for ion exchanged samples. These improvements may outweigh the increases in energy consumption required to regenerate the adsorbents. Less frequent regeneration (larger capacity) and less frequent adsorbent replacement (larger regeneration efficiency) provide energy improvements that may justify use of these materials. Based on capacity and regeneration efficiency alone, Li-ETS-10 and Ba-ETS-10 are strong candidates for microwave

regeneration when loaded with water (e.g. drying applications). Li-ETS-10, however, requires 30% less energy during regeneration and has ~5 times smaller penetration depth, which make it more favorable adsorbent for industrial use.

3.6. References

1. Abrioux, C., Coasne, B., Maurin, G., Henn, F., Boutin, A., Di Lella, A., Nieto-Draghi, C. and Fuchs, A. H. (2008). "A molecular simulation study of the distribution of cation in zeolites." Adsorption **14**(4-5): 743-754.

2. Adams, F., de Jong, M. and Hutcheon, R. (1992). "Sample shape correction factors for cavity perturbation measurements." Journal of Microwave Power and Electromagnetic Energy **27**(3): 131-135.

3. Al-Baghli, N. A. and Loughlin, K. F. (2005). "Adsorption of methane, ethane, and ethylene on titanosilicate ETS-10 zeolite." Journal of Chemical & Engineering Data **50**(3): 843-848.

4. Anderson, M. W., Terasaki, O., Ohsuna, T., Phllippou, A., MacKay, S. P., Ferreira, A., Rocha, J. and Lidin, S. (1994). "Structure of the microporous titanosilicate ETS-10." Nature **367**(6461): 347-351.

5. Ania, C. O., Parra, J. B., Menéndez, J. A. and Pis, J. J. (2005). "Effect of microwave and conventional regeneration on the microporous and mesoporous network and on the adsorptive capacity of activated carbons." Microporous and Mesoporous Materials **85**(1-2): 7-15.

6. Anson, A., Lin, C. C. H., Kuznicki, S. M. and Sawada, J. A. (2009). "Adsorption of carbon dioxide, ethane, and methane on titanosilicate type molecular sieves." Chemical Engineering Science **64**(16): 3683-3687.

7. Anson, A., Lin, C. C. H., Kuznicki, T. M. and Kuznicki, S. M. (2010). "Separation of ethylene/ethane mixtures by adsorption on small-pored titanosilicate molecular sieves." Chemical Engineering Science **65**(2): 807-811.

8. Anson, A., Wang, Y., Lin, C. C. H., Kuznicki, T. M. and Kuznicki, S. M. (2008). "Adsorption of ethane and ethylene on modified ETS-10." Chemical Engineering Science **63**(16): 4171-4175.

9. Atkinson, J. D., Zhang, Z., Yan, Z. and Rood, M. J. (2013). "Evolution and impact of acidic oxygen functional groups on activated carbon fiber cloth during NO oxidation." Carbon **54**: 444-453.

10. Bathen, D. (2003). "Physical waves in adsorption technology—an overview." Separation and Purification Technology **33**(2): 163-177.

11. Bellat, J. P., Paulin, C., Jeffroy, M., Boutin, A., Paillaud, J. L., Patarin, J., Lella, A. D. and Fuchs, A. (2009). "Unusual hysteresis loop in the adsorption-desorption of water in NaY zeolite at very low pressure." Journal of Physical Chemistry C **113**(19): 8287-8295.

12. Camarinha, E. D., Lito, P. F., Antunes, B. M., Otero, M., Lin, Z., Rocha, J., Pereira, E., Duarte, A. C. and Silva, C. M. (2009). "Cadmium(II) removal from aqueous solution using microporous titanosilicate ETS-10." Chemical Engineering Journal **155**(1-2): 108-114.

13. Cherbański, R., Komorowska-Durka, M., Stefanidis, G. D. and Stankiewicz, A. I. (2011). "Microwave swing regeneration Vs temperature swing regeneration - Comparison of desorption kinetics." Industrial & Engineering Chemistry Research **50**(14): 8632-8644.

14. Cherbański, R. and Molga, E. (2009). "Intensification of desorption processes by use of microwaves-An overview of possible applications and industrial perspectives." Chemical Engineering and Processing: Process Intensification **48**(1): 48-58.

15. Choi, J. H., Kim, S. D., Kwon, Y. J. and Kim, W. J. (2006). "Adsorption behaviors of ETS-10 and its variant, ETAS-10 on the removal of heavy metals, Cu2+, Co2+, Mn2+ and Zn2+ from a waste water." Microporous and Mesoporous Materials **96**(1-3): 157-167.

16. Chowdhury, T., Shi, M., Hashisho, Z. and Kuznicki, S. M. (2013). "Indirect and direct microwave regeneration of Na-ETS-10." Chemical Engineering Science **95**: 27-32.

17. Chowdhury, T., Shi, M., Hashisho, Z., Sawada, J. A. and Kuznicki, S. M. (2012). "Regeneration of Na-ETS-10 using microwave and conductive heating." Chemical Engineering Science **75**: 282-288.

18. Hashisho, Z., Rood, M. and Botich, L. (2005). "Microwave-swing adsorption to capture and recover vapors from air streams with activated carbon fiber cloth." Environmental Science and Technology **39**(17): 6851-6859.

19. Hutcheon, R. M., de Jong, M. and Adams, F. P. (1992). "A System for Rapid Measurements of RF and Microwave Properties Up to 1400°C." Journal of Microwave Power and Electromagnetic Energy **27(2)**: 87.

20. Jänchen, J., Ackermann, D., Stach, H. and Brösicke, W. (2004). "Studies of the water adsorption on Zeolites and modified mesoporous materials for seasonal storage of solar heat." Solar Energy **76**(1–3): 339-344.

21. Kim, K.-J. and Ahn, H.-G. (2012). "The effect of pore structure of zeolite on the adsorption of VOCs and their desorption properties by microwave heating." Microporous and Mesoporous Materials **152**(0): 78-83.

22. Kraus, M., Kopinke, F. D. and Roland, U. (2011). "Influence of moisture content and temperature on the dielectric permittivity of zeolite NaY." Physical Chemistry Chemical Physics **13**(9): 4119-4125.

23. Kurzweil, P., Maunz, W. and Plog, C. (1995). "Impedance of zeolite-based gas sensors." Sensors and Actuators B: Chemical **25**(1-3): 653-656.

24. Kuznicki, S. M. (1991). Large-pored crystalline titanium molecular sieve zeolites.

25. Lv, L., Tsoi, G. and Zhao, X. S. (2004). "Uptake equilibria and mechanisms of heavy metal ions on microporous titanosilicate ETS-10." Industrial & Engineering Chemistry Research **43**(24): 7900-7906.

26. Magnowski, N. B. K., Avila, A. M., Lin, C. C. H., Shi, M. and Kuznicki, S. M. (2011). "Extraction of ethane from natural gas by adsorption on modified ETS-10." Chemical Engineering Science **66**(8): 1697-1701.

27. Nak, C. J., Young, J. L., Park, J. H., Lim, H., Shin, C. H., Cheong, H. and Kyung, B. Y. (2009). "New insights into ETS-10 and titanate quantum wire: A comprehensive characterization." Journal of the American Chemical Society **131**(36): 13080-13092.

28. Nakada, K. and Ishii, A. (2011). DFT Calculation for Adatom Adsorption on Graphene.

29. National Research Council (1994). Microwave processing of materials, The National Academies Press.

30. Ohgushi, T., Sakai, Y., Adachi, Y. and Satoh, H. (2009). "Comparisons between measured and calculated properties in the microwave heating of Na-A, K-A, and Na,Ca-A zeolites." Journal of Physical Chemistry C **113**(19): 8206-8210.

31. Ohsuna, T., Terasaki, O., Watanabe, D., Anderson, M. W. and Lidin, S. (1994). "Microporous titanosilicate ETS-10: electron microscopy study." Studies in Surface Science and Catalysis **84**: 413-420.

32. Olivier, J. P. (1998). "Improving the models used for calculating the size distribution of micropore volume of activated carbons from adsorption data." Carbon **36**(10): 1469-1472.

33. Park, S. W., Yun, Y. H., Kim, S. D., Yang, S. T., Ahn, W. S., Seo, G. and Kim, W. J. (2010). "CO2 retention ability on alkali cation exchanged titanium silicate, ETS-10." Journal of Porous Materials **17**(5): 589-595.

34. Polaert, I., Estel, L., Huyghe, R. and Thomas, M. (2010). "Adsorbents regeneration under microwave irradiation for dehydration and volatile organic compounds gas treatment." Chemical Engineering Journal **162**(3): 941-948.

35. Reuß, J., Bathen, D. and Schmidt-Traub, H. (2002). "Desorption by microwaves: Mechanisms of multicomponent mixtures." Chemical Engineering & Technology **25**(4): 381-384.

36. Rocha, J. and Anderson, M. W. (2000). "Microporous titanosilicates and other novel mixed octahedral-tetrahedral framework oxides." European Journal of Inorganic Chemistry(5): 801-818.

37. Roussy, G. and Chenot, P. (1981). "Selective energy supply to adsorbed water and nonclassical thermal process during microwave dehydration of zeolite." Journal of Physical Chemistry **85**(15): 2199-2203.

38. Roussy, G., Zoulalian, A., Charreyre, M. and Thiebaut, J. M. (1984). "How microwaves dehydrate zeolites." Journal of physical Chemistry **88**(23): 5702-5708.

39. Rybakov, K. I., Semenov, V. E., Egorov, S. V., Eremeev, A. G., Plotnikov, I. V. and Bykov, Y. V. (2006). "Microwave heating of conductive powder materials." Journal of Applied Physics **99**(2).

40. Shi, M., Avila, A. M., Yang, F., Kuznicki, T. M. and Kuznicki, S. M. (2011). "High pressure adsorptive separation of ethylene and ethane on Na-ETS-10." Chemical Engineering Science **66**(12): 2817-2822.

41. Shi, M., Lin, C. C. H., Kuznicki, T. M., Hashisho, Z. and Kuznicki, S. M. (2010). "Separation of a binary mixture of ethylene and ethane by adsorption on Na-ETS-10." Chemical Engineering Science **65**(11): 3494-3498.

42. Tanchuk, B., Sawada, J. A., Rezaei, S. and Kuznicki, S. M. (2013). "Adsorptive drying of CO2 using low grade heat and humid, ambient air." Separation and Purification Technology **120**: 354-361.

43. Uma, S., Rodrigues, S., Martyanov, I. N. and Klabunde, K. J. (2004). "Exploration of photocatalytic activities of titanosilicate ETS-10 and transition metal incorporated ETS-10." Microporous and Mesoporous Materials **67**(2-3): 181-187.

44. Waghmode, S. B., Vetrivel, R., Hegde, S. G., Gopinath, C. S. and Sivasanker, S. (2003). "Physicochemical investigations of the basicity of the cation exchanged ETS-10 molecular sieves." Journal of Physical Chemistry B **107**(33): 8517-8523.

Chapter 4. TAILORING THE ELECTRICAL RESISTIVITY OF DEALUMINATED ZEOLITE Y BY CARBON ADDITION TO ALLOW RESISTIVE HEATING

4.1. Chapter Overview

This chapter describes a proof of concept study that assesses the feasibility and performance of multiple techniques for carbon addition to decrease the resistivity of a highly resistive molecular sieve and allow its resistive heating without sacrificing its adsorption properties. Carbon was added to zeolite by physical mixing with powdered carbon, chemical vapor deposition of ethanol and benzene, carbon nanotube growth via catalytic CH_4 decomposition, and thermal decomposition of organic polymer.

ETS-10 was initially selected for carbon addition experiment. However, common methods for carbon addition require high temperature treatment which can affect ETS-10 thermal stability and structural properties. Figure 4-1 demonstrates the change in ETS-10 structure at 400ºC and 600ºC. Therefore, dealuminated zeolite Y, a highly resistive molecular sieve with high mechanical and thermal stability, was selected to study the effect of carbon addition methods on its electric properties.

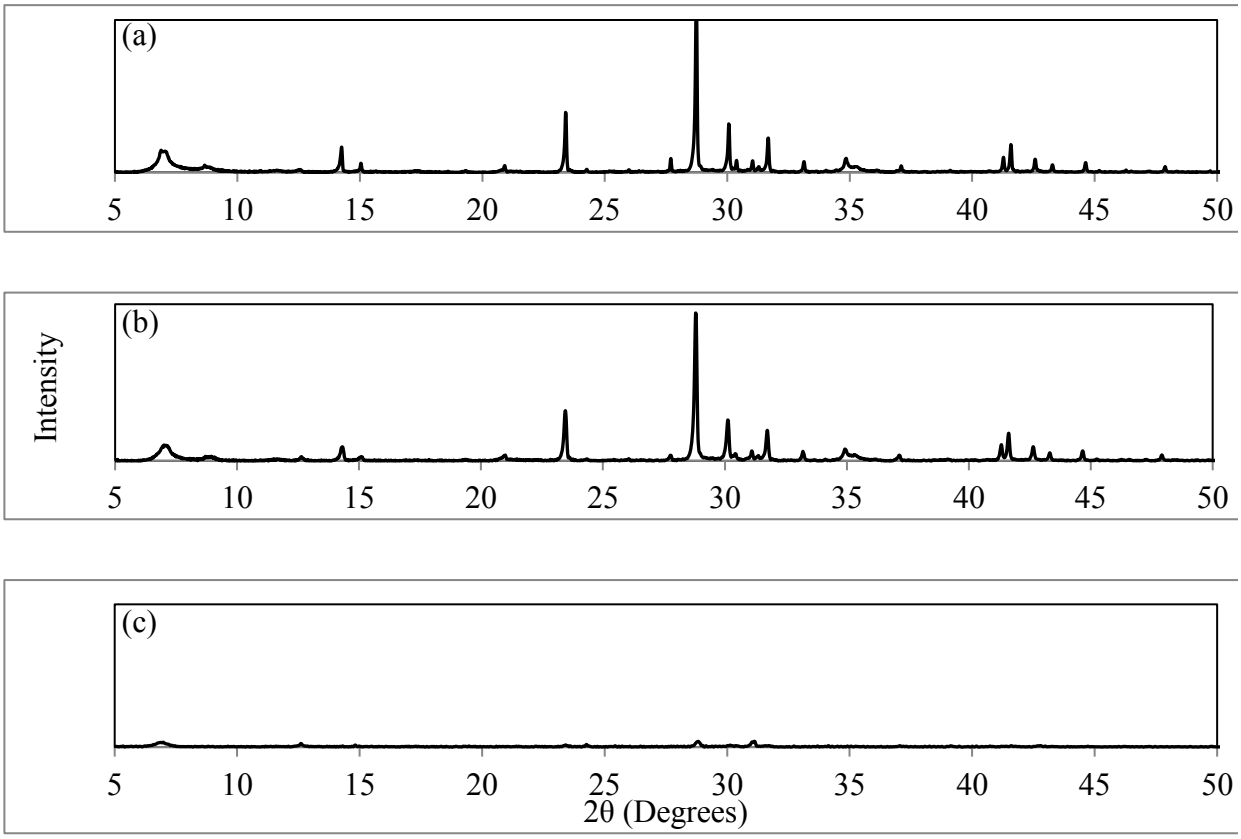

Figure 4-1. XRD pattern for original (a) and heated ETS-10 at 400ºC (b) and 600ºC (c)

4.2. Introduction

Pressure swing regeneration (PSR) and temperature swing regeneration (TSR) are established techniques for recovering adsorption capacity of saturated adsorbents. Conventional PSR and TSR techniques (applying steam, hot gas, conductive heating, or vacuum regeneration), however, have high energy consumption, are slow, and/or alter the physical/chemical properties of adsorbents and adsorbates (Al-Baghli and Loughlin 2005, Ania et al. 2005, Cherbański and Molga 2009, Cherbański et al. 2011, Chowdhury et al. 2012, Fayaz et al. 2015, Kamravaei et al. 2017, Shariaty

et al. 2017). Resistive heating regeneration, also known as electrothermal regeneration, passes electric current through a material with sufficiently low resistivity to generate heat by the Joule effect (Russell and Cohn 2012). This allows for rapid adsorbent regeneration that is decoupled from the purge gas. Compared to PSR and TSR, resistive heating is faster, has higher desorption efficiency, and requires less energy to achieve a desired desorption efficiency (Sullivan et al. 2001, 2004). Performance of resistive heating, however, is largely dependent on the electrical resistivity of the adsorbent (Subrenat et al. 2001, Luo et al. 2006, Park et al. 2007, 2009, Ribeiro et al. 2014).

Accordingly, resistive heating is established for regenerating carbonaceous adsorbents (resistivity = 0.2-0.8 Ω.m) (Subrenat et al. 2001, Luo et al. 2006, Hashisho et al. 2008, Johnsen et al. 2011, Ramirez et al. 2011, Johnsen and Rood 2012, Johnsen et al. 2014, Niknaddaf et al. 2016). Most inorganic adsorbents, including zeolites (resistivity $>10^7$ Ω.m), have low conductivity (Álvaro et al. 2006) and cannot be heated resistively. This work, for the first time, proposes that addition of carbon to low conductivity materials can increase the effective conductivity of the adsorbent bed, enabling resistive heating regeneration, without sacrificing its adsorption performance. To fundamentally address this hypothesis, different structural forms, sizes, and amounts of carbon are added to a commercial zeolite to increase net resistivity.

Carbon can be added to solid substrates by chemical vapor deposition (CVD) (Kim et al. 1999, Lu et al. 2004, Song et al. 2012), thermal degradation of polymers (Nath and Sahajwalla 2011, Nath and Sahajwalla 2011, Yang et al. 2012, Uda et al. 2013), and physical mixing (Bueche 1973, Park et al. 2007, 2009). Depending on method, carbon may be added to the substrate as (1) individual particles (Fan et al. 2014, Jiang et al. 2014), (2) monolayer or multilayer surface coverage (Kim et al. 1999, Song et al. 2012), or (3) carbon nanotubes (CNTs) grown from catalyst roots on the substrate's surface (Kumar and Ando 2005, Khatri et al. 2010, Nath and Sahajwalla

2011, Janas and Koziol 2014). If added carbon has a well-organized structure (i.e., carbon nanotube, graphene), no electrons will be scattered. Electrons have greater probability of scattering if the structure is imperfect (i.e., amorphous carbon). Less scattered electrons (i.e., structured carbon) will result in lower electrical resistivity, improving resistive heating potential (Jullien 1989, Singleton 2001). These carbon-addition methods, while individually well described in the literature, have never been considered as techniques to allow resistive heating of zeolites. Carbon coatings, for example, are the first step in preparation of zeolite-templated porous carbons (Song et al. 2012). Nanotubes grown from zeolite bases are used for catalytic reactions (Cao et al. 2013, Sano et al. 2013, Qi et al. 2015) and membrane separations (Liang et al. 2005, Sarno et al. 2013, Zhang et al. 2014). Mixed carbon/zeolite materials are applied in multi-pollutant control adsorption applications (Jha et al. 2008, Li and Chung 2008, Miyake et al. 2008).

The objective of this manuscript is to investigate the impact of different methods for carbon addition on the electrical and adsorptive properties of zeolites, with the goal of allowing resistive heating regeneration of adsorbents. This paper provides a proof of concept methodology for improving zeolite conductivity through the addition of carbon, highlighting potential for resistive heating with minimal impact on adsorption performance. Because different carbon addition methods add different amounts and forms of carbon to the substrate, variable impacts on resistivity are anticipated. The objective of this work, therefore, is to compare these methods and assess their effectiveness based on changes to dealuminated zeolite Y's resistivity without compromising its physical structure and adsorption properties. This manuscript is the first to report methods that allow resistive heating of a highly resistive inorganic adsorbent.

4.3. Experimental Methods

4.3.1. Sample Preparation

Dealuminated zeolite Y (CBV-901, Zeolyst, average particle size of 7 μm) was the base material for this study. Dealuminated zeolite Y is considered as a representative, non-conductive zeolite because of its high thermal stability and electrical resistivity due to its high Si/Al ratio (Si/Al = 80, providing a worst case scenario). Carbon was added to CBV-901 using methods described below, which were developed based on previous reports (Kim et al. 1999, Moisala et al. 2003, Lu et al. 2004, Song et al. 2012, Uda et al. 2013, Janas and Koziol 2014).

Physical mixing: CBV-901 and powdered carbon (Jacobi Carbons, average particle size = 26 μm) were mixed at different ratios (5, 10, 20, 30, 40 carbon wt%) after drying for > 12 h at 120 ^{o}C. These samples are referred to as wt% C/CBV-901.

Ethanol or benzene chemical vapor deposition (CVD)*:* 5 g powdered CBV-901 was added to a quartz boat and placed in a tube furnace. Temperature was ramped (20 ^{o}C/min) to 600 ^{o}C in 0.5 standard liters per minute (SLPM, 25 ^{o}C and 1 atm) N_2. After reaching the set point temperature, ethanol (90.5%, Rica Chemical Company) or benzene (> 99%, Sigma–Aldrich) was introduced into the furnace for 2 h at 0.07 and 0.18 ml/min (calculated based on saturation vapor pressures), respectively using a bubbler purged with N_2 (0.5 SLPM). Following vapor addition, the sample was cooled to 25 ^{o}C in 0.5 SLPM N_2. These samples are referred to as ethanol/CBV-901 or benzene/CBV-901.

CH_4 decomposition on cobalt impregnated zeolite: 8 g $Co(NO_3)_2.6H_2O$ (≥ 98%, Sigma-Aldrich) was dissolved in 100 ml deionized water, and 5 g CBV-901 was added to the solution. The solution was mixed for 1 h and then dried at 90 ºC for > 12 h. The collected powder was added

to a quartz boat and put in a tube furnace. Temperature was ramped (20 ºC/min) to 600 ºC in 0.5 SLPM N_2. The sample was then calcined in air (0.5 SLPM) at 600 ºC for 1 h and then reduced in 10% H_2 in N_2 (0.5 SLPM) for 1 h at the same temperature. Finally, 0.5 SLPM CH_4 was added to the tube furnace at 600 ºC for 0.5 h. This sample is referred to as CNT/CBV-901.

Polymer carbonization: 1.25 g polyvinyl alcohol (PVA, molecular weight of 89,000 – 98,000 g/mole, 99+% hydrolyzed, Sigma-Aldrich) was dissolved in 100 ml deionized water at 80 ºC before adding 5 g CBV-901. The solution was sonicated for 1 h and then dried at 90 ºC for > 12 h. Resulting samples were put in the tube furnace and heated at 600 ºC (ramp rate = 20 ºC/min) for 2 h in 2 SLPM N_2 before cooling to room temperature in N_2. This sample is referred to as PVA/CBV-901.

4.3.2. Material Characterization

Bulk Elemental Analysis*:* Added carbon was measured with Organic Elemental Analysis (OEA) (Flash 2000, Thermo Fisher Scientific Inc.), using furnace and gas chromatograph column temperatures of 950 and 65 ^{0}C, respectively. He (carrier gas), He (reference), and O_2 flow rates were 140, 250, and 100 ml/min, respectively. A 5 sec oxygen dose was used and the run time was 12 min.

Scanning Electron Microscopy (SEM)*:* Field emission SEM (JAMP-9500F Auger microprobe, JEOL) was completed using 15 kV accelerating voltage, 8 nA emission current, 24 mm working distance, and 30º sample rotation. An M5 lens with 0.6% energy resolution was used for Auger spectroscopy and imaging.

Raman Spectroscopy*:* Raman spectra (Nicolet Almega XR micro-Raman Analysis System) were acquired at room temperature with 532 nm (2.33 eV) laser wavelength at 24 mW power. All

spectra were collected by fine-focusing a 50× microscope objective and averaging five, 10 sec exposures.

X-Ray Diffraction (XRD)*:* Powder XRD patterns (Rigaku Ultima IV unit equipped with a D/Tex detector and Fe filter) were acquired using a cobalt tube (38 kV, 38 mA) with average Kα wavelength of 1.790260 Å. Samples were run from 5 to 90° using a top-pack mount at 2° 2θ/min and step size of 0.02°.

Resistivity Measurements and Resistive Heating: 2 g of each sample (no binder) was pressed at 5 kPSI to form discs. Resistivity of prepared discs was measured by inserting them between two electrodes connected to a digital multimeter (Agilent Technologies) (Figure 4-2). During resistivity measurements, samples were purged with 0.5 SLPM N_2. Resistive heating of the modified samples was performed using the same setup and gas flow rate, only replacing the digital multimeter with a power source. During resistive heating, the temperature of the samples was measured using a thermocouple (Type K, Omega).

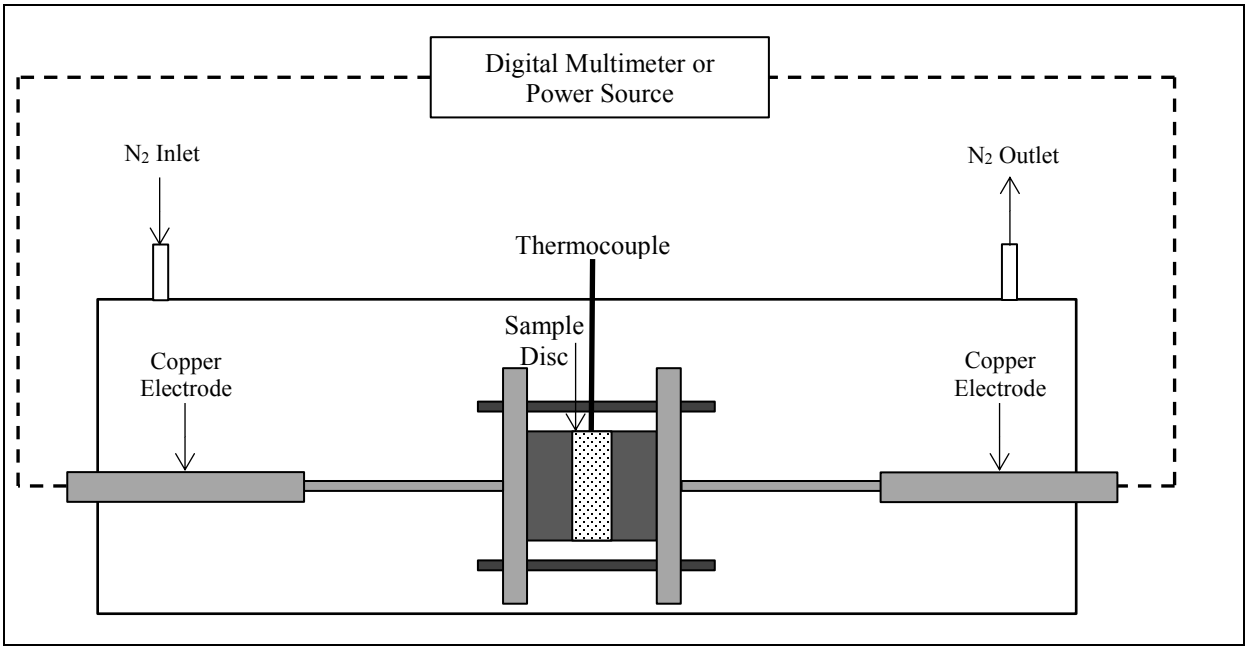

Figure 4-2. Schematic of setup for resistivity measurements and resistive heating

N_2 Adsorption: Micropore surface analysis (IQ2MP, Quantachrome) with N_2 (relative pressures from 10^{-7} to 0.995) at 77 K was used to characterize physical properties of prepared materials. 60 – 70 mg of sample was degassed at 120 °C for 5 h to remove moisture before analysis. Specific surface area and micropore volume were obtained from relative pressure ranges of 0.01 − 0.07 and 0.2 − 0.5 using the BET equation and the V-t method, respectively.

Toluene Adsorption: Toluene, a common VOC, was used as a surrogate adsorbate to assess the adsorption properties of the samples. The adsorption isotherms (99.9%, Fisher Chemicals) were obtained gravimetrically using a sorption analyzer (TA Instruments, model VTI-SA) at 25 °C with N_2 carrier gas and varying concentrations of toluene. The system logged the equilibrium weight of the sample (5 – 7 mg) in response to a step change in toluene concentration (0.01 – 0.9 relative pressure). Equilibrium for a given toluene concentration was assumed when the weight change was < 0.001 wt% in 5 min.

4.4. Result and Discussion

Bulk carbon contents of untreated and modified zeolites are shown in Figure 4-3. For physically mixed samples, consistent carbon/zeolite mass ratios for three randomly selected allotments (difference of ~ 0.9 wt%) indicates homogeneity. Lower carbon contents (1-3 wt%) compared to intended mass loadings are attributed to the presence of other elements (i.e., O and H) in the powdered carbon. For all surface-modified samples, consistent thermal processing conditions (2 h, 600 ^oC) were applied. Although the selected temperature (600 ^oC) is lower than what is typical for carbon deposition experiments, appreciable carbon loadings were obtained (Figure 4-3). Different loading methods resulted in different amounts of deposited carbon. Of all surface-modified samples, CNT/CBV-901 has the highest bulk carbon content. It also has the darkest color and is fluffier than other surface-modified samples. A color change was still present for the other

modified samples, but gray tints were more common than the black color associated with CNT/CBV-901. Higher carbon deposition in this case was expected because a metal catalyst was used to enhance methane decomposition at the lower temperature. Un-catalyzed methane decomposition requires > 1000 ^{o}C (Guéret et al. 1997). Moreover, comparing samples modified by CVD, more carbon deposition was obtained using ethanol than benzene, which is particularly relevant because deposited carbon mass via ethanol is 9 times higher than via benzene. This is attributed to higher carbon deposition by ethanol's decomposition at the performed thermal condition compared to benzene (decomposition conversion rate of ~50% (Gallego et al. 2011) compared to ~7% (Zanetti and Egloff 1917), respectively) (Figure 4-3).

Carbon deposition yields are highest for PVA/CBV-901 (33%) and CNT/CBV-901 (31%) (Figure 4-3). To obtain higher carbon loadings for PVA modified samples, however, input PVA mass should be increased. To deposit the same amount of carbon (1.55 g) as CNT/CBV-901, input PVA mass would be greater than the zeolite's mass (13 g mixed with 5 g zeolite), likely preventing homogenous loading across the zeolite's surface. CVD approaches have low carbon yields because ethanol and benzene do not rapidly carbonize at 600 ^{o}C and residence times upstream of the substrate are 3.5 min. Based only on carbon yields and loading potential, the CNT/CBV-901 method is preferred at the considered conditions.

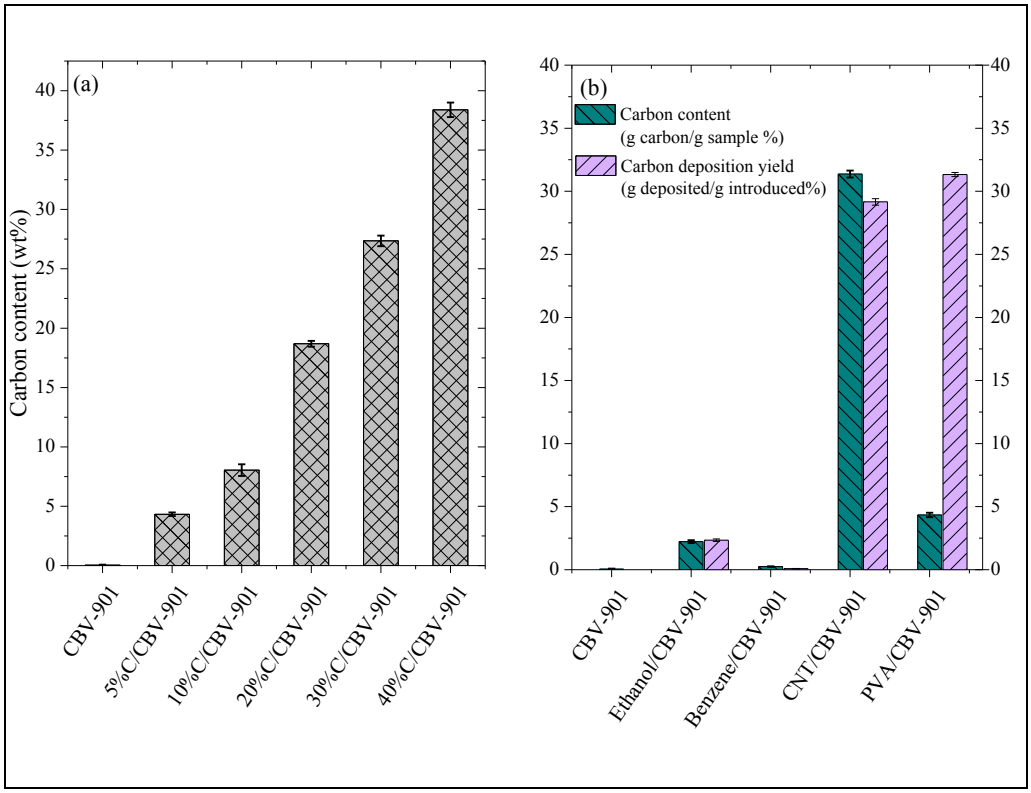

Figure 4-3. Carbon content for (a) physically mixed (b) and surface-modified samples obtained from bulk elemental analysis. Values are an average of triplicates ± standard deviation.

Scanning electron micrographs (Figure 4-4) highlight differences between surface-modified samples. For PVA/CBV-901, individual carbon particles are visible between zeolite particles, similar to physically mixed samples, however, they are considerably smaller than zeolite crystals. Carbon particle size was 1-2 orders of magnitude smaller for PVA/CBV-901 compared to physically mixed samples (< 0.5 μm vs. 26 μm). For equal mass loadings, small diameter carbon particles better coat the zeolite to provide a more continuous path for electric current to move through the carbon/zeolite material, decreasing interference and resistivity. Since improved conductivity is expected to result from improved electron mobility through added carbon, for a constant carbon wt%, covering zeolite crystals with smaller particles is more likely to result in

higher conductivity. For samples modified by CVD, carbon particles are not visible (Figure 4-4), implying that carbon is added to the zeolite as mono- or multi-layer coatings. Carbon nanotubes are visible on the CNT/CBV-901 sample, grown from metal catalyst seeds that are also visible and identified with BSEM (bright spots) and EDX (Figure 4-5.a).

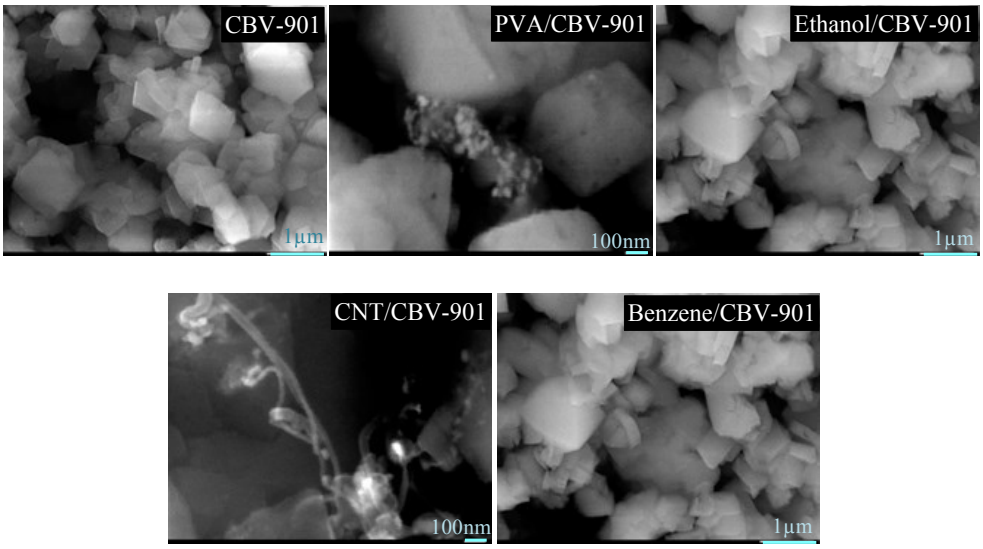

Figure 4-4. SEM images of modified samples

Raman spectroscopy confirms the formation of carbon nanotubes in CNT/CBV-901 (Figure 4-5.b). Four bands are observed for CNT/CBV-901, and the presence of D (1343 cm^{-1}), G (1573 cm^{-1}), and G' (2671 cm^{-1}) bands confirm CNT formation, consistent with SEM observations (Triantafyllidis et al. 2008). The additional band at 673 cm^{-1} represents the zeolite framework (Moteki et al. 2011).

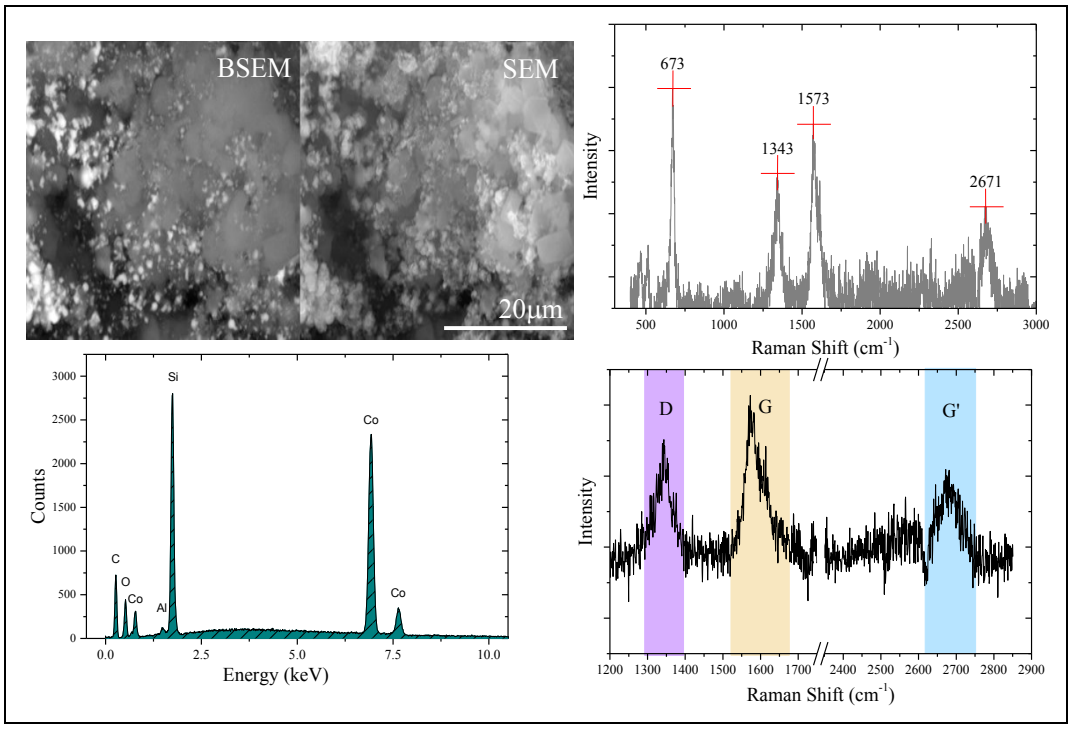

Figure 4-5. SEM, BSEM, and EDX (a) and Raman spectroscopy (b) results obtained for the CNT/CBV-901 sample

Zeolite crystallinity is stable after carbon addition – all samples have matching XRD profiles (Figure 4-6). Heat treatments for carbon deposition does not impact crystallinity. The high Si/Al ratio of dealuminated zeolite Y makes it thermally stable until ~900 ºC, due to silicon/aluminum ordering in the tetrahedral zeolite lattice (Alsdorf et al. 1985). This prevents baseline effects on the zeolite's physical and adsorptive properties associated with heating, isolating differences associated with carbon addition. XRD results also confirm no significant change in zeolite's crystalline lattice.

Differences in XRD peak intensities are attributed to added carbon diluting the zeolite signal (Figure 4-6). CNT/CBV-901 and PVA/CBV-901 have more carbon (31.4 and 4.3 wt%) than other samples (Figure 4-3), generating correspondingly weak zeolite signals. For CNT/CBV-901, peaks observed near 30, 50, and 60 degrees correspond to cobalt oxide (30 degrees) and CNT (~50 and

60 degree), consistent with Raman results (Figure 4-5) (Pełech et al. 2014). The absence of new peaks for other surface-modified samples indicates that added carbon is amorphous.

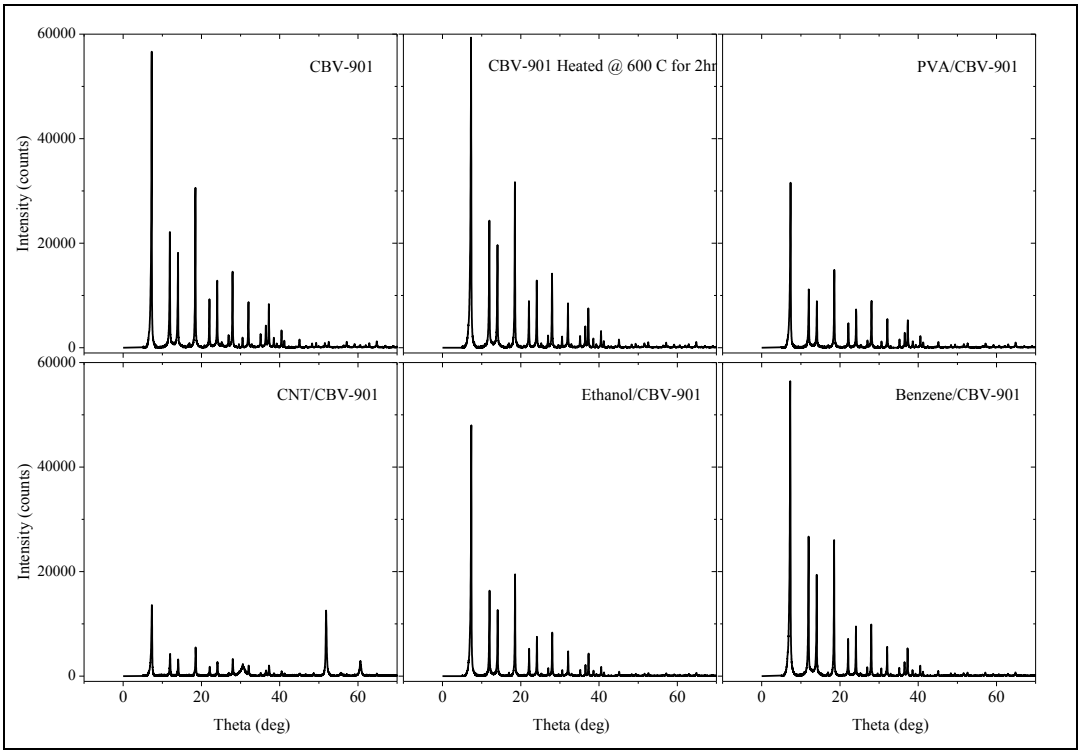

Figure 4-6. XRD pattern for all thermally modified samples.

Resistivity of mixed and modified samples was compared to the untreated zeolite (Figure 4-7). Six and seven-order of magnitude resistivity decreases occurred for physically mixed samples with 30 and 40 wt% carbon, respectively. For surface-modified samples, only CNT/CBV-901 had sufficiently low resistivity (0.7 Ω.m) for resistive heating, attributed to its high carbon content. Resistivity of CBV-901 loaded with cobalt catalysts (likely oxidized in air) is > 10^7 Ω.m, confirming that gains after carbon addition are attributed exclusively to structured CNT (Kaneto et al. 1999). Consistent with this, while CNT/CBV-901 and 30%C/CBV-901 have similar carbon content, the resistivity of CNT/CBV-901 is two orders of magnitude lower because 30%C/CBV-901 contains amorphous carbon. Although sample discs were pressed using high pressure (5 kPSI),

void spaces between carbon and zeolite particles may add resistance to electron and heat flow. This additional resistance is not anticipated for CNT/CBV-901, however, because CNTs are attached to the zeolite (via diffusion of carbon atoms into catalyst seeds) (Moisala et al. 2003). This is an advantage of the CNT-loading method compared to physical mixing.

Comparing other surface-modified samples to CNT/CBV-901, low carbon deposition (i.e., < 3%) results in no notable change in zeolite resistivity. This implies that a minimum amount of carbon must be deposited to form, hypothetically, a continuous "carbon chain" across the full length of the pressed disc. To make other techniques practical, therefore, higher temperature (Ethanol, Benzene/CBV-901) or more carbon precursor (PVA/CBV-901) should be used, potentially at the expense of consistent adsorbent physical properties. The deposited carbon in CNT/CBV-901, while not optimized in this work, is clearly large enough to form the desired "carbon chain" and decrease resistivity. In all, high carbon loading potential, high carbon deposition efficiency, and direct zeolite-carbon contact all convey that CNT addition is the preferred carbon loading technique for the prescribed thermal decomposition conditions.

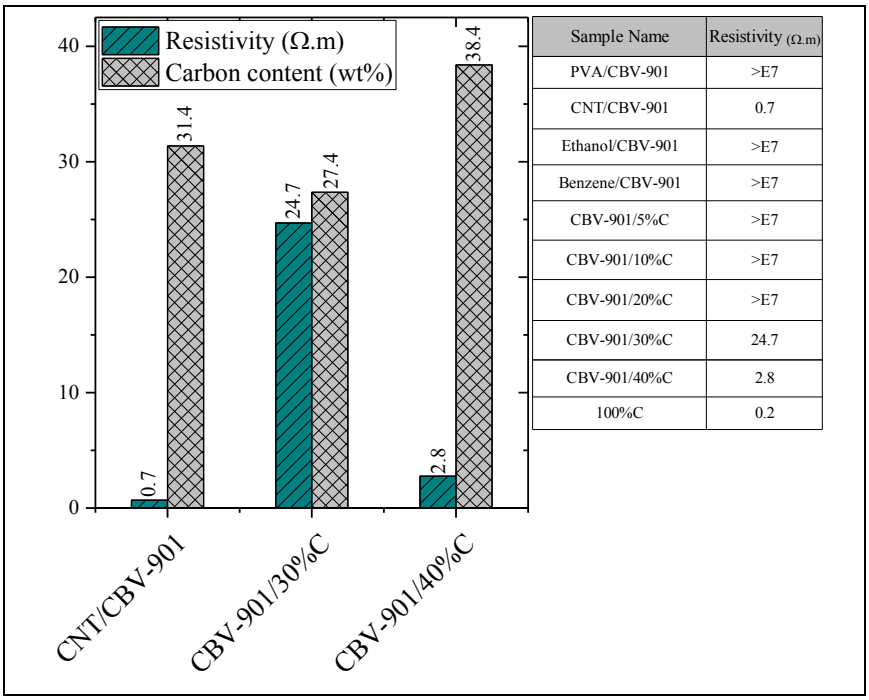

Sample Name	Resistivity (Ω.m)
PVA/CBV-901	>E7
CNT/CBV-901	0.7
Ethanol/CBV-901	>E7
Benzene/CBV-901	>E7
CBV-901/5%C	>E7
CBV-901/10%C	>E7
CBV-901/20%C	>E7
CBV-901/30%C	24.7
CBV-901/40%C	2.8
100%C	0.2

Figure 4-7. Resistivity of prepapred samples

Since the objective of this work is to decrease zeolite resistivity without compromising adsorption properties, physical properties and adsorption performance of surface-modified samples were determined. CNT/CBV-901, the only surface-modified sample that met resistive heating requirements, was characterized using micropore surface analysis and toluene adsorption (Figure 4-8). Compared to virgin zeolite, BET surface area and total pore volume of CNT/CBV-901 decreased by 23% and 16%, respectively. This may be due to CNT deposition on the surface of the zeolite; however, one might expect an overall increase in pore volume when adding a porous material to the surface of another porous material (Ciambelli et al. 2005). More likely, the addition of large cobalt catalyst particles (~10 to 40 Å) to the zeolite surface, before carbon growth, blocks narrow zeolite pores (7.4 Å (Kim and Ahn 2012)) (Garrido Pedrosa et al. 2006). CNT growth will, consequently, add pore volume to the samples, but apparently not enough to overcome catalyst pore blockage. When comparing adsorption capacities at different relative pressures (0.02 – 0.9),

the toluene adsorption isotherm suggests that most (66 ± 2%) zeolite adsorption sites are available after carbon addition (Figure 4-8). Because the kinetic diameter of toluene is 5.85 Å (Dehdashti et al. 2011) is close to zeolite Y's pore size (7.4 Å (Kim and Ahn 2012)), its adsorption is a good indicator of zeolite pore availability.

The reduction in toluene adsorption capacity at 0.995 relative pressure is > 2 times that of pore volume, attributed to the larger size of toluene compared to nitrogen (used for micropore surface analysis). While additional porosity is obtained from added CNTs, these pores are only accessible to molecules small enough to pass through the CNT wall. This CNT "sieving-effect" observation is consistent with results from Lu et al. (2007). Consequently, high CNT content in the sample is not favorable for adsorption of most volatile organic compounds. The CNT loading method described here, therefore, requires optimization to reduce CNT content while maintaining resistivity decreases. This may be possible by reducing the population and size of deposited CNTs through the tuning of deposition conditions (e.g. reducing deposition time and temperature).

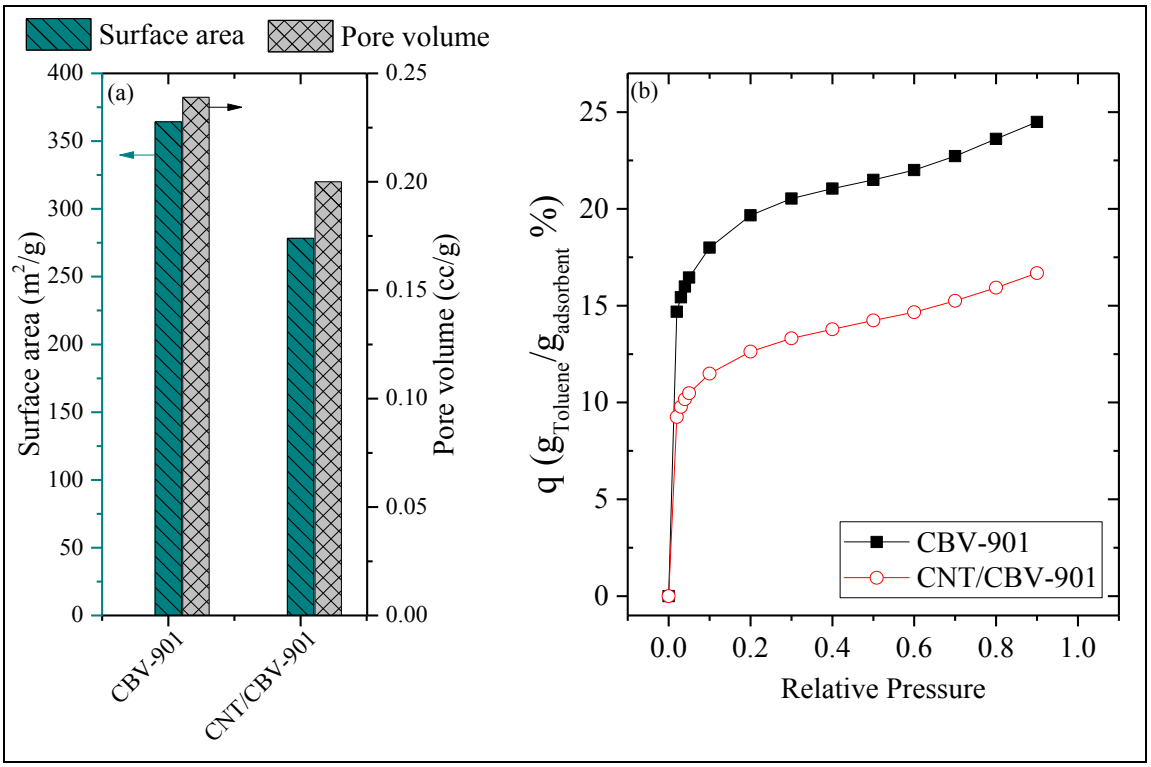

Figure 4-8.Adsorption properties of CNT/CBV-901 with respect to untreated adsorbent, (a) micropore surface analysis and (b) Toluene adsorption isotherm

CNT/CBV-901 was resistively heated in N_2 at 130 ºC (Figure 4-8). Temperature was controlled by manually adjusting the output voltage of the power source. The material can be quickly heated (120 ºC/min) at the beginning of the heating period, while the heating rate can be changed by changing the applied voltage. Figure 4-9 also shows the possibility to control the temperature using this technique as a constant temperature condition. These results represent the first resistive heating of an inorganic adsorbent material with high resistivity, providing a new opportunity to regenerate industrial inorganic adsorbents efficiently and quickly.

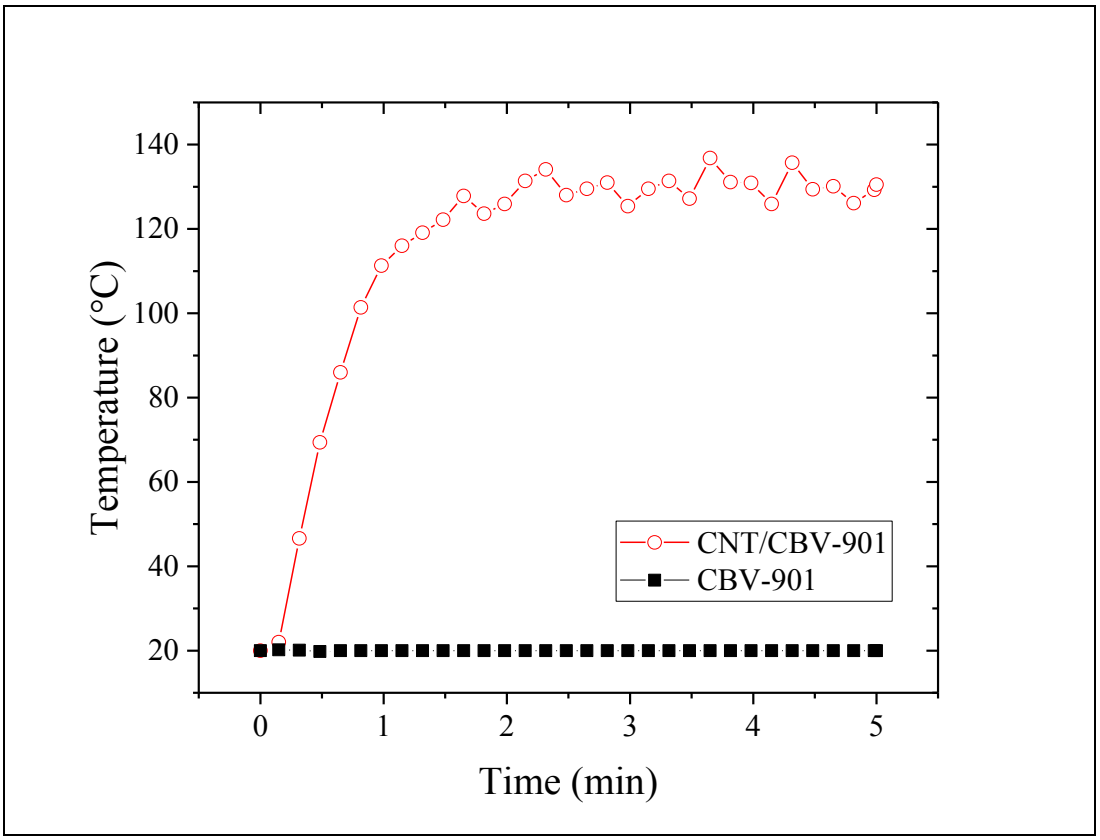

Figure 4-9. Temperature profile during resistive heating of CNT/CBV-901 at constant temperature.

4.5. Conclusions

In this work, the effect of carbon addition on the electrical resistivity of zeolite CBV-901 was investigated. The results indicate that resistivity can be decreased from > 10^7 to 2.8 Ω.m, which is suitable for resistive heating, by physically mixing the zeolite with 40 wt% carbon powders. While this method decreases zeolite resistivity, it was shown that resistivity is further reduced by adding carbon directly to the zeolite's structure in the form of CNTs. CNT growth increased the carbon content of zeolites to 31.4 wt% and decreased resistivity by eight orders of magnitude (to 0.7 Ω.m) while preserving the majority of zeolite pores for adsorption. This zeolite modified by CNT growth was successfully heated by resistive heating at 120 ºC /min. The results from this work show the

potential of using CNT addition for decreasing the resistivity of highly resistive adsorbents to a level suitable for resistive heating. This technique, however, could be further optimized to reduce its effect on the adsorption properties of the adsorbent.

4.6. Acknowledgement

We would like to acknowledge financial support for this research from the Natural Science and Engineering Research Council (NSERC) of Canada, and Alberta Innovates Graduate Student Scholarship program.

4.7. References

1. Al-Baghli, N. A. and Loughlin, K. F. (2005). "Adsorption of methane, ethane, and ethylene on titanosilicate ETS-10 zeolite." Journal of Chemical Engineering Data **50**(3): 843-848.

2. Alsdorf, E., Lohse, U. and Feist, M. (1985). "Thermoanalytical and adsorption investigations on dealuminated Y-zeolites of different preparation." Thermochimica Acta **93**: 553-556.

3. Álvaro, M., Cabeza, J. F., Fabuel, D., García, H., Guijarro, E. and De Juan, J. L. M. (2006). "Electrical conductivity of zeolite films: Influence of charge balancing cations and crystal structure." Chemistry of Materials **18**(1): 26-33.

4. Ania, C. O., Parra, J. B., Menéndez, J. A. and Pis, J. J. (2005). "Effect of microwave and conventional regeneration on the microporous and mesoporous network and on the adsorptive capacity of activated carbons." Microporous and Mesoporous Materials **85**(1-2): 7-15.

5. Bueche, F. (1973). "A new class of switching materials." Journal of Applied Physics **44**(1): 532-533.

6. Cao, Y., Yu, H., Tan, J., Peng, F., Wang, H., Li, J., Zheng, W. and Wong, N. B. (2013). "Nitrogen-, phosphorous- and boron-doped carbon nanotubes as catalysts for the aerobic oxidation of cyclohexane." Carbon **57**: 433-442.

7. Cherbański, R., Komorowska-Durka, M., Stefanidis, G. D. and Stankiewicz, A. I. (2011). "Microwave swing regeneration Vs temperature swing regeneration - Comparison of desorption kinetics." Industrial & Engineering Chemistry Research **50**(14): 8632-8644.

8. Cherbański, R. and Molga, E. (2009). "Intensification of desorption processes by use of microwaves-An overview of possible applications and industrial perspectives." Chemical Engineering and Processing: Process Intensification **48**(1): 48-58.

9. Chowdhury, T., Shi, M., Hashisho, Z., Sawada, J. A. and Kuznicki, S. M. (2012). "Regeneration of Na-ETS-10 using microwave and conductive heating." Chemical Engineering Science **75**: 282-288.

10. Ciambelli, P., Sannino, D., Sarno, M., Fonseca, A. and Nagy, J. B. (2005). "Selective formation of carbon nanotubes over Co-modified beta zeolite by CCVD." Carbon **43**(3): 631-640.

11. Dehdashti, A., Khavanin, A., Rezaee, A., Assilian, H. and Motalebi, M. (2011). "Application of microwave irradiation for the treatment of adsorbed volatile organic compounds on granular activated carbon." Iranian Journal of Environmental Health Science and Engineering **8**(1): 85-94.

12. Fan, R. J., Sun, Q., Zhang, L., Zhang, Y. and Lu, A. H. (2014). "Photoluminescent carbon dots directly derived from polyethylene glycol and their application for cellular imaging." Carbon **71**: 87-93.

13. Fayaz, M., Shariaty, P., Atkinson, J. D., Hashisho, Z., Phillips, J. H., Anderson, J. E. and Nichols, M. (2015). "Using microwave heating to improve the desorption efficiency of high molecular weight VOC from beaded activated carbon." Environmental Science and Technology **49**(7): 4536-4542.

14. Gallego, J., Sierra, G., Mondragon, F., Barrault, J. and Batiot-Dupeyrat, C. (2011). "Synthesis of MWCNTs and hydrogen from ethanol catalytic decomposition over a Ni/La2O3 catalyst produced by the reduction of LaNiO3." Applied Catalysis A: General **397**(1–2): 73-81.

15. Garrido Pedrosa, A. M., Souza, M. J. B., Melo, D. M. A. and Araujo, A. S. (2006). "Cobalt and nickel supported on HY zeolite: Synthesis, characterization and catalytic properties." Materials Research Bulletin **41**(6): 1105-1111.

16. Guéret, C., Daroux, M. and Billaud, F. (1997). "Methane pyrolysis: thermodynamics." Chemical Engineering Science **52**(5): 815-827.

17. Hashisho, Z., Emamipour, H., Rood, M. J., Hay, K. J., Kim, B. J. and Thurston, D. (2008). "Concomitant adsorption and desorption of organic vapor in dry and humid air streams using microwave and direct electrothermal swing adsorption." Environmental Science and Technology **42**(24): 9317-9322.

18. Janas, D. and Koziol, K. K. (2014). "A review of production methods of carbon nanotube and graphene thin films for electrothermal applications." Nanoscale **6**(6): 3037-3045.

19. Jha, V. K., Matsuda, M. and Miyake, M. (2008). "Sorption properties of the activated carbon-zeolite composite prepared from coal fly ash for Ni2+, Cu2+, Cd2+ and Pb2+." Journal of Hazardous Materials **160**(1): 148-153.

20. Jiang, Z., Nolan, A., Walton, J. G. A., Lilienkampf, A., Zhang, R. and Bradley, M. (2014). "Photoluminescent carbon dots from 1,4-addition polymers." Chemistry - A European Journal **20**(35): 10926-10931.

21. Johnsen, D. L., Mallouk, K. E. and Rood, M. J. (2011). "Control of electrothermal heating during regeneration of activated carbon fiber cloth." Environmental Science and Technology **45**(2): 738-743.

22. Johnsen, D. L. and Rood, M. J. (2012). "Temperature control during regeneration of activated carbon fiber cloth with resistance-feedback." Environmental Science and Technology **46**(20): 11305-11312.

23. Johnsen, D. L., Zhang, Z., Emamipour, H., Yan, Z. and Rood, M. J. (2014). "Effect of isobutane adsorption on the electrical resistivity of activated carbon fiber cloth with select physical and chemical properties." Carbon **76**: 435-445.

24. Jullien, A. G. a. R. (1989). The Solid State: From Superconductors to Superalloys. New York, Oxford Science Publications.

25. Kamravaei, S., Shariaty, P., Jahandar Lashaki, M., Atkinson, J. D., Hashisho, Z., Phillips, J. H., Anderson, J. E. and Nichols, M. (2017). "Effect of Beaded Activated Carbon Fluidization on Adsorption of Volatile Organic Compounds." Industrial & Engineering Chemistry Research **56**(5): 1297-1305.

26. Kaneto, K., Tsuruta, M., Sakai, G., Cho, W. Y. and Ando, Y. (1999). "Electrical conductivities of multi-wall carbon nano tubes." Synthetic Metals **103**(1–3): 2543-2546.

27. Khatri, I., Kishi, N., Zhang, J., Soga, T., Jimbo, T., Adhikari, S., Aryal, H. R. and Umeno, M. (2010). "Synthesis and characterization of carbon nanotubes via ultrasonic spray pyrolysis method on zeolite." Thin Solid Films **518**(23): 6756-6760.

28. Kim, J. H., Ikoma, Y. and Niwa, M. (1999). "Control of the pore-opening size of HY zeolite by CVD of silicon alkoxide." Microporous and Mesoporous Materials **32**(1-2): 37-44.

29. Kim, K.-J. and Ahn, H.-G. (2012). "The effect of pore structure of zeolite on the adsorption of VOCs and their desorption properties by microwave heating." Microporous and Mesoporous Materials **152**: 78-83.

30. Kumar, M. and Ando, Y. (2005). "Controlling the diameter distribution of carbon nanotubes grown from camphor on a zeolite support." Carbon **43**(3): 533-540.

31. Li, Y. and Chung, T. S. (2008). "Exploratory development of dual-layer carbon-zeolite nanocomposite hollow fiber membranes with high performance for oxygen enrichment and natural gas separation." Microporous and Mesoporous Materials **113**(1-3): 315-324.

32. Liang, Y., Zhang, H., Yi, B., Zhang, Z. and Tan, Z. (2005). "Preparation and characterization of multi-walled carbon nanotubes supported PtRu catalysts for proton exchange membrane fuel cells." Carbon **43**(15): 3144-3152.

33. Lu, D., Kondo, J. N., Domen, K., Begum, H. A. and Niwa, M. (2004). "Ultra-fine tuning of microporous opening size in zeolite by CVD." Journal of Physical Chemistry B **108**(7): 2295-2299.

34. Lu, L., Shao, Q., Huang, L. and Lu, X. (2007). "Simulation of adsorption and separation of ethanol–water mixture with zeolite and carbon nanotube." Fluid Phase Equilibria **261**(1–2): 191-198.

35. Luo, L., Ramirez, D., Rood, M. J., Grevillot, G., Hay, K. J. and Thurston, D. L. (2006). "Adsorption and electrothermal desorption of organic vapors using activated carbon adsorbents with novel morphologies." Carbon **44**(13): 2715-2723.

36. Miyake, M., Kimura, Y., Ohashi, T. and Matsuda, M. (2008). "Preparation of activated carbon-zeolite composite materials from coal fly ash." Microporous and Mesoporous Materials **112**(1-3): 170-177.

37. Moisala, A., Nasibulin, A. G. and Kauppinen, E. I. (2003). "The role of metal nanoparticles in the catalytic production of single-walled carbon nanotubes - A review." Journal of Physics Condensed Matter **15**(42): S3011-S3035.

38. Moteki, T., Murakami, Y., Noda, S., Maruyama, S. and Okubo, T. (2011). "Zeolite Surface As a Catalyst Support Material for Synthesis of Single-Walled Carbon Nanotubes." The Journal of Physical Chemistry C **115**(49): 24231-24237.

39. Nath, D. C. D. and Sahajwalla, V. (2011). "Application of fly ash as a catalyst for synthesis of carbon nanotube ribbons." Journal of Hazardous Materials **192**(2): 691-697.

40. Nath, D. C. D. and Sahajwalla, V. (2011). "Growth mechanism of carbon nanotubes produced by pyrolysis of a composite film of poly (vinyl alcohol) and fly ash." Applied Physics A: Materials Science and Processing **104**(2): 539-544.

41. Niknaddaf, S., Atkinson, J. D., Shariaty, P., Jahandar Lashaki, M., Hashisho, Z., Phillips, J. H., Anderson, J. E. and Nichols, M. (2016). "Heel formation during volatile organic compound desorption from activated carbon fiber cloth." Carbon **96**: 131-138.

42. Park, S., Kwon, Y. P., Kwon, H. C., Lee, J. H., Lee, H. W. and Lee, J. C. (2007). "Electrothermal properties of porous ceramic fiber media containing carbon materials." Journal of Nanoscience and Nanotechnology **7**(11): 3776-3779.

43. Park, S., Kwon, Y. P., Kwon, H. C., Lee, J. H., Lee, H. W. and Lee, J. C. (2009). "Electrothermal properties of regenerable carbon contained porous ceramic fiber media." Journal of Electroceramics **22**(1-3): 315-318.

44. Pełech, I., Narkiewicz, U., Kaczmarek, A. and Jędrzejewska, A. (2014). "Preparation and characterization of multi-walled carbon nanotubes grown on transition metal catalysts." Polish Journal of Chemical Technology **16**(1): 117-122.

45. Qi, J., Benipal, N., Chadderdon, D. J., Huo, J., Jiang, Y., Qiu, Y., Han, X., Hu, Y. H., Shanks, B. H. and Li, W. (2015). "Carbon nanotubes as catalysts for direct carbohydrazide fuel cells." Carbon **89**: 142-147.

46. Ramirez, D., Emamipour, H., Vidal, E. X., Rood, M. J. and Hay, K. J. (2011). "Capture and recovery of methyl ethyl ketone with electrothermal-swing adsorption systems." Journal of Environmental Engineering **137**(9): 826-832.

47. Ribeiro, R. P. P. L., Grande, C. A. and Rodrigues, A. E. (2014). "Electric Swing Adsorption for Gas Separation and Purification: A Review." Separation Science and Technology (Philadelphia) **49**(13): 1985-2002.

48. Russell, J. and Cohn, R. (2012). Joule Heating, Book on Demand.

49. Sano, N., Kodama, T. and Tamon, H. (2013). "Direct synthesis of carbon nanotubes on stainless steel electrode for enhanced catalyst efficiency in a glucose fuel cell." Carbon **55**: 365-368.

50. Sarno, M., Tamburrano, A., Arurault, L., Fontorbes, S., Pantani, R., Datas, L., Ciambelli, P. and Sarto, M. S. (2013). "Electrical conductivity of carbon nanotubes grown inside a mesoporous anodic aluminium oxide membrane." Carbon **55**: 10-22.

51. Shariaty, P., Jahandar Lashaki, M., Hashisho, Z., Sawada, J., Kuznicki, S. and Hutcheon, R. (2017). "Effect of ETS-10 ion exchange on its dielectric properties and adsorption/microwave regeneration." Separation and Purification Technology **179**: 420-427.

52. Singleton, J. (2001). Band Theory and Electronic Properties of Solids. New York, Oxford University Press.

53. Song, X. H., Teo, W. S. and Wang, K. (2012). "Synthesis and characterization of activated carbons prepared from benzene CVD on zeolite y." Journal of Porous Materials **19**(2): 211-215.

54. Subrenat, A., Baléo, J. N., Le Cloirec, P. and Blanc, P. E. (2001). "Electrical behaviour of activated carbon cloth heated by the joule effect: Desorption application." Carbon **39**(5): 707-716.

55. Sullivan, P. D., Rood, M. J., Dombrowski, K. D. and Hay, K. J. (2004). "Capture of organic vapors using adsorption and electrothermal regeneration." Journal of Environmental Engineering **130**(3): 258-267.

56. Sullivan, P. D., Rood, M. J., Hay, K. J. and Qi, S. (2001). "Adsorption and electrothermal desorption of hazardous organic vapors." Journal of Environmental Engineering **127**(3): 217-223.

57. Triantafyllidis, K. S., Karakoulia, S. A., Gournis, D., Delimitis, A., Nalbandian, L., Maccallini, E. and Rudolf, P. (2008). "Formation of carbon nanotubes on iron/cobalt oxides supported on zeolite-Y: Effect of zeolite textural properties and particle morphology." Microporous and Mesoporous Materials **110**(1): 128-140.

58. Uda, A., Morita, S. and Ozaki, Y. (2013). "Thermal degradation of a poly(vinyl alcohol) film studied by multivariate curve resolution analysis." Polymer (United Kingdom) **54**(8): 2130-2137.

59. Yang, H., Xu, S., Jiang, L. and Dan, Y. (2012). "Thermal decomposition behavior of poly (vinyl alcohol) with different hydroxyl content." Journal of Macromolecular Science, Part B: Physics **51**(3): 464-480.

60. Zanetti, J. E. and Egloff, G. (1917). "The Thermal Decomposition of Benzene." Journal of Industrial & Engineering Chemistry **9**(4): 350-356.

61. Zhang, L., Zhao, B., Wang, X., Liang, Y., Qiu, H., Zheng, G. and Yang, J. (2014). "Gas transport in vertically-aligned carbon nanotube/parylene composite membranes." Carbon **66**: 11-17.

Chapter 5. CARBON NANOTUBE ADDITION AS AN EFFECTIVE METHOD TO TAILOR THE ELECTRIC CONDUCTIVITY OF DEALUMINATED ZEOLITE Y FOR RESISTIVE HEATING REGENERATION

5.1. Chapter Overview

The previous chapter demonstrated the addition of CNT through CH_4 decomposition on cobalt impregnated dealuminated zeolite Y at 600^{o}C as a method to reduce its electrical resistivity so that it can be heated by resistive heating. However, due to the relatively high temperature and the change in adsorption properties of zeolite, the method need to be further optimized. In this chapter, CNT deposition was optimized aiming for achieving low resistivity of zeolite Y for regeneration with resistive heating as well as lower modification temperature, shorter time for CNT deposition, and smaller change to the adsorption properties.

5.2. Introduction

Temperature swing regeneration (TSR) and pressure swing regeneration (PSR) are widely used for regenerating and recovering the adsorption capacity of adsorbents. The conventional TSR and PSR techniques (such as steam, hot gas, conductive heating, and vacuum regeneration), however, have high energy consumption, are slow, and/or can alter the physical/chemical properties of the adsorbents and adsorbates (Al-Baghli and Loughlin 2005, Ania et al. 2005, Cherbański and Molga 2009, Cherbański et al. 2011, Chowdhury et al. 2012, Fayaz et al. 2015, Niknaddaf et al. 2016, Kamravaei et al. 2017).

Resistive heating is an adsorbent regeneration technique whereby electric current is passed through a material with sufficiently low resistivity and heat is generated by the Joule effect (Russell and Cohn 2012). This allows for rapid adsorbent regeneration that is decoupled from the purge gas flow. Compared to conventional TSR and PSR methods, resistive heating regeneration is faster, can have higher desorption efficiency, and requires less energy to achieve a desired desorption efficiency (Sullivan et al. 2001, 2004). The feasibility and performance of resistive heating, however, are highly dependent on the electrical resistivity of the adsorbent (Subrenat et al. 2001, Luo et al. 2006, Park et al. 2007, 2009, Ribeiro et al. 2014).

Resistive heating has been extensively tested for regeneration of carbonaceous adsorbents (resistivity of 0.2-0.8 Ω.m) (Subrenat et al. 2001, Luo et al. 2006, Hashisho et al. 2008, Johnsen et al. 2011, Ramirez et al. 2011, Johnsen and Rood 2012, Johnsen et al. 2014). Most inorganic adsorbents, including zeolites (resistivity of $>10^7$ Ω.m), however, have low electric conductivity (Álvaro et al. 2006) and cannot be heated resistively. Our previous work showed that addition of carbon nanotube (CNT) at 600ºC to the zeolite reduces its electrical resistivity, while maintaining 70% of the zeolite adsorption properties (Shariaty et al. 2017). While it was proven that this technique resulted in 8 orders of magnitude change in the electrical resistivity of zeolite, around 30% reduction in adsorption properties was obtained. Since the size and population of deposited CNT are important factors affecting both resistivity and adsorption properties of the zeolite sample, its deposition condition should be studied aiming for optimum condition and reducing the CNT deposition effect on zeolite adsorption properties.

The CNT deposition in this work is expected to follow the “root” growth mechanism, where the metal catalysts deposited on the zeolite are pinned at the zeolite surface. The process led to catalytic decomposition of methane into carbon atoms, and the released carbon atoms diffuse into

the metal catalyst particles. CNTs are then grown from the metal particles. In theory, cobalt particles are located inside the CNTs, generally at one their end, therefore, the nanotube inner diameter is equal to the dimension of these particles. Additionally, the released carbon atoms depend on the methane conversion rate at the used thermal condition. Consequently, both cobalt catalyst impregnation and formation/diffusion of carbon atoms are important factors affecting the deposited CNTs (Anna et al. 2003).

Previous studies on CNT deposition showed the importance of deposition temperature and time during the process affecting its size, form, and population (Anna et al. 2003, Moisala et al. 2003, Liang et al. 2005, Janas and Koziol 2014, Pełech et al. 2014). Sengupta and Jacob (2009) showed that an increase in the CNT growth temperature resulted in increased CNT diameter due to agglomeration of the metal catalysts at higher temperatures. The thermal condition during hydrogen treatment of metal catalyst is also an important factor affecting the form of deposited CNT due to the degree of oxide removal from the catalyst surface (Takagi et al. 2007). Additionally, decomposition of carbon precursor and solubility of carbon in the metal catalyst particle are temperature-dependent properties affecting the population of deposited CNT on the substrate (Anna et al. 2003). The CNT growth temperature was also mentioned to be a key factor in defining its form (single- vs. multi-walled) (Resasco et al. 2002).

The objective of this work, therefore, is to investigate CNT growth condition on the properties of dealuminated zeolite Y to find the optimum condition to improve its electrical conductivity without compromising its adsorption properties. CNT was deposited on zeolite through methane chemical vapor decomposition (CVD) on cobalt catalyst impregnated sample. Specifically, the CNT growth process was divided into three different steps (calcination, metal catalyst formation,

and methane decomposition), and the effects of temperature and duration variation in each step on the adsorption and desorption properties of the zeolite were studied.

5.3. Experimental setup and Method

5.3.1. Sample Preparation

Dealuminated zeolite Y (CBV-901, Zeolyst, average particle size of 7 μm) was the base material for this study (ZY used as abbreviation for the original zeolite). The method used for CNT deposition is developed based on the previously reported methods summarized as below (Resasco et al. 2002, Anna et al. 2003):

4 g $Co(NO_3)_2.6H_2O$ (≥ 98%, Sigma-Aldrich) was dissolved in 100 ml deionized water, and 4 g CBV-901 was added to the solution. The solution was sonicated for 1 h and then dried in an oven at 90 ºC overnight. 0.5g of collected powder was then added to a tubular boat without edge (to enhance the gas/solid contact) and placed in a tube furnace. The thermal condition applied for CNT deposition consists of: increasing the temperature at 20 ^oC/min in 0.5 standard (25^oC and 1 atm) liter per minute (SLPM) N_2 (99.998%, Praxair) to reach the target temperature, calcination in 0.5 SLPM air to remove the remaining NO3-1, metal catalyst formation in 0.5 SLPM of 10% H2 (99.999%, Praxair) in N_2, and CH_4 (99.99%, Praxair) decomposition in 0.5 SLPM CH_4. Calcination, catalyst formation, and CH_4 decomposition were performed at different temperatures and durations, as described in Table 5-1, to find out the optimum condition. The change in thermal condition for each step was varied one at a time and the lowest possible temperature and duration were used for the following steps.

Table 5-1.Different thermal conditions applied for CNT growth (shaded area for a sample indicates the parameter changed compared to the previous sample)

Sample ID	Calcination		Cobalt Catalyst Formation		CH_4 Thermal Decomposition	
	Duration (min)	Temperature (^oC)	Duration (min)	Temperature (^oC)	Duration (min)	Temperature (^oC)
ZY-605-305-605	60	500	30	500	60	500
ZY-604-305-605	60	400	30	500	60	500
ZY-603-305-605	60	300	30	500	60	500
ZY-303-305-605	30	300	30	500	60	500
ZY-153-305-605	15	300	30	500	60	500
ZY-153-304-605	15	300	30	400	60	500
ZY-153-303-605	15	300	30	300	60	500
ZY-153-153-605	15	300	15	300	60	500
ZY-153-153-604	15	300	15	300	60	400
ZY-153-153-603	15	300	15	300	60	300
ZY-153-153-304	15	300	15	300	30	400

*Sample ID represents time and temperature applied for each step as:

ZY-(time(T/100))$_{\text{calcination}}$-(time(T/100))$_{\text{Cobalt catalyst formation}}$-(time(T/100))$_{\text{CH4 thermal decomposition}}$

5.3.2. Material Characterization

***Bulk Elemental Analysis**:* Added carbon was measured using Organic Elemental Analysis (OEA) (Flash 2000, Thermo Fisher Scientific Inc.) with furnace and gas chromatograph column

temperatures of 950 and 65 ^{0}C, respectively. He (carrier gas), He (reference), and O_2 flow rates were 140, 250, and 100 ml/min, respectively. A 5 sec oxygen dose was used and the run time was 12 min.

Scanning Electron Microscopy (SEM)*:* Field emission SEM was completed using a JAMP-9500F Auger microprobe (JEOL). The accelerating voltage, emission current, working distance, and sample rotation were 15 kV, 8 nA, 24 mm, and 30^o, respectively. A M5 lens with 0.6% energy resolution was used for Auger spectroscopy and imaging.

Raman Spectroscopy*:* All Raman spectra were acquired at room temperature using a Nicolet Almega XR micro-Raman Analysis System. Laser wavelength has been set to 532 nm (2.33 eV). Maximum power has been set to 24 mW, 100% of which has been used for this spectroscopic study. All Raman spectra were collected by fine-focusing a 50 × microscope objective and five 10 seconds exposure.

X-Ray Diffraction (XRD)*:* Powder XRD patterns were acquired with a Rigaku Ultima IV unit equipped with a D/Tex detector and Fe filter. Results were obtained using a cobalt tube (38 kV, 38 mA) with average Kα wavelength of 1.790260 Å. Samples were run from 5 to 90° on a continuous scan using a top-pack mount at 2° 2θ/min and step size of 0.02°.

Resistivity Measurements and Resistive Heating: Samples (no binder) were pressed at 5 kPSI to form discs. Conductivity of prepared discs was measured by inserting them between two stainless steel electrodes (adjusting the pressure applied to the sample from the electrode at 10 PSI using torque meter) connected to a digital multimeter (Agilent Technologies) (Figure 5-1). During resistivity measurement, the samples were placed in a quartz enclosure which purged with 0.5 SLPM N_2. Resistive heating of the modified samples was performed using the same setup after

replacing the digital multimeter with a power source. During resistive heating the temperature of the sample was measured using a Type K thermocouple (Omega).

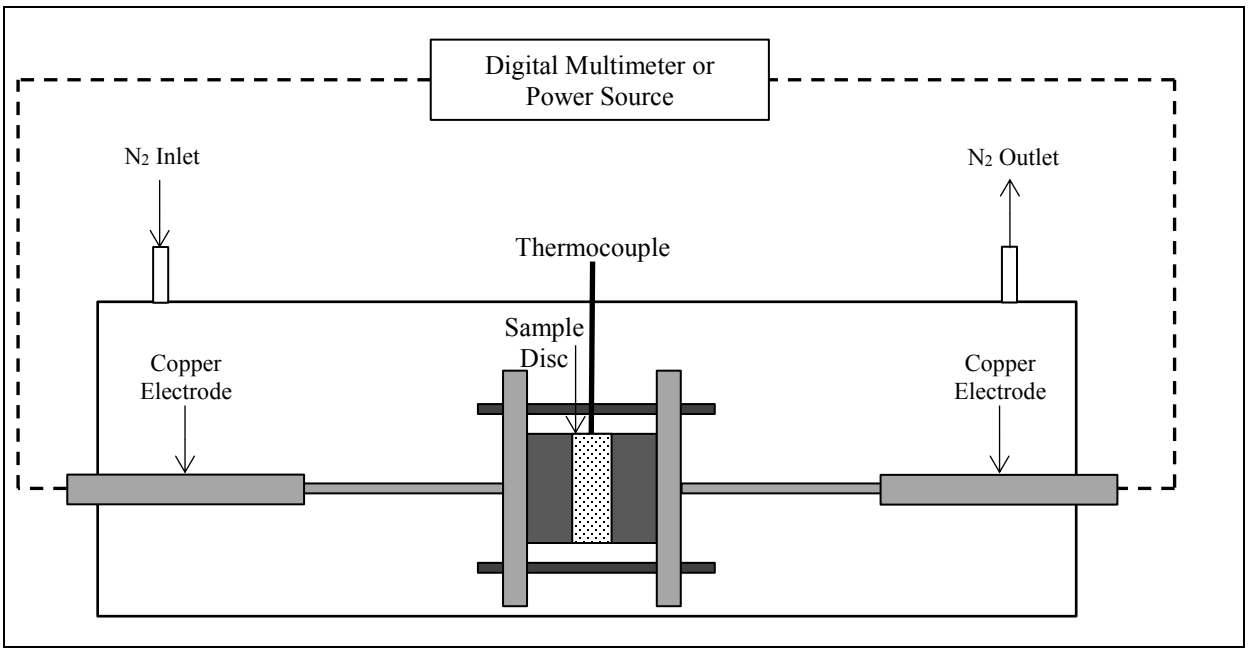

Figure 5-1. Schematic of setup for resistivity measurements and resistive heating

N_2 Adsorption*:* Micropore surface analysis (IQ2MP, Quantachrome) with N_2 (relative pressures from 10−7 to 0.995) at 77 K was used to characterize physical properties of prepared materials. 60 – 70 mg of sample was degassed at 120 °C for 5 h to remove moisture before analysis.

Methyl Ethyl Ketone (MEK) Adsorption Isotherm: Adsorption isotherms of MEK (99.9%, Fisher Chemicals) were obtained gravimetrically using a sorption analyzer (TA Instruments, model VTI-SA) at 25 °C with N_2 carrier gas and varying concentrations of toluene (99.9%, Fisher Chemicals). The system logged the equilibrium weight of the sample (5–7 mg) in response to a step change in the concentration of the adsorbate (relative pressure range of 0.01–0.9). Equilibrium was assumed when the weight changed by < 0.001 wt% in 5 min.

5.4. Result and Discussion

5.4.1. Calcination

Different calcination conditions (calcination temperature 300-500^{o}C and calcination duration 15-60 min) resulted in different CNT deposition on the zeolite surface. Figure 5-2 shows the SEM pictures of the samples. It can be seen that a decrease in calcination temperature resulted in a decrease in population of deposited CNT. Similar trend can be noticed by decreasing the calcination temperature.

During calcination, purging the sample with ultra-pure air would oxidize the deposited salt on the surface of the zeolite resulting in production of cobalt oxide on the zeolite surface and removal of other impurities (specifically in our case NO_3^- remained from the initial solution). Cobalt oxides are then reduced in cobalt catalyst particles by purging the sample with the reducing agent (H_2/N_2 mixture). Lower number of produced cobalt oxides in the calcination procedure, therefore, would result in formation of fewer cobalt catalyst particles and as a result less deposited CNTs on the surface of zeolite. The obtained results show that by decreasing the calcination time and temperature, the oxidation reaction of the cobalt could not get completed, which led to a reduction in the number of deposited CNTs on the zeolite surface.

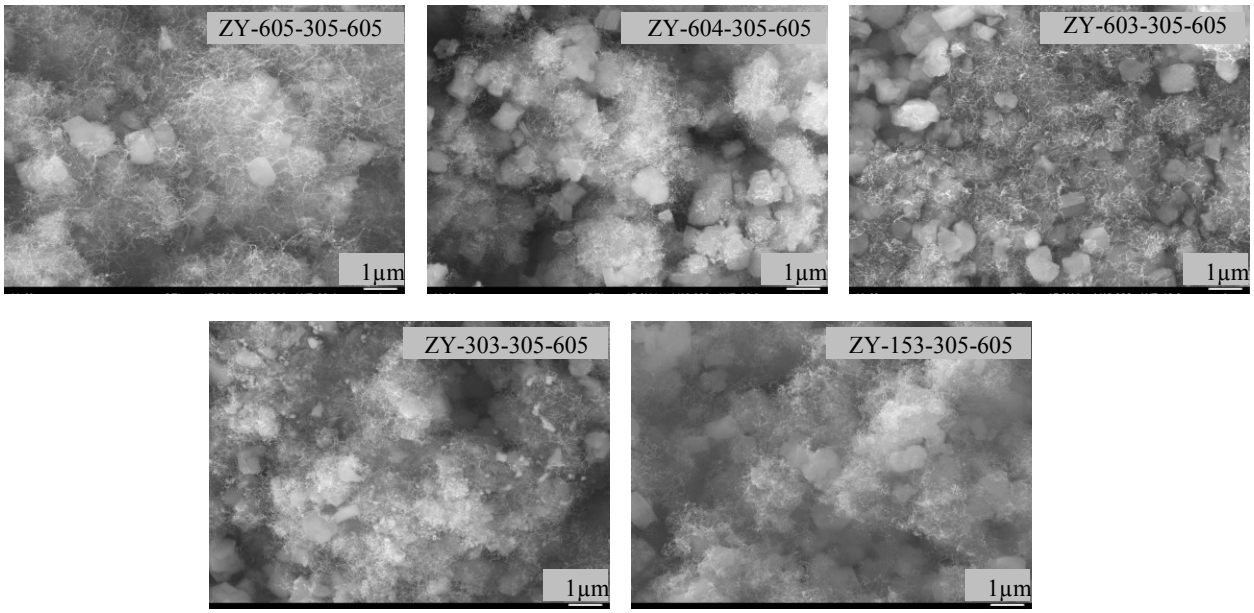

Figure 5-2. SEM pictures obtained for CNT deposition using different calcination conditions

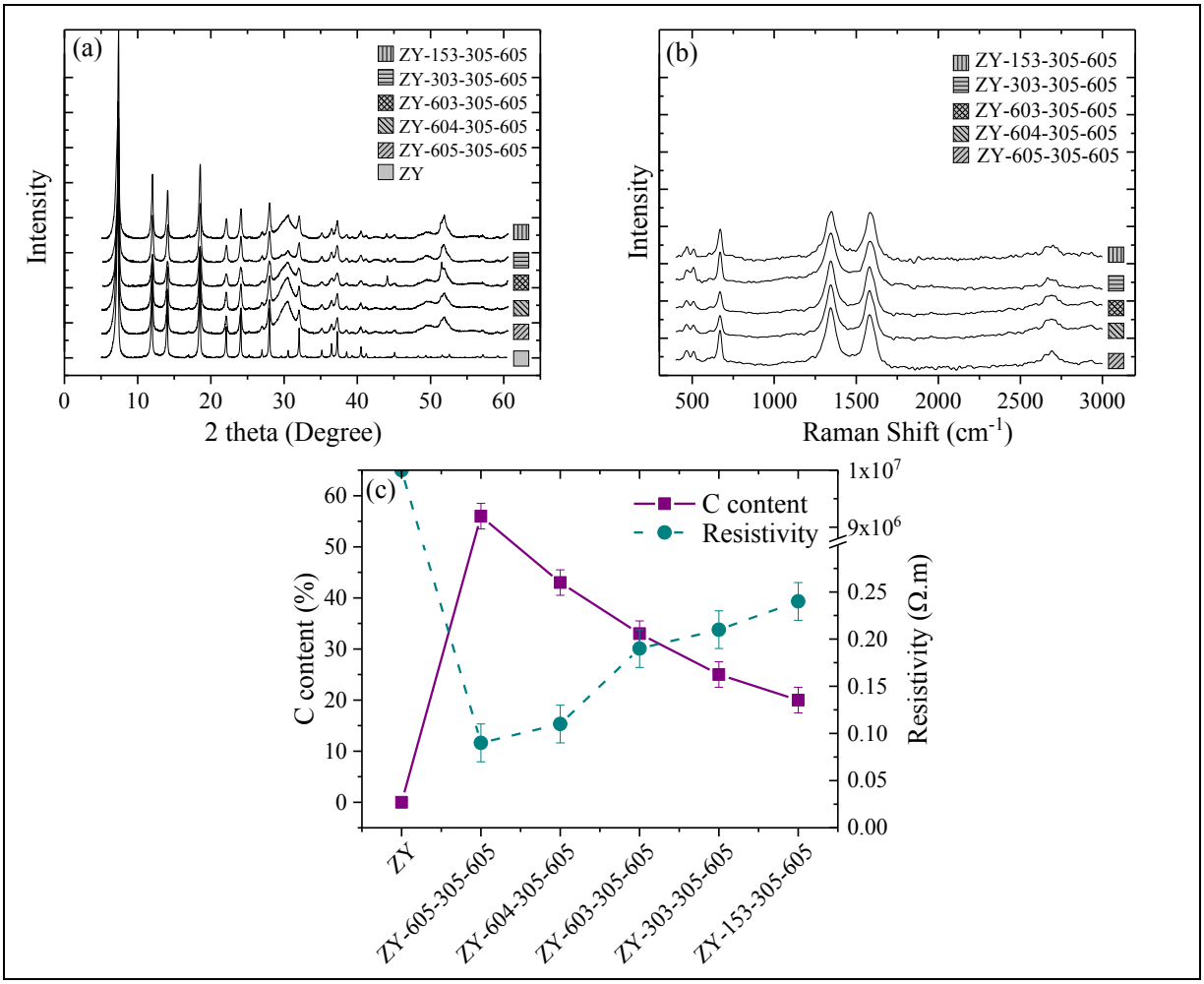

Figure 5-3. (a) XRD pattern, (b) Raman spectra, and (c) carbon content and resistivity obtained for CNT deposition using different calcination conditions

.a also shows the XRD profiles after changing the calcination thermal condition. It can be seen that after CNT deposition procedure, there are two additional peaks introduced to the original XRD pattern. The additional peaks correspond to the cobalt oxide (~30 degree) and CNT (~50 degree) (Pełech et al. 2014). As illustrated in

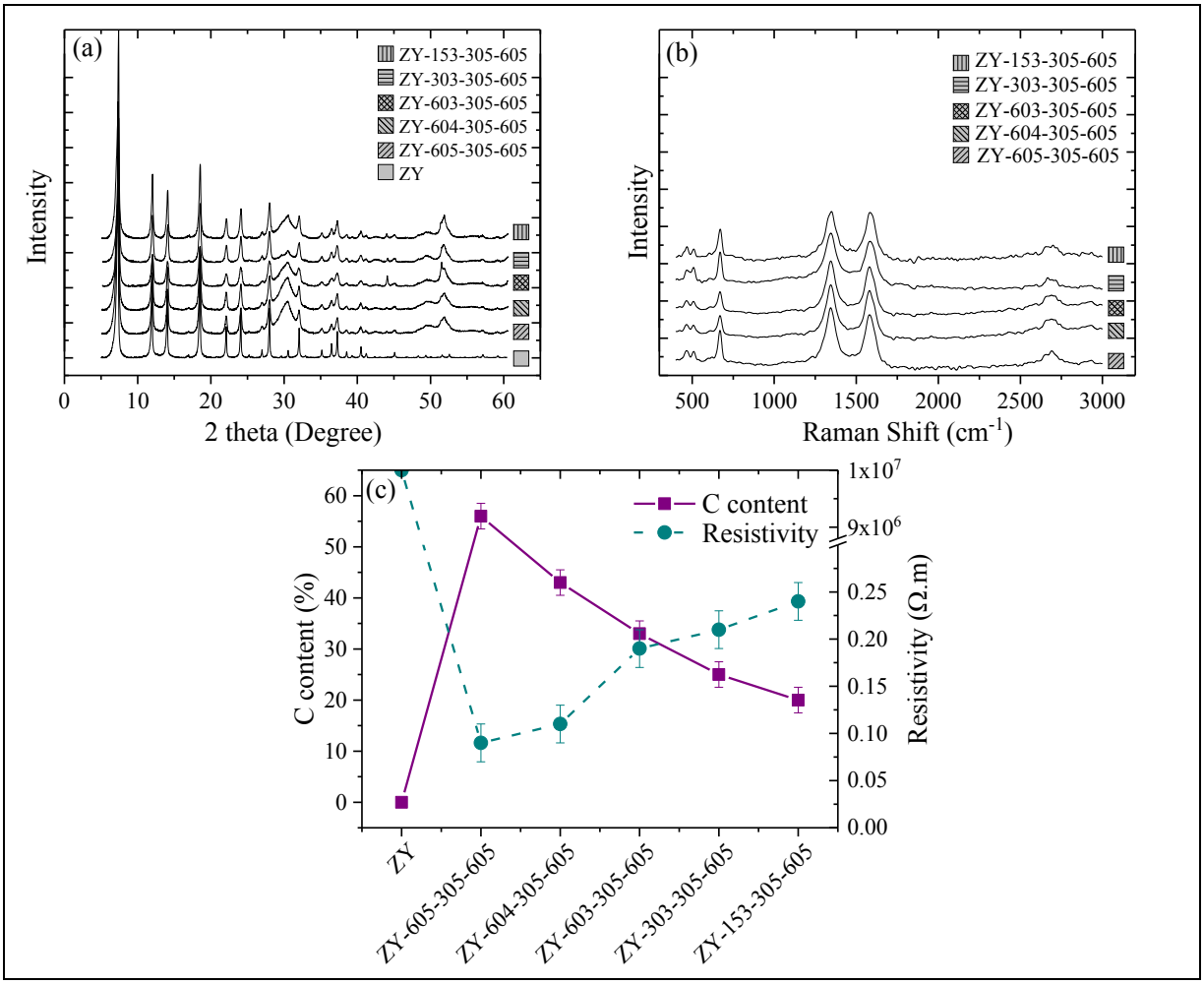

Figure 5-3. (a) XRD pattern, (b) Raman spectra, and (c) carbon content and resistivity obtained for CNT deposition using different calcination conditions

.a, by decreasing the calcination temperature and duration, there is a decrease in the intensity of the peak corresponding to the cobalt oxide, confirming the incomplete oxidation of cobalt on the zeolite.

The Raman spectroscopies of the samples were also obtained (Figure 5-3.b), which further confirms the formation of CNT for all samples. Four bands are observed for modified zeolites, and the presence of D (1343 cm^{-1}), G (1573 cm^{-1}), and G' (2671 cm^{-1}) bands confirm the nanotube

structure of deposited carbon, consistent with SEM observations (Triantafyllidis et al. 2008). The additional band at 673 cm^{-1} represents the zeolite framework (Moteki et al. 2011). The results suggest that changing the calcination condition did not change the form of deposited carbon.

The carbon content and electrical resistivity of the samples were obtained as demonstrated in Figure 5-3c. The carbon content confirms that by reducing the number of cobalt oxides on the zeolite surface (as a result of decreasing the calcination temperature and duration), a decreasing trend in the amount of deposited CNT can be observed. The resistivity results, however, showed that even by decreasing the CNT content of the samples from 56 to 20 wt%, 7 orders of magnitude reduction in resistivity of the zeolite was still achieved for all samples.

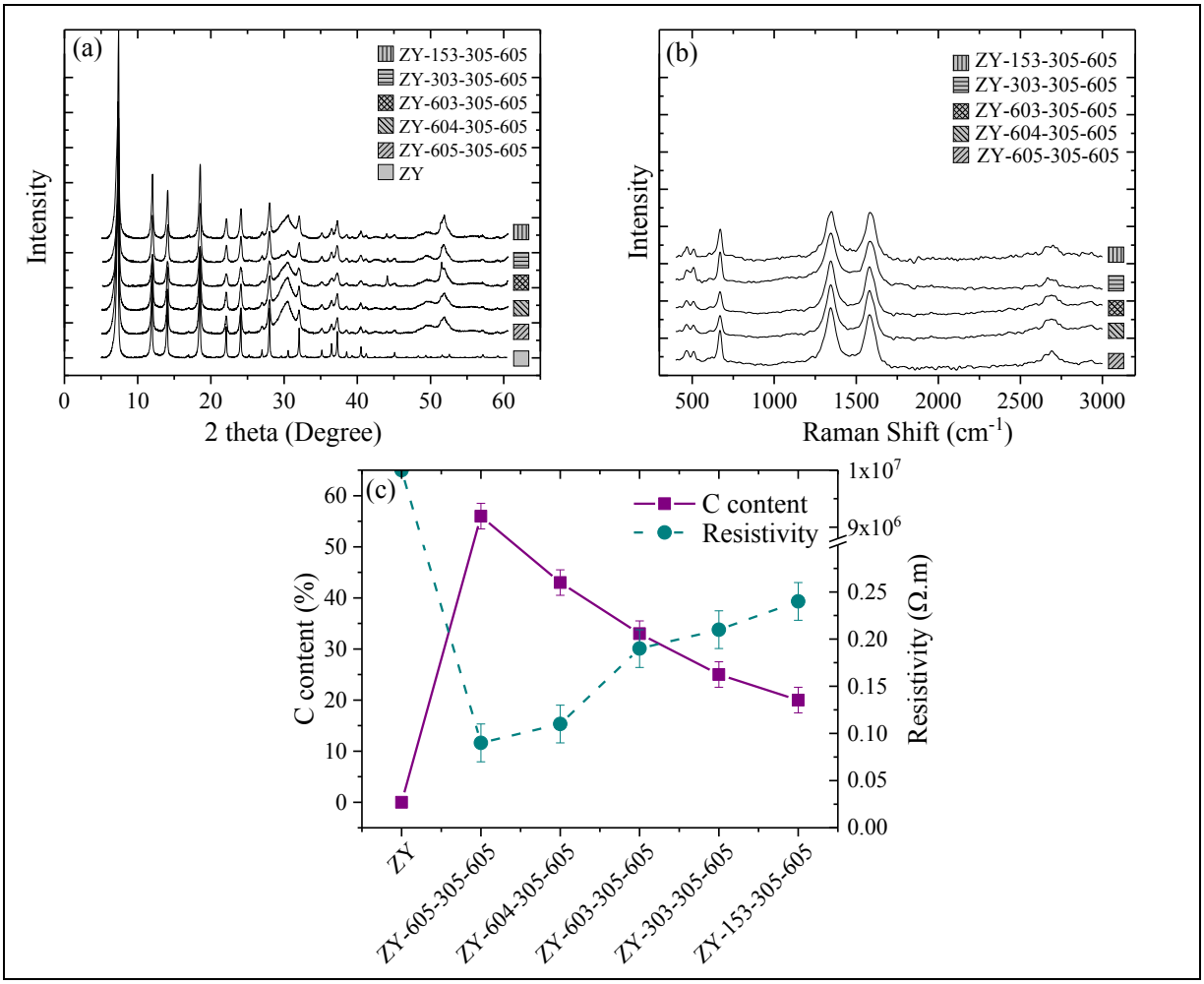

Figure 5-3. (a) XRD pattern, (b) Raman spectra, and (c) carbon content and resistivity obtained for CNT deposition using different calcination conditions

In summary, the reduction in calcination temperature and duration resulted in reduced number of produced cobalt oxide, which consequently reduced the CNT content of the zeolite. This reduction, however, still kept the resistivity of zeolite within the suitable range for resistive heating (typically, ~1 Ω.m (Liang et. al. 2005)).

5.4.2. Cobalt Catalyst Formation

During this step, the metallic cobalt is generated by reducing the cobalt oxide using H_2 as a reducing agent. The conditions applied during this step affect the size of the formed metallic cobalt on the zeolite, which ultimately influence the deposited CNTs diameter.

Figure 5-4 shows a reduction in CNT diameter after reducing the temperature during this step, which is in agreement with the literature (Sengupta and Jacob 2009). As previously reported by Sengupta and Jacob (2009), this could be due to larger diameter of formed metal catalysts at higher temperature as a result of metal particles agglomeration. The temperature effect was more significant when reducing the temperature from 500 to 400 ^{o}C, while more reduction could not notably change the CNTs diameter. Decreasing the reduction reaction time, however, led to minor change in the CNT diameter size. This means that 15 minutes is suitable enough for completion of reduction reaction and formation of cobalt metal particles.

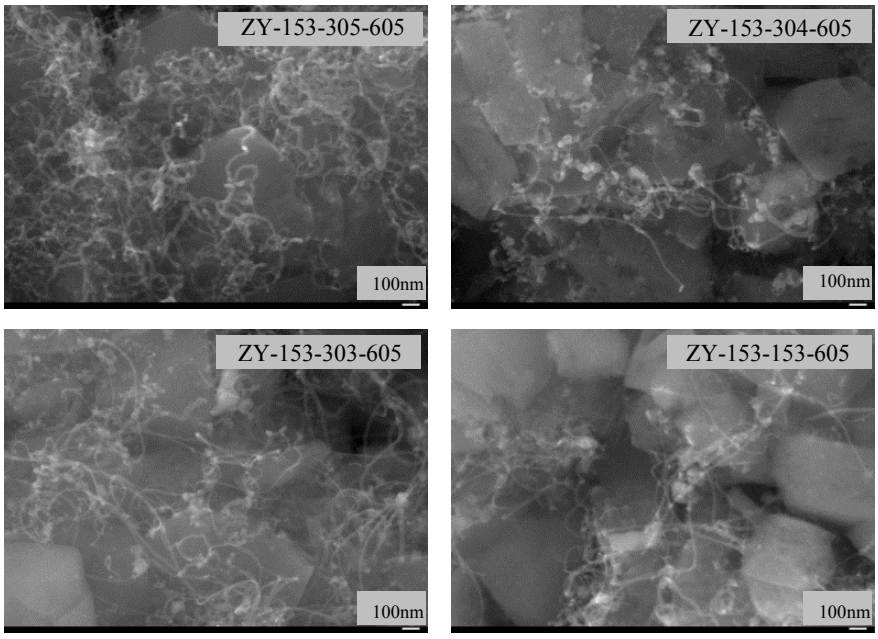

Figure 5-4. SEM pictures obtained for CNT deposition using different cobalt catalyst formation conditions

Additionally, XRD and Raman spectroscopy results show that the change in the cobalt catalyst formation condition would reduce the intensities of the peaks corresponding to the CNT. This is more obvious in Figure 5-5.b, where the intensities of D and G gaps got close to the intensity of zeolite crystal peak (673 cm^{-1}), while they had larger intensities before decreasing the temperature and duration of the reduction reaction (

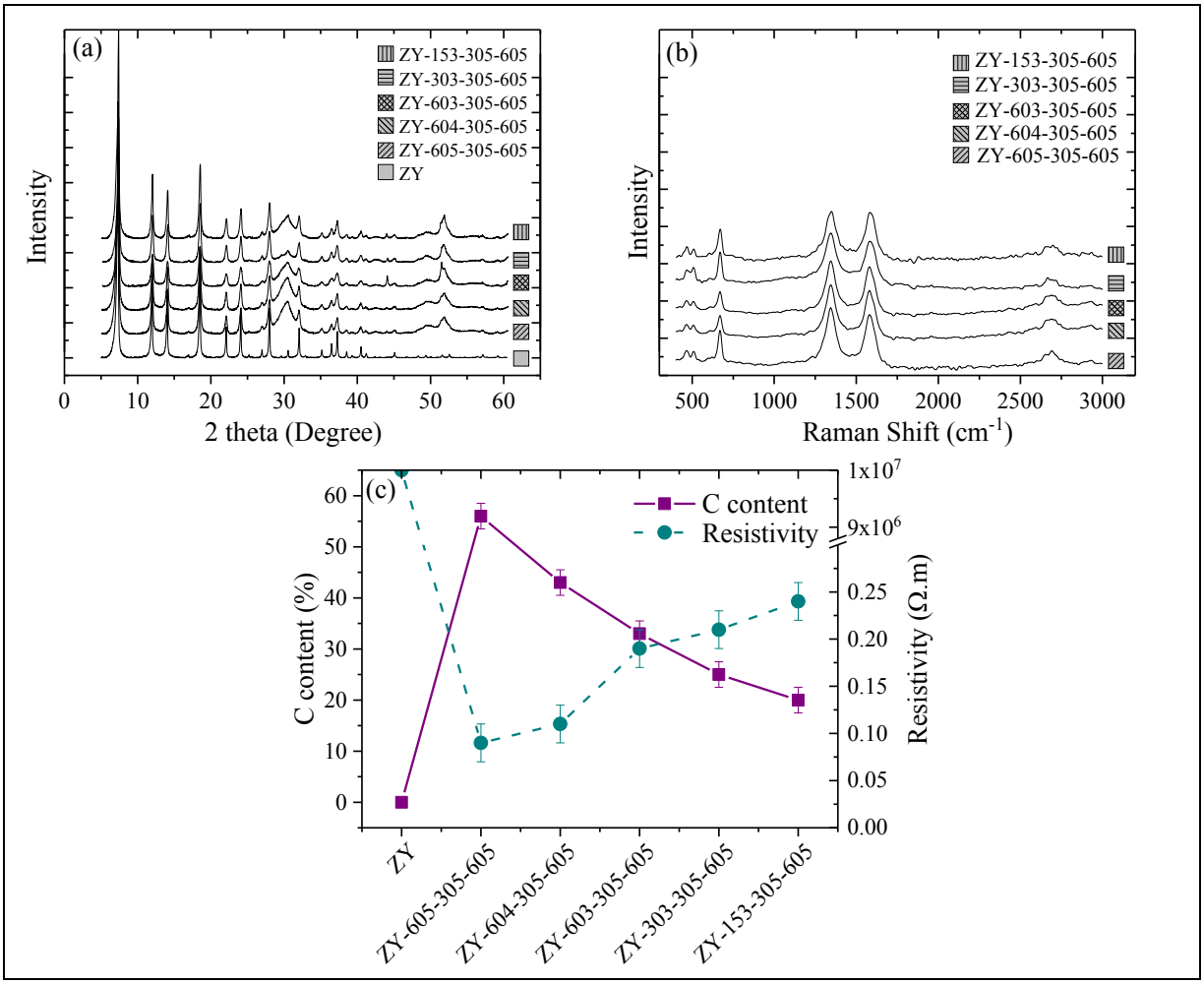

Figure 5-3. (a) XRD pattern, (b) Raman spectra, and (c) carbon content and resistivity obtained for CNT deposition using different calcination conditions

.b). This is in agreement with the reduction in carbon content of the zeolite after CNT deposition. Figure 5-5.c also confirms that the reduction in temperature affected the CNT deposition more than changing the duration, where a notable reduction in carbon content were found after reducing the temperature from 500 to 400ºC. Similar carbon contents, however, were observed for other samples by further changing the cobalt catalyst formation condition.

Furthermore, although reducing the carbon content resulted in ~6 times larger resistivity for the zeolite, however, the resistivity is still in a range that is suitable for resistive heating application.

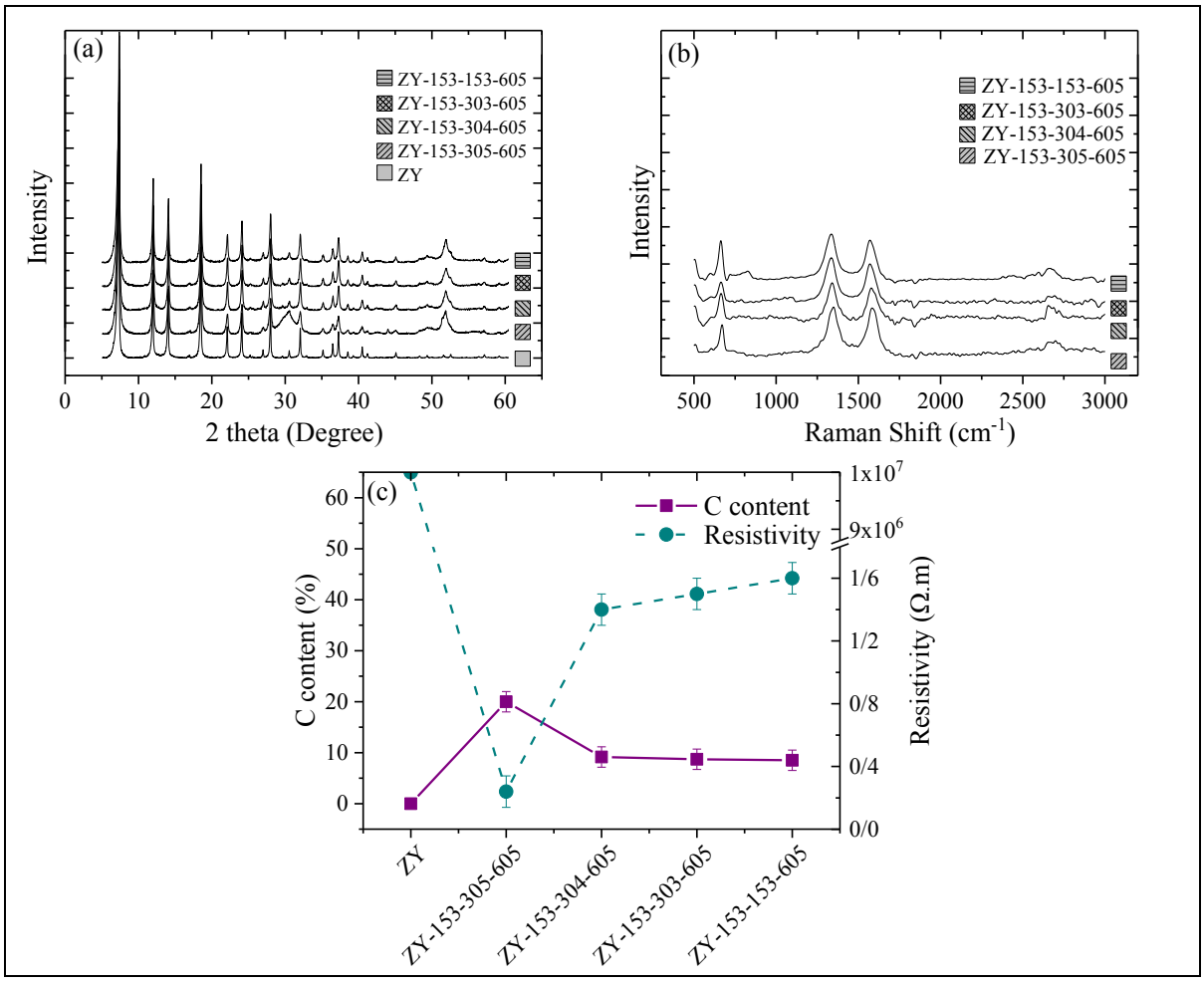

Figure 5-5. (a) XRD pattern, (b) Raman spectra, and (c) carbon content and resistivity obtained for CNT deposition using different cobalt catalyst formation conditions

In summary, decreasing the temperature of cobalt oxide reduction resulted in formation of smaller cobalt catalyst particles. These smaller particles would result in deposition of CNT with smaller diameter, and consequently lower carbon content of the final product. However, further decrease in the temperature from 400 to 300°C led to similar products indicating that the change in the catalyst size within this temperature range is minimal, the temperature between 400 and 500

^{o}C is a breakthrough point that could provide enough energy for catalyst reduction reaction, which significantly increases the metal catalyst diameter.

5.4.3. CH_4 Thermal Decomposition

The final step for deposition of CNT on zeolite is catalytic decomposition of CH_4 on the zeolite. As previously mentioned, methane decomposes to carbon atoms and the carbon atoms dissolve into the cobalt catalyst resulting in CNT growth on top of the cobalt catalyst. (Anna et al. 2003) As expected, any change in decomposition temperature could result in a change of methane conversion rate to carbon. Furthermore, lower temperature reduces the solubility of the carbon atoms into the metal catalysts.(Anna et al. 2003) The cumulative effect of decreasing the conversion rate and carbon atoms solubility, therefore, led to a reduction in the length of CNT deposited on zeolite surface. This can be clearly seen in Figure 5-6, where a significant reduction in CNT length was observed by changing the temperature from 500 to 400^{o}C. Further decrease in temperature to 300 ^{o}C resulted in no conversion of methane as it can be seen for CNT-3/2 sample. Additionally, by reducing the duration of methane decomposition, it was observed that the available cobalt catalysts got saturated even within 15 minutes. So, no significant change in the amount of deposited CNT has been observed in this case.

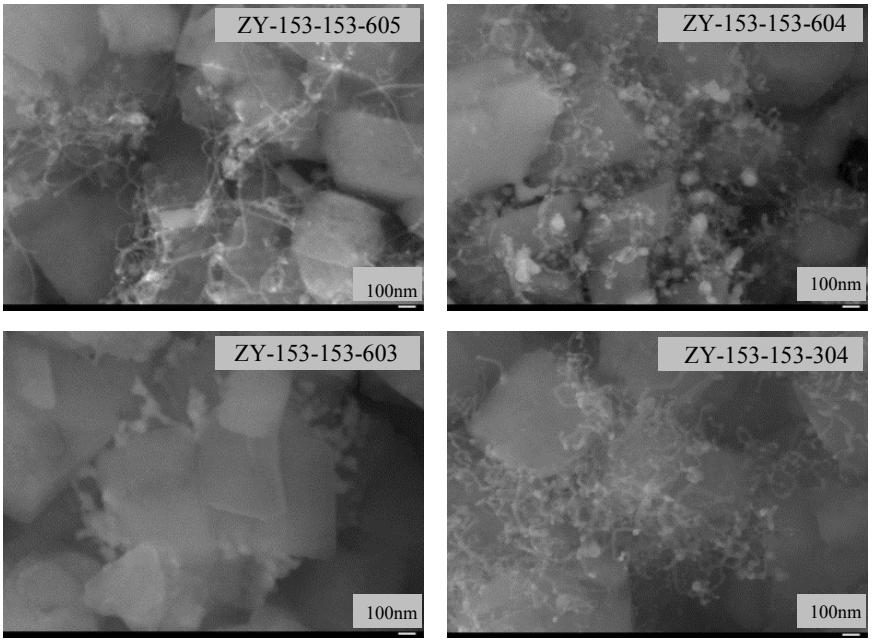

Figure 5-6. SEM pictures obtained for CNT deposition using different methane thermal decomposition conditions

The reduction in the CNT length by decreasing the methane decomposition temperature was also confirmed with results of XRD and Raman spectroscopy results (Figure 5-7. a and b). Specifically, all XRD patterns after reducing the decomposition temperature are matching the original zeolite XRD with additional three weak peaks around 50 and 40 degree. Looking at the XRD pattern for CNT-3/2 sample, that has almost no CNT, two peaks between 40 degree and 50 degree can still be observed. These peaks represent the unsaturated cobalt catalysts on the surface of zeolite. These peaks are still visible in other samples after reducing the decomposition temperature; however, they are weaker than CNT peak (after 50 degree). This implies that the reduction in produced carbon atoms would result in excess cobalt catalysts on the zeolite, which remain unsaturated after the CNT deposition process.

Furthermore, the resistivity results were in agreement with XRD and Raman spectroscopy results, showing small increase (while still within the resistive heating range) in resistivity with the decrease in carbon content at lower decomposition temperature.

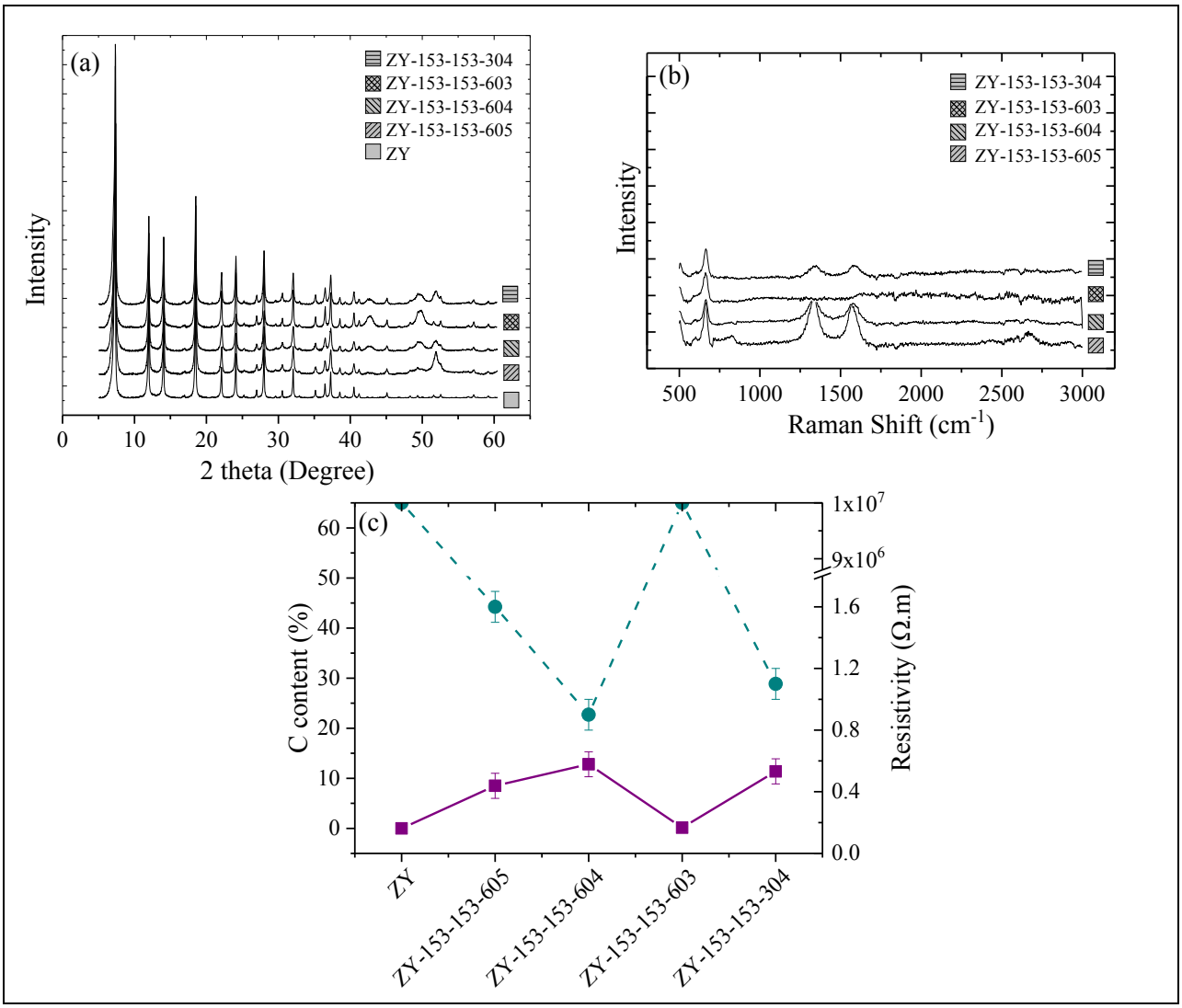

Figure 5-7. (a) XRD pattern, (b) Raman spectra, and (c) carbon content and resistivity obtained for CNT deposition using different methane thermal decomposition conditions

In summary, the results showed that by decreasing the CNT deposition temperature and duration, still a significant reduction in resistivity of zeolite could be obtained while minimizing the change in the crystalline structure of the zeolite. Therefore, the conditions used for preparation

of CNT-3/3 sample can be selected as the optimum condition. The range of temperature used for CNT deposition in this case was within the typical TSR range, which avoid any additional damage to the zeolite structure due to the modification.

Since this sample had minimal effect on crystalline properties of the zeolite, additional investigation was completed to check the influence of the optimized CNT deposition condition on the zeolite adsorption properties. Figure 5-8 shows the nitrogen and MEK isotherms for both CNT-3/3 and original zeolite without modification. Because the kinetic diameter of MEK is 5.25 Å (Monneyron et al. 2003), close to the zeolite Y pore size (7.4 Å (Kim and Ahn 2012)), its adsorption is a good indicator for the zeolite's available pores and presence of any pore restriction due to carbon nanotube addition. Obtained adsorption capacities of zeolite for both N_2 and MEK after CNT addition were on average 8.5% less than the original zeolite (before CNT addition). Since the calculated adsorption capacities are based on the gram samples, and considering that CNT-3/3 obtained 9wt% CNT, by normalization of the adsorption capacities to gram original zeolite used for modification similar values could be obtained for zeolite before and after CNT deposition. Additionally, the contribution of the deposited CNT towards adsorption is expected to be negligible due to its size and its closed-end (i.e. adsorption due to "sieving effect" (Lu et al. 2007) through CNT walls is less probable). This is an important finding shows that by addition of CNT to the zeolite, using the optimized condition, there is almost no change in its adsorption properties, while its resistivity decreased to the value (from $>10^7$ to 1.1 Ω.m) suitable for resistive heating applications.

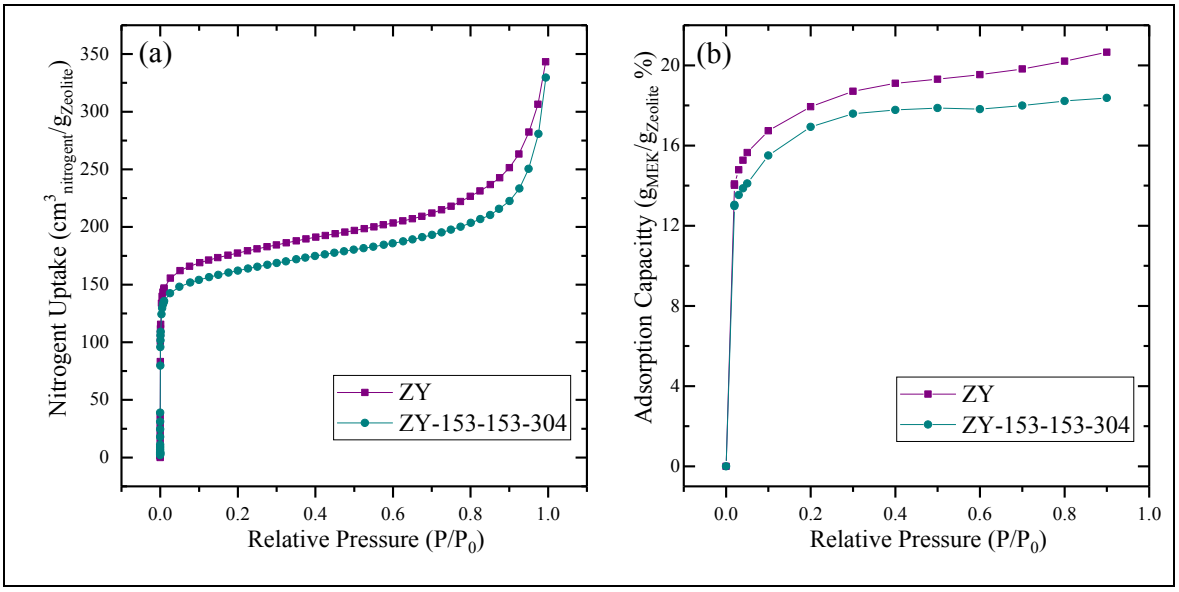

Figure 5-8. Adsorption properties of zeolite before and after CNT deposition, (a) nitrogen adsorption isotherm and (b) MEK adsorption isotherm

Finally, to prove that the current sample can be heated resistively, it was heated using this technique and compared to the original zeolite samples (Figure 5-9). While temperature of the original sample cannot be increased even by 1°C, the modified sample can be heated resistively and its temperature can be controlled. The possibility of controlling the temperature is of interest since constant-temperature is mainly used for thermal regeneration of the adsorbents. The temperature profile was merely presented to show the possibility of resistive heating of the adsorbent using the proposed condition for modification, which opens up a new venue for regeneration of inorganic adsorbents using resistive heating technique. Further studies, however, should be done to compare the efficiency of this technique with conventional regeneration methods for different applications.

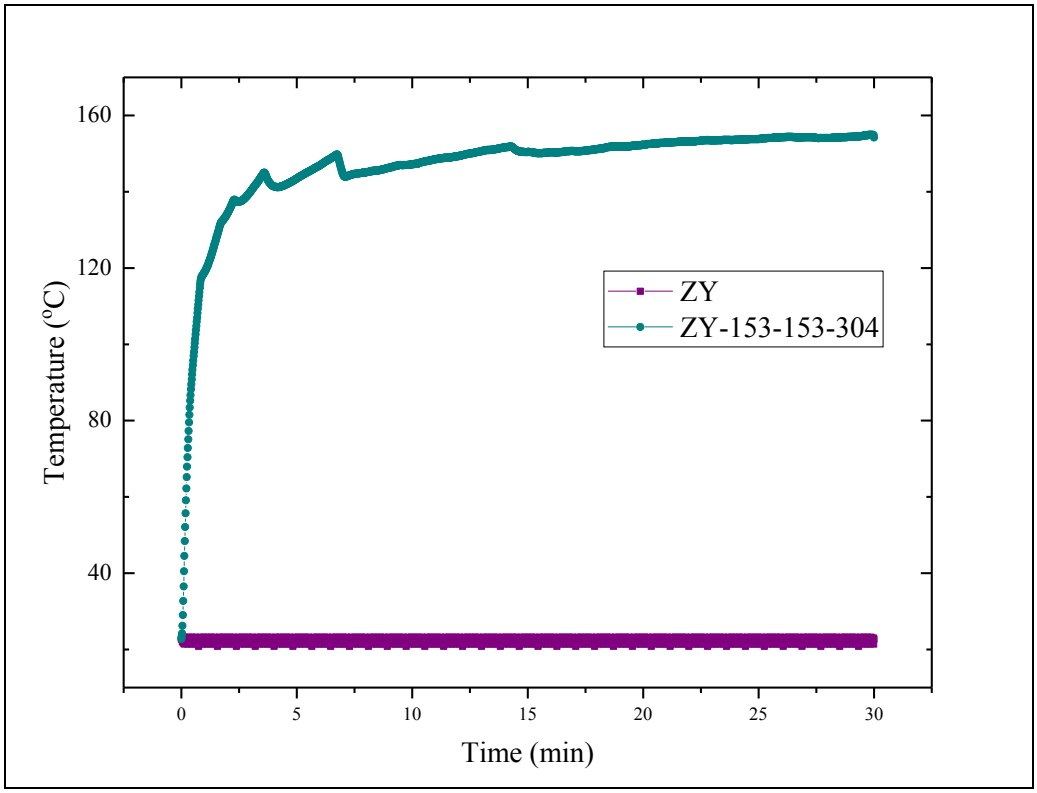

Figure 5-9. Temperature profile during resistive heating of zeolite before and after CNT deposition at constant temperature.

5.5. Conclusion

Different thermal conditions have been tested for CNT growth on the surface of zeolites, as a technique to reduce its electrical resistivity. Specifically, temperature and duration of three main steps in CNT thermal deposition have been studied. It was found this change in calcination, cobalt catalyst formation, and CH_4 thermal decomposition influenced the CNT population, diameter, and length, respectively. Based on the obtained results, the optimized thermal condition for CNT deposition was found as 300°C for 15 minutes (calcination), 300°C for 15 minutes (cobalt catalyst formation), and 400°C for 30 minutes (CH_4 thermal decomposition). This condition led to more than 6 orders of magnitude reduction in zeolite resistivity with minor in its adsorption properties. The obtained thermal condition was within the conventional temperature range used for

regeneration, which makes this technique applicable for inorganic adsorbents even with low thermal stability with no additional change in their properties. Finally, the modified zeolite with the optimized condition was successfully heated using resistive heating, which proves the effectiveness of the applied modification method for tuning the electrical resistivity of the zeolite.

5.6. Acknowledgement

We would like to acknowledge financial support for this research from the Natural Science and Engineering Research Council (NSERC) of Canada and Alberta Innovates Graduate Student Scholarship program.

5.7. References

1. Al-Baghli, N. A. and Loughlin, K. F. (2005). "Adsorption of methane, ethane, and ethylene on titanosilicate ETS-10 zeolite." Journal of Chemical Engineering Data **50**(3): 843-848.

2. Álvaro, M., Cabeza, J. F., Fabuel, D., García, H., Guijarro, E. and De Juan, J. L. M. (2006). "Electrical conductivity of zeolite films: Influence of charge balancing cations and crystal structure." Chemistry of Materials **18**(1): 26-33.

3. Ania, C. O., Parra, J. B., Menéndez, J. A. and Pis, J. J. (2005). "Effect of microwave and conventional regeneration on the microporous and mesoporous network and on the adsorptive capacity of activated carbons." Microporous and Mesoporous Materials **85**(1-2): 7-15.

4. Anna, M., Albert, G. N. and Esko, I. K. (2003). "The role of metal nanoparticles in the catalytic production of single-walled carbon nanotubes—a review." Journal of Physics: Condensed Matter **15**(42): S3011.

5. Cherbański, R., Komorowska-Durka, M., Stefanidis, G. D. and Stankiewicz, A. I. (2011). "Microwave swing regeneration Vs temperature swing regeneration - Comparison of desorption kinetics." Industrial & Engineering Chemistry Research **50**(14): 8632-8644.

6. Cherbański, R. and Molga, E. (2009). "Intensification of desorption processes by use of microwaves-An overview of possible applications and industrial perspectives." Chemical Engineering and Processing: Process Intensification **48**(1): 48-58.

7. Chowdhury, T., Shi, M., Hashisho, Z., Sawada, J. A. and Kuznicki, S. M. (2012). "Regeneration of Na-ETS-10 using microwave and conductive heating." Chemical Engineering Science **75**: 282-288.

8. Fayaz, M., Shariaty, P., Atkinson, J. D., Hashisho, Z., Phillips, J. H., Anderson, J. E. and Nichols, M. (2015). "Using microwave heating to improve the desorption efficiency of high molecular weight VOC from beaded activated carbon." Environmental Science and Technology **49**(7): 4536-4542.

9. Hashisho, Z., Emamipour, H., Rood, M. J., Hay, K. J., Kim, B. J. and Thurston, D. (2008). "Concomitant adsorption and desorption of organic vapor in dry and humid air streams using microwave and direct electrothermal swing adsorption." Environmental Science and Technology **42**(24): 9317-9322.

10. Janas, D. and Koziol, K. K. (2014). "A review of production methods of carbon nanotube and graphene thin films for electrothermal applications." Nanoscale **6**(6): 3037-3045.

11. Johnsen, D. L., Mallouk, K. E. and Rood, M. J. (2011). "Control of electrothermal heating during regeneration of activated carbon fiber cloth." Environmental Science and Technology **45**(2): 738-743.

12. Johnsen, D. L. and Rood, M. J. (2012). "Temperature control during regeneration of activated carbon fiber cloth with resistance-feedback." Environmental Science and Technology **46**(20): 11305-11312.

13. Johnsen, D. L., Zhang, Z., Emamipour, H., Yan, Z. and Rood, M. J. (2014). "Effect of isobutane adsorption on the electrical resistivity of activated carbon fiber cloth with select physical and chemical properties." Carbon **76**(0): 435-445.

14. Kamravaei, S., Shariaty, P., Jahandar Lashaki, M., Atkinson, J. D., Hashisho, Z., Phillips, J. H., Anderson, J. E. and Nichols, M. (2017). "Effect of Beaded Activated Carbon Fluidization

on Adsorption of Volatile Organic Compounds." Industrial & Engineering Chemistry Research **56**(5): 1297-1305.

15. Kim, K.-J. and Ahn, H.-G. (2012). "The effect of pore structure of zeolite on the adsorption of VOCs and their desorption properties by microwave heating." Microporous and Mesoporous Materials **152**: 78-83.

16. Liang, Y., Zhang, H., Yi, B., Zhang, Z. and Tan, Z. (2005). "Preparation and characterization of multi-walled carbon nanotubes supported PtRu catalysts for proton exchange membrane fuel cells." Carbon **43**(15): 3144-3152.

17. Lu, L., Shao, Q., Huang, L. and Lu, X. (2007). "Simulation of adsorption and separation of ethanol–water mixture with zeolite and carbon nanotube." Fluid Phase Equilibria **261**(1–2): 191-198.

18. Luo, L., Ramirez, D., Rood, M. J., Grevillot, G., Hay, K. J. and Thurston, D. L. (2006). "Adsorption and electrothermal desorption of organic vapors using activated carbon adsorbents with novel morphologies." Carbon **44**(13): 2715-2723.

19. Moisala, A., Nasibulin, A. G. and Kauppinen, E. I. (2003). "The role of metal nanoparticles in the catalytic production of single-walled carbon nanotubes - A review." Journal of Physics Condensed Matter **15**(42): S3011-S3035.

20. Monneyron, P., Manero, M. H. and Foussard, J. N. (2003). "Measurement and modeling of single- and multi-component adsorption equilibria of VOC on high-silica zeolites." Environmental Science and Technology **37**(11): 2410-2414.

21. Moteki, T., Murakami, Y., Noda, S., Maruyama, S. and Okubo, T. (2011). "Zeolite Surface As a Catalyst Support Material for Synthesis of Single-Walled Carbon Nanotubes." The Journal of Physical Chemistry C **115**(49): 24231-24237.

22. Niknaddaf, S., Atkinson, J. D., Shariaty, P., Jahandar Lashaki, M., Hashisho, Z., Phillips, J. H., Anderson, J. E. and Nichols, M. (2016). "Heel formation during volatile organic compound desorption from activated carbon fiber cloth." Carbon **96**: 131-138.

23. Park, S., Kwon, Y. P., Kwon, H. C., Lee, J. H., Lee, H. W. and Lee, J. C. (2007). "Electrothermal properties of porous ceramic fiber media containing carbon materials." Journal of Nanoscience and Nanotechnology **7**(11): 3776-3779.

24. Park, S., Kwon, Y. P., Kwon, H. C., Lee, J. H., Lee, H. W. and Lee, J. C. (2009). "Electrothermal properties of regenerable carbon contained porous ceramic fiber media." Journal of Electroceramics **22**(1-3): 315-318.

25. Pełech, I., Narkiewicz, U., Kaczmarek, A. and Jędrzejewska, A. (2014). "Preparation and characterization of multi-walled carbon nanotubes grown on transition metal catalysts." Polish Journal of Chemical Technology **16**(1): 117-122.

26. Ramirez, D., Emamipour, H., Vidal, E. X., Rood, M. J. and Hay, K. J. (2011). "Capture and recovery of methyl ethyl ketone with electrothermal-swing adsorption systems." Journal of Environmental Engineering **137**(9): 826-832.

27. Resasco, D. E., Alvarez, W. E., Pompeo, F., Balzano, L., Herrera, J. E., Kitiyanan, B. and Borgna, A. (2002). "A Scalable Process for Production of Single-walled Carbon Nanotubes

(SWNTs) by Catalytic Disproportionation of CO on a Solid Catalyst." Journal of Nanoparticle Research **4**(1): 131-136.

28. Ribeiro, R. P. P. L., Grande, C. A. and Rodrigues, A. E. (2014). "Electric Swing Adsorption for Gas Separation and Purification: A Review." Separation Science and Technology (Philadelphia) **49**(13): 1985-2002.

29. Russell, J. and Cohn, R. (2012). Joule Heating, Book on Demand.

30. Sengupta, J. and Jacob, C. (2009). "Growth temperature dependence of partially Fe filled MWCNT using chemical vapor deposition." Journal of Crystal Growth **311**(23–24): 4692-4697.

31. Shariaty, P., Jahandar Lashaki, M., Hashisho, Z., Sawada, J., Kuznicki, S. and Hutcheon, R. (2017). "Effect of ETS-10 ion exchange on its dielectric properties and adsorption/microwave regeneration." Separation and Purification Technology **179**: 420-427.

32. Subrenat, A., Baléo, J. N., Le Cloirec, P. and Blanc, P. E. (2001). "Electrical behaviour of activated carbon cloth heated by the joule effect: Desorption application." Carbon **39**(5): 707-716.

33. Sullivan, P. D., Rood, M. J., Dombrowski, K. D. and Hay, K. J. (2004). "Capture of organic vapors using adsorption and electrothermal regeneration." Journal of Environmental Engineering **130**(3): 258-267.

34. Sullivan, P. D., Rood, M. J., Hay, K. J. and Qi, S. (2001). "Adsorption and electrothermal desorption of hazardous organic vapors." Journal of Environmental Engineering **127**(3): 217-223.

35. Takagi, D., Hibino, H., Suzuki, S., Kobayashi, Y. and Homma, Y. (2007). "Carbon Nanotube Growth from Semiconductor Nanoparticles." Nano Letters **7**(8): 2272-2275.

36. Triantafyllidis, K. S., Karakoulia, S. A., Gournis, D., Delimitis, A., Nalbandian, L., Maccallini, E. and Rudolf, P. (2008). "Formation of carbon nanotubes on iron/cobalt oxides supported on zeolite-Y: Effect of zeolite textural properties and particle morphology." Microporous and Mesoporous Materials **110**(1): 128-140.

Chapter 6. APPLICATION OF RESISTIVE HEATING FOR REGENERATION OF ELECTRICALLY MODIFIED DEALUMINATED ZEOLITE Y

6.1. Chapter Overview

The optimum condition for CNT addition to dealuminated zeolite Y was described in the previous chapter. In this chapter, the performance of dealuminated zeolite Y modified under the optimum condition described in the previous chapter was evaluated via lab scale adsorption/regeneration cycles to demonstrate the feasibility of the proposed modification method and to evaluate the performance of resistive heating regeneration of the modified zeolite. Adsorption and resistive heating regeneration properties of modified zeolite were investigated and compared to adsorption and conventional conduction-convection thermal regeneration of original zeolite. This is the first time that resistive heating has been used for regeneration of a zeolite.

6.2. Introduction

Application of molecular sieves in adsorption processes demonstrates substantial selectivity and adsorption capacity for adsorptive separation of hydrocarbons and purification/speciation of natural gas, which could result in less greenhouse gas and VOCs emissions. Different molecular sieves have been conventionally used for different abatement systems. For instance, zeolite 13x is a conventional adsorbent used in CO_2 capture and storage process (CCS) (Ben-Mansour et al. 2016), zeolite Y is used for VOCs abatement (Kim and Ahn 2012), zeolite 5A is typically used for natural gas purification (Nugent et al. 2013, Eyer et al. 2014), and natural zeolite and mixed coordination zeolites (ETS-10, ETS-2) are good adsorbents for natural gas separation and gas

drying applications (Anson et al. 2009, Avila et al. 2011, Chowdhury et al. 2012, Shariaty et al. 2017).

After adsorption, however, the adsorbents should be regenerated for reuse. Temperature swing regeneration (TSR) is widely used for regenerating and recovering the adsorption capacity of loaded adsorbents. The conventional TSR techniques (such as steam and hot gas regeneration), however, have high energy consumption, are slow, and/or can alter the physical/chemical properties of the adsorbents and adsorbates (Al-Baghli and Loughlin 2005, Ania et al. 2005, Cherbański and Molga 2009, Cherbański et al. 2011, Chowdhury et al. 2012, Fayaz et al. 2015, Kamravaei et al. 2017, Shariaty et al. 2017).

Resistive (Joule) heating is an alternative method for thermal regeneration of adsorbents whereby electric current is passed through a material with sufficiently low resistivity and heat is generated by the Joule effect (Russell and Cohn 2012). This allows for rapid adsorbent regeneration that is decoupled from the purge gas flow. Compared to conventional TSR methods, resistive heating regeneration is faster, can have higher desorption efficiency, and requires less energy to achieve a desired desorption efficiency (Sullivan et al. 2001, 2004). The feasibility and performance of resistive heating, however, is highly dependent on the electrical resistivity of the adsorbent (Subrenat et al. 2001, Luo et al. 2006, Park et al. 2007, Ribeiro et al. 2014).

Resistive heating has been used for regenerating carbonaceous adsorbents (resistivity of ~1 Ω.m (Johnsen et al. 2014)) (Subrenat et al. 2001, Luo et al. 2006, Hashisho et al. 2008, Johnsen et al. 2011, Ramirez et al. 2011, Johnsen and Rood 2012, Johnsen et al. 2014, Niknaddaf et al. 2016). Most inorganic adsorbents, including zeolites (resistivity of $>10^7$ Ω.m), however, are highly resistive and cannot be heated resistively. Consequently, to the best of our knowledge, there is no study evaluating application of resistive heating for regeneration of inorganic adsorbents due to

their high resistivity. Our previous work showed that addition of carbon nanotube (CNT) to the zeolite using optimized thermal condition of up to 400^{o}C reduces its electrical resistivity without compromising its adsorption properties (Hashisho and Shariaty 2016). Therefore, using this modification method allows for resistive heating of the zeolite. The performance of resistive heating for regeneration of modified zeolites, however, should be evaluated compared to conventional thermal regeneration methods.

The objective of this work, therefore, is to assess the performance of resistive heating for regeneration of modified dealuminated zeolite Y. Specifically, dealuminated zeolite Y is modified through CNT addition and saturated with Methyl Ethyl Ketone (MEK) as a test adsorbate. The saturated zeolite was then regenerated using resistive heating. The efficiency of the method was then evaluated by comparing the regeneration efficiency, desorption rate, and energy consumption obtained using resistive heating and conventional conduction-convection heating regeneration.

6.3. Materials and Methods

6.3.1. Sample Preparation

Dealuminated zeolite Y (CBV-901, Zeolyst, average particle size of 7 μm) was the base material for this study. The method used for CNT deposition was developed based on a previously reported method (Hashisho and Shariaty 2016) and is summarized here:

CBV-901 was added (1:1 wt) to $Co(NO_3)_2.6H_2O$ (≥ 98%, Sigma-Aldrich). The solution was sonicated for 1 h and then dried at 90 ºC overnight. Collected powder was then added to a tubular boat without edge (to enhance the gas/solid contact) and placed in a tube furnace. The sample was heated at 20 ºC/min in 0.5 standard (25ºC and 1 atm) liter per minute (SLPM) N_2 to reach 300 ºC followed by 15 min calcination in 0.5 SLPM air and 15 min metal catalyst formation in 0.5 SLPM of 10% H_2 in N_2. The temperature was further increased at 20 ºC/min in 0.5 SLPM N_2 to reach 400 ºC followed by 30 min CNT deposition in 0.5 SLPM CH_4. The sample was then cooled down to the room temperature in 0.5 SLPM N_2.

Modified (CNT/CBV-901) and as-synthesized (CBV-901) zeolite were pressed at 5 kPSI and the cake was then crushed and sieved to 20 – 50 mesh prior to adsorption/regeneration tests. The characterization tests were performed on powder samples.

6.3.2. Material Characterization

Bulk Elemental Analysis*:* Added carbon was measured using Organic Elemental Analysis (Flash 2000, Thermo Fisher Scientific Inc.) with furnace and gas chromatography column temperatures of 950 and 65 ^{0}C, respectively. He (carrier gas), He (reference), and O_2 flow rates were 140, 250, and 100 ml/min, respectively. A 5 sec oxygen dose was used and the run time was 12 min.

Scanning Electron Microscopy (SEM)*: Field emission* SEM was completed using a JAMP-9500F Auger microprobe (JEOL). The accelerating voltage, emission current, working distance, and sample rotation were 15 kV, 8 nA, 24 mm, and 30^{o}, respectively. An M5 lens with 0.6% energy resolution was used for Auger spectroscopy and imaging.

X-Ray Diffraction (XRD)*:* Powder XRD patterns were acquired with a Rigaku Ultima IV unit equipped with a D/Tex detector and Fe filter. Results were obtained using a cobalt tube (38 kV, 38 mA) with average Kα wavelength of 1.790260 Å. Samples were run from 5 to 90° on a continuous scan using a top-pack mount at 2° 2θ/min and step size of 0.02°.

N_2 Adsorption Isotherm*:* Micropore surface analyzer (IQ2MP, Quantachrome) was used to obtain N_2 adsorption isotherms (relative pressures from 10^{-7} to 0.995) at 77 K. 60 – 70 mg of sample was degassed at 120 °C for 5 h to remove moisture before analysis.

MEK Adsorption Isotherm: Adsorption isotherms of MEK (99.9%, Fisher Chemicals) were obtained gravimetrically using a sorption analyzer (TA Instruments, model VTI-SA) at 25 °C with N_2 carrier gas and varying concentrations of MEK (99.9%, Fisher Chemicals). The system logged the equilibrium weight of the sample (5–7 mg) in response to a step change in the concentration of the adsorbate (relative pressure range of 0.01–0.9). Equilibrium was assumed when the weight changed by < 0.001 wt% in 5 min.

For both N_2 and MEK adsorption capacities, the obtained values were normalized based on the weight of the original zeolite used for modification.

6.3.3. Adsorption/Regeneration Experiments

MEK adsorption

The adsorption setup consisted of an adsorption tube, adsorbate vapor generation system, gas detection system, and data acquisition system (Figure 6-1.a). The tube was made of quartz (1.44 cm inner diameter, 15 cm length) for resistive heating regeneration (for CNT/CBV-901) and stainless steel (1.44 cm inner diameter, 15 cm length) for conventional conduction-convection base heating regeneration (for CBV-901). Note that different adsorption tube materials were used to allow the lowest energy requirement for each regeneration technique. Each was filled with 2± 0.1 g of dry zeolite resulting in a bed height of approximately 3 cm. For the quartz tube, stainless steel meshes at the top and bottom held the adsorbent bed in place (a stainless steel spring was used to avoid any gap between the meshes and adsorbents). For the stainless steel tube, glass wool was used to retain the adsorbents. The adsorbate vapor generation system consisted of a syringe pump (KD Scientific, KDS-220) that injected liquid MEK into a dry, 5 SLPM air stream to achieve a concentration of 500 ppmv. The air flow rate was set using a mass flow controller (Alicat Scientific). The gas detection system consisted of a flame-ionization detector (FID, Baseline-Mocon Inc., series 9000) that monitored VOC concentration at the tube's outlet. The FID was calibrated before each test using the adsorbate stream generated with the vapor generation system. When the outlet concentration matched the inlet concentration, the adsorbent was considered to be saturated with the adsorbate. The adsorbent was fully loaded during all adsorption experiments, requiring 60 min of exposure to the 5 SLPM, 500 ppmv vapor stream. The data acquisition system consisted of a LabVIEW program (National Instruments) and a data logger (National Instruments, Compact DAC) equipped with analogue input modules for recording temperature and outlet VOC concentration. After adsorbent saturation, the adsorption capacity was determined gravimetrically using Eq 1.

$$Adsorption\ capacity\% = \frac{W_{AA} - W_{BA}}{W_{BA}} \times 100 \qquad \text{Eq. 9}$$

where W_{BA} and W_{AA} are weight of adsorbent bed before and after adsorption, respectively. Adsorption capacities for modified zeolite were normalized based on the weight of the original zeolite used for modification.

Regeneration

After adsorption, resistive heating and conventional conduction-convection heating were used to heat the saturated adsorbents. The samples were heated using a constant power of 70 W and 4.25 W for conventional and resistive heating, respectively. The power was adjusted to reach complete regeneration within similar duration (15 min) for both methods. Detailed description of the regeneration setup for each method is as follow:

Resistive heating regeneration: During resistive heating regeneration, the stainless steel meshes (used for holding the adsorbents) were connected to a DC power supply (PS-1030, Circuit-Test Electronics) to apply voltage to both sides of the adsorbent bed. The pressure applied to the adsorbent bed from the stainless steel meshes was adjusted at 10 PSI using a torque meter. A 0.9-mm outer diameter (OD), ungrounded, type K thermocouple (Omega) was used to measure the temperature at the center of the adsorbent bed during regeneration. The schematic diagram of the setup is demonstrated in Figure 6-1.b.

Conventional conduction-convection heating (indirect resistive heating) regeneration: For conventional heating regeneration, the heat application module consisted of a heating tape (Omega) wrapped around the stainless steel tube. A glass-fiber insulation tape (Omega) was wrapped around the heating tape to minimize heat loss. A 0.9-mm OD type K thermocouple (Omega) inserted at the center of the reactor was used to measure the temperature of the adsorbent bed during regeneration. A solid-state relay connected to the DAC system was used to control the

power application to the heating tape. This method is referred to as conventional heating. The schematic diagram of the setup is demonstrated in Figure 6-1.c

During each regeneration test, the data logger was interfaced to the FID and thermocouple to record outlet VOC concentration and adsorbent bed temperature. A N_2 flow of 0.5 SLPM was also used to purge the adsorbent bed during regeneration experiments.

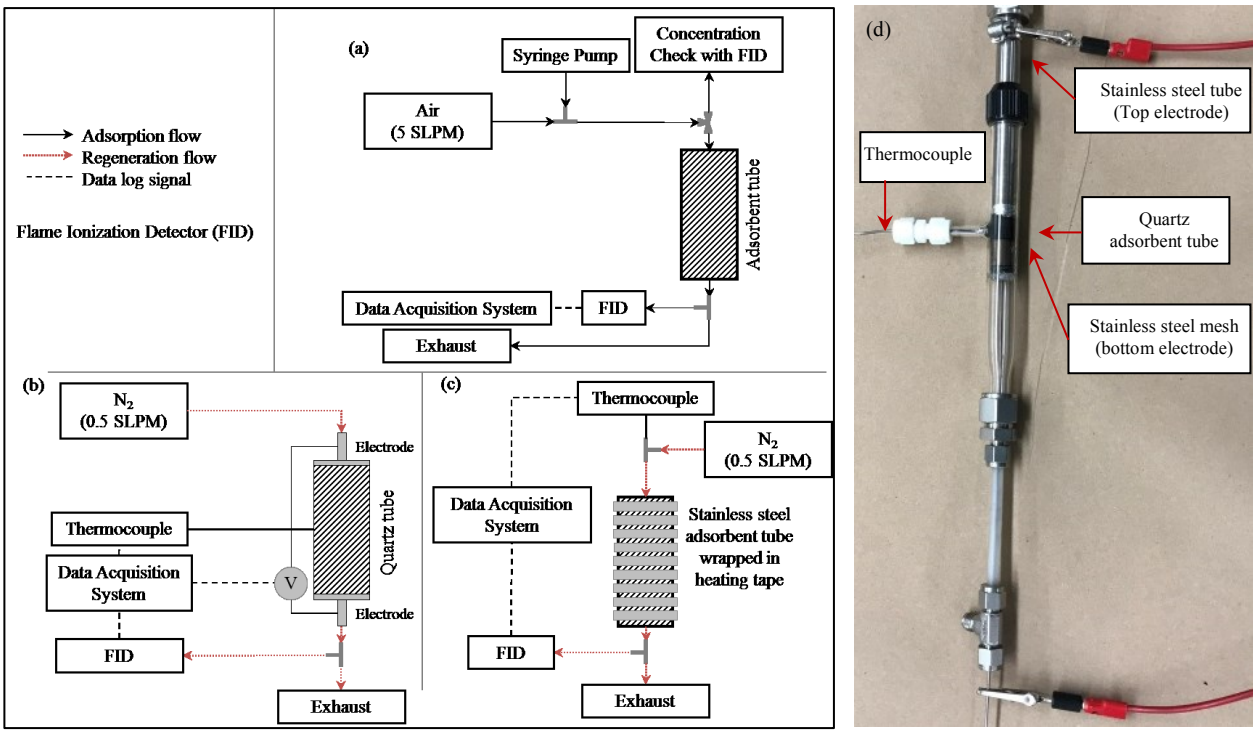

Figure 6-1. Schematic diagram of (a) adsorption, (b) conventional heating regeneration, and (c) resistive heating regeneration setups. (d) shows a picture of resistive heating regeneration setup.

6.4. Results and Discussion

Adsorption and physical properties

The adsorption and physical properties of the zeolite were measured before and after modification. The modification resulted in addition of 11 wt% carbon in form of carbon nanotube (Figure 6-2.a), which reduced the electrical resistivity of the zeolite from $>10^7$ to 1.1 Ω.m. As demonstrated in Figure 6-2.b, XRD patterns also show the similar crystalline structure of the zeolite before and after modification with additional peaks around 50^o due to addition of carbon nanotubes (Pełech et al. 2014). Furthermore, after normalization of the N_2 and MEK adsorption isotherms (Figure 6-2.c and d), similar results were obtained for modified and original zeolite. This confirms that the applied modification has marginal (<2%) effect on adsorption properties of the zeolite.

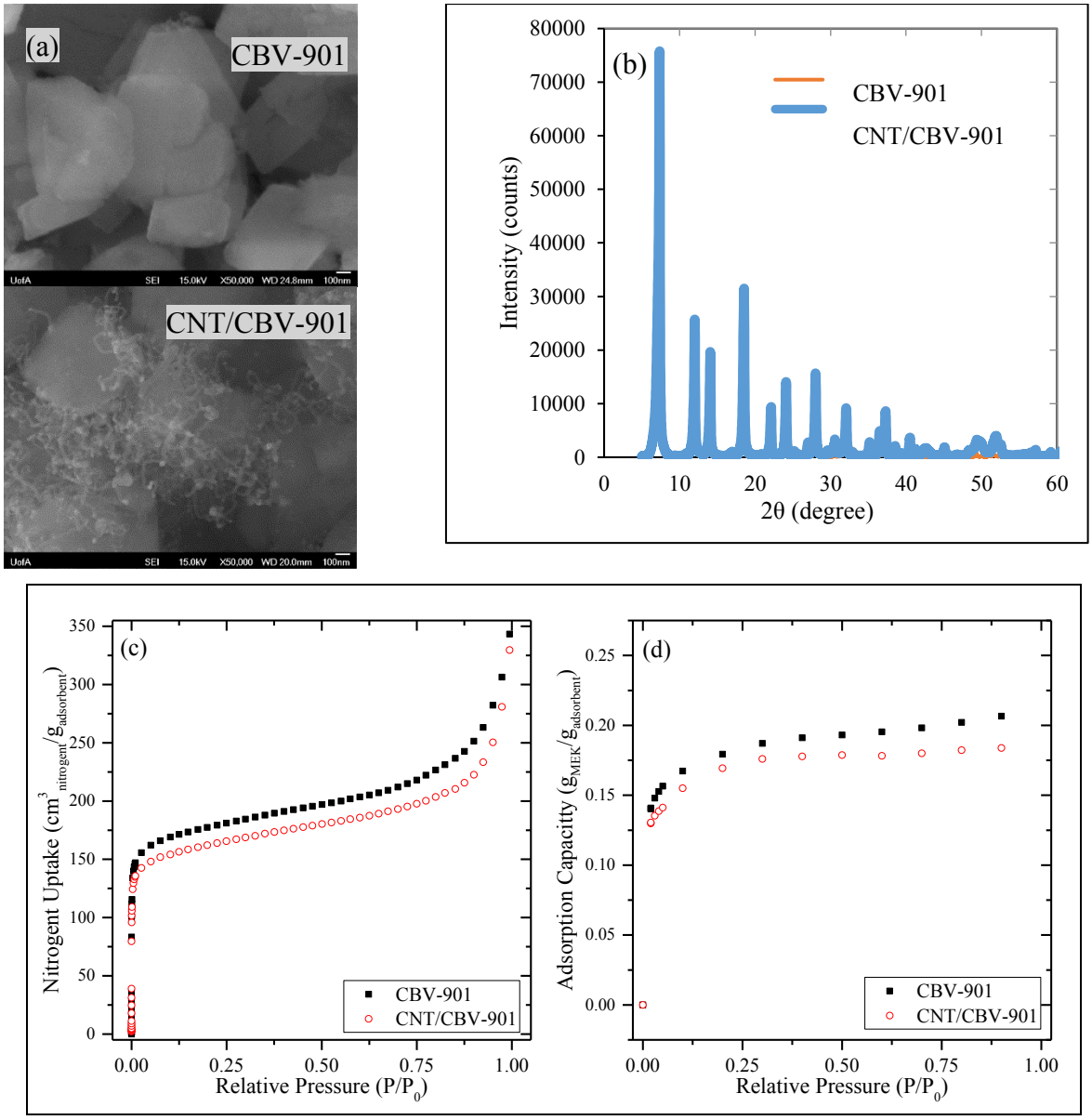

Figure 6-2. (a) SEM pictures, (b) XRD patterns, (c) nitrogen adsorption isotherms, and (d) MEK adsorption isotherms obtained for original (CBV-901) and modified (CNT/CBV-901) zeolite samples

The adsorption breakthrough curves of MEK on modified and original zeolites are illustrated in Figure 6-3. The breakthrough curves were obtained for 5 consecutive adsorption/resistive heating regeneration of modified zeolite (Figure 6-3.a) and adsorption/ conventional heating

regeneration of original zeolite (Figure 6-3.b) Using the obtained breakthrough curves, the throughput ratio (TPR) and the length of unused bed (LUB) were calculated for both modified and original zeolite to assess the adsorption performance of the zeolite before and after modification. TPR values ($TPR = \frac{t_{5\%}}{t_{50\%}}$, where $t_{5\%}$ and $t_{50\%}$ are time required to achieve 5% and 50% breakthrough, respectively) show how steep is the breakthrough curve. Higher TPR implies that transient mass-transfer limitations become less important in the adsorption. The LUB ($LUB = 1 - \frac{W_{5\%}}{W_{100\%}}$, where $W_{5\%}$ and $W_{100\%}$ are mass of the organic vapor adsorbed at time $t_{5\%}$ and $t_{100\%}$) also describes the effective fraction of the adsorbent that is not utilized when the adsorption cycle is stopped at 5% breakthrough (Hashisho et al. 2005).

For original and modified zeolite samples the TPR were calculated as 0.52±0.02 and 0.50±0.02 (average of five cycles), respectively. The obtained values for both samples, however, can be considered similar as their difference is within the experimental error. Additionally, similar values were also calculated for the LUB (0.43±0.02 and 0.45±0.02 for the zeolite before and after modification, respectively). Consequently, there was no change in the kinetic of adsorption after modification of the zeolite. The additional carbon nanotubes, therefore, did not restrict the diffusion of the adsorbates to the zeolite adsorption sites.

Additionally, normalizing the adsorption capacities based on the zeolite mass before the modification, similar (within 2%) adsorption capacities were obtained for modified and original zeolite during the adsorption experiments. This also was confirmed by calculating the area above the breakthrough curves for both original and modified zeolite which were within 5%. This was expected as similar adsorption isotherms were obtained (Figure 6-2.d). The adsorption capacities for both modified and original zeolite were constant throughout the cycles, indicating the complete

regeneration of the saturated adsorbents after each adsorption cycle. This can also be confirmed by the superimposed breakthrough curves.

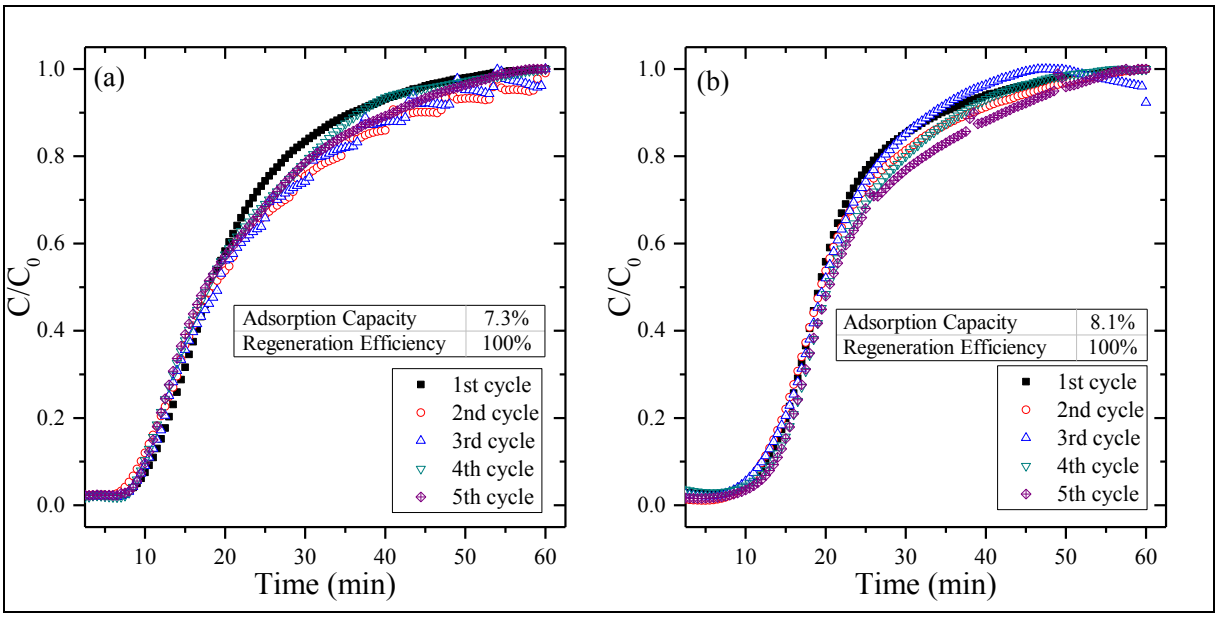

Figure 6-3. Adsorption breakthrough curves of MEK on modified zeolite (a) and original zeolite (before modification) (b)

In summary, there was minimal change in the adsorption properties and crystalline structure of the zeolite after implementation of the modification method except for zeolite electrical resistivity. The resistivity decreased from $>10^7$ to 1.1 Ω.m after modification, which allows for resistive heating of the zeolite.

Comparison of conventional and resistive heating as regeneration method

As mentioned in the Materials and Methods section, the regeneration using conventional and resistive heating was completed at constant power and for the same duration. Figure 6-4 shows that using both regeneration methods, the final temperature was around 160°C, which resulted

in the complete regeneration of the saturated adsorbents. Figure 6-4 further shows 4 times faster heating (44 ^{o}C/min versus 11.5 ^{o}C/min) and cooling in case of resistive heating compared to conventional heating. This is expected since resistive heating the adsorbent bed is used as a heating medium (heat is generated due to the electrical resistance of the medium)(Russell and Cohn 2012), while in conventional heating the heat is generated through an external source and is transferred to the adsorbent bed center, where the thermal resistance (inversely related to the adsorbent thermal conductivity) of the adsorbents is a limiting factor, reducing the heating rate. Additionally, the energy consumed to reach similar temperature within the same duration was 63.1 kJ and 3.8 kJ for conventional and resistive heating methods, respectively. Hence, resistive heating allows 94% less energy consumption, higher heating rate, and faster cooling time which demonstrates the efficiency of resistive heating as a potential alternative to conventional heating methods for regenerating zeolite adsorbents.

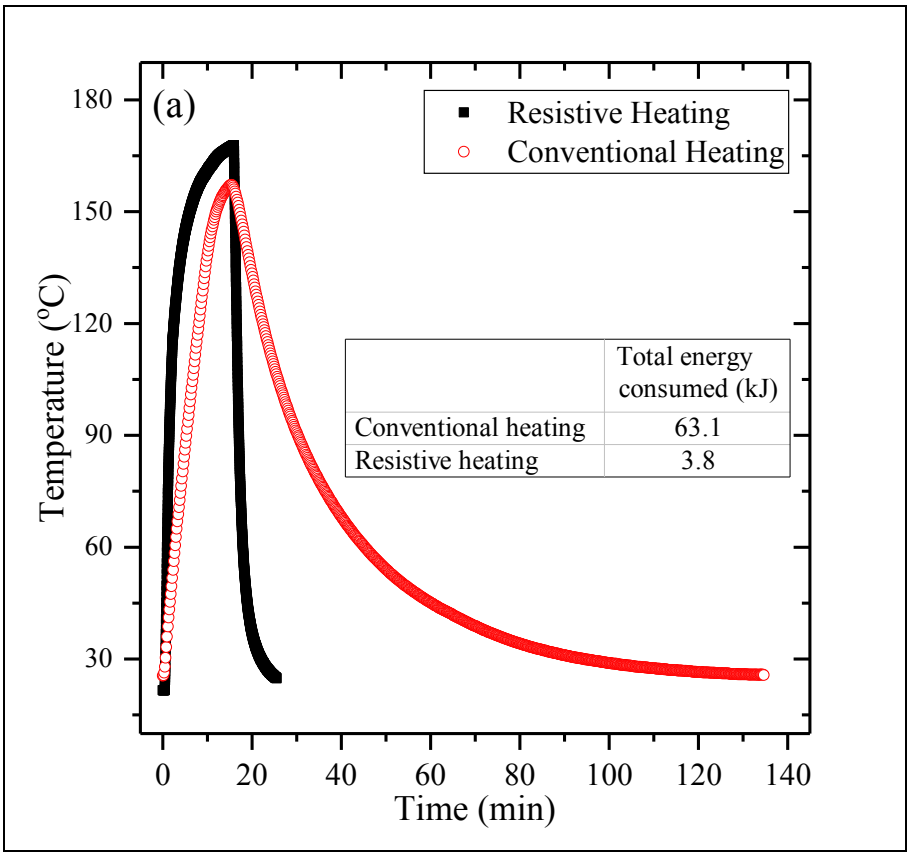

Figure 6-4. Temperature profile and energy consumed during resistive and conventional heating regeneration

The concentration of desorbed VOC at the outlet of the tube during regeneration was monitored for both heating methods (Figure 6-5). The desorption rate using resistive heating is approximately 4 times higher than conventional heating (9374 ppm/min versus 2175 ppm/min), resulting in faster desorption of the adsorbed gas in shorter duration. While it took 10 min for conventional heating regeneration to remove most of the adsorbed VOC from the adsorbent, for resistive heating the corresponding time was around 5min.

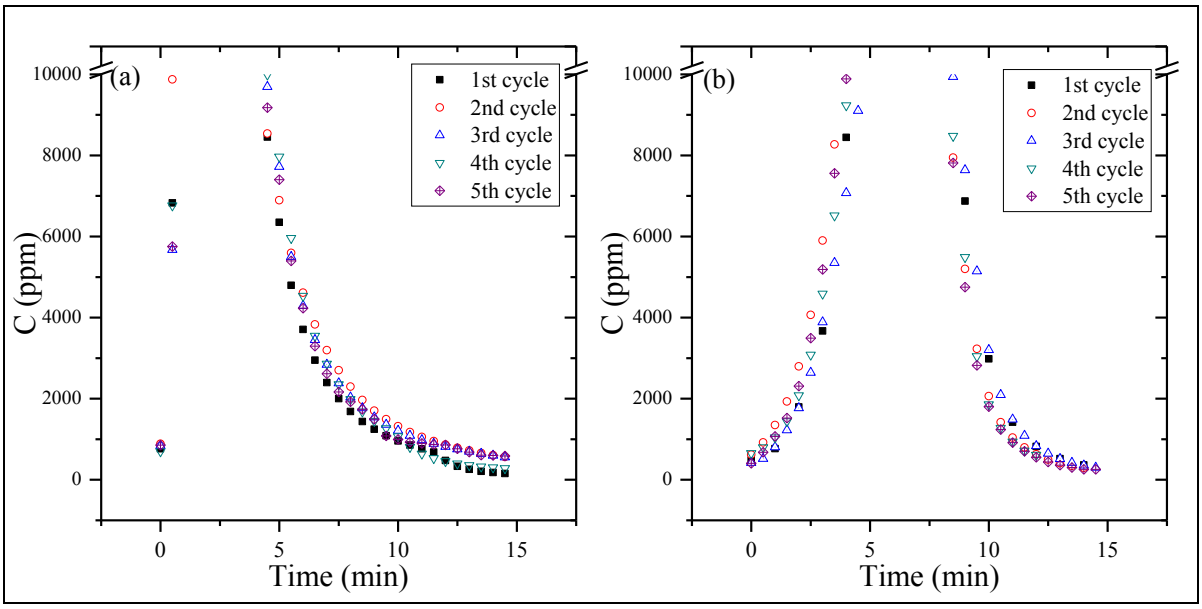

Figure 6-5. Desorption profiles during regeneration of modified zeolite samples using resistive heating (a) and original zeolite samples using conventional heating (b) (The detection range of the FID system was up to 10,000 ppm)

In summary, the efficiency of resistive heating as an alternative method for regenerating zeolite adsorbents has been demonstrated based on its higher heating rate, higher desorption rate, and lower energy consumption compared to conventional heating method to reach complete regeneration within the same duration.

6.5. Conclusion

The thermal regeneration of dealuminated zeolite Y was investigated using two different heating methods, resistive and conventional conduction-convection heating. The electrical resistivity of the zeolite was initially modified by carbon nanotube addition. The modification did not change the crystalline structure of the zeolite, based on XRD patterns before and after CNT addition. Additionally, negligible changes in zeolite adsorption properties were detected after modification, as supported by N_2 and MEK adsorption isotherms. However, the electric resistivity deceased from $>10^7$ to 1.1 Ω.m which allowed for resistive heating of the saturated zeolite for its thermal regeneration.

The performance of resistive and conventional heating regeneration was then compared. Using the same duration for both methods, resistive heating demonstrated 94% less energy consumption, 4 times higher heating rate, and 4 times higher desorption rate to reach complete regeneration. This proves resistive heating as a potential alternative of conventional heating methods for regenerating zeolite adsorbents. Implementing the proposed modification method on inorganic adsorbents could ultimately allow for resistive heating of the saturated adsorbent as a more efficient regeneration method, without compromising its adsorption performance.

6.6. Acknowledgements

We would like to acknowledge financial support for this research from the Natural Science and Engineering Research Council (NSERC) of Canada and Alberta Innovates Graduate Student Scholarship program.

6.7. References

1. Al-Baghli, N. A. and Loughlin, K. F. (2005). "Adsorption of methane, ethane, and ethylene on titanosilicate ETS-10 zeolite." Journal of Chemical Engineering Data **50**(3): 843-848.

2. Ania, C. O., Parra, J. B., Menéndez, J. A. and Pis, J. J. (2005). "Effect of microwave and conventional regeneration on the microporous and mesoporous network and on the adsorptive capacity of activated carbons." Microporous and Mesoporous Materials **85**(1-2): 7-15.

3. Anson, A., Lin, C. C. H., Kuznicki, S. M. and Sawada, J. A. (2009). "Adsorption of carbon dioxide, ethane, and methane on titanosilicate type molecular sieves." Chemical Engineering Science **64**(16): 3683-3687.

4. Avila, A. M., Yang, F., Shi, M. and Kuznicki, S. M. (2011). "Extraction of ethane from natural gas at high pressure by adsorption on Na-ETS-10." Chemical Engineering Science **66**(13): 2991-2996.

5. Ben-Mansour, R., Habib, M. A., Bamidele, O. E., Basha, M., Qasem, N. A. A., Peedikakkal, A., Laoui, T. and Ali, M. (2016). "Carbon capture by physical adsorption: Materials, experimental investigations and numerical modeling and simulations - A review." Applied Energy **161**: 225-255.

6. Cherbański, R., Komorowska-Durka, M., Stefanidis, G. D. and Stankiewicz, A. I. (2011). "Microwave swing regeneration Vs temperature swing regeneration - Comparison of desorption kinetics." Industrial & Engineering Chemistry Research **50**(14): 8632-8644.

7. Cherbański, R. and Molga, E. (2009). "Intensification of desorption processes by use of microwaves-An overview of possible applications and industrial perspectives." Chemical Engineering and Processing: Process Intensification **48**(1): 48-58.

8. Chowdhury, T., Shi, M., Hashisho, Z., Sawada, J. A. and Kuznicki, S. M. (2012). "Regeneration of Na-ETS-10 using microwave and conductive heating." Chemical Engineering Science **75**: 282-288.

9. Eyer, S., Stadie, N. P., Borgschulte, A., Emmenegger, L. and Mohn, J. (2014). "Methane preconcentration by adsorption: A methodology for materials and conditions selection." Adsorption **20**(5-6): 657-666.

10. Fayaz, M., Shariaty, P., Atkinson, J. D., Hashisho, Z., Phillips, J. H., Anderson, J. E. and Nichols, M. (2015). "Using microwave heating to improve the desorption efficiency of high molecular weight VOC from beaded activated carbon." Environmental Science and Technology **49**(7): 4536-4542.

11. Hashisho, Z., Emamipour, H., Rood, M. J., Hay, K. J., Kim, B. J. and Thurston, D. (2008). "Concomitant adsorption and desorption of organic vapor in dry and humid air streams using microwave and direct electrothermal swing adsorption." Environmental Science and Technology **42**(24): 9317-9322.

12. Hashisho, Z., Rood, M. and Botich, L. (2005). "Microwave-swing adsorption to capture and recover vapors from air streams with activated carbon fiber cloth." Environmental Science and Technology **39**(17): 6851-6859.

13. Hashisho, Z. and Shariaty, P. (2016). Method for Tailoring Electrical Resistivity of Molecular Sieve Absorbents for Resistive Heating Application. **US Provisional application 62/419,798**.

14. Johnsen, D. L., Mallouk, K. E. and Rood, M. J. (2011). "Control of electrothermal heating during regeneration of activated carbon fiber cloth." Environmental Science and Technology **45**(2): 738-743.

15. Johnsen, D. L. and Rood, M. J. (2012). "Temperature control during regeneration of activated carbon fiber cloth with resistance-feedback." Environmental Science and Technology **46**(20): 11305-11312.

16. Johnsen, D. L., Zhang, Z., Emamipour, H., Yan, Z. and Rood, M. J. (2014). "Effect of isobutane adsorption on the electrical resistivity of activated carbon fiber cloth with select physical and chemical properties." Carbon **76**(0): 435-445.

17. Kamravaei, S., Shariaty, P., Jahandar Lashaki, M., Atkinson, J. D., Hashisho, Z., Phillips, J. H., Anderson, J. E. and Nichols, M. (2017). "Effect of Beaded Activated Carbon Fluidization on Adsorption of Volatile Organic Compounds." Industrial & Engineering Chemistry Research **56**(5): 1297-1305.

18. Kim, K. J. and Ahn, H. G. (2012). "The effect of pore structure of zeolite on the adsorption of VOCs and their desorption properties by microwave heating." Microporous and Mesoporous Materials **152**: 78-83.

19. Luo, L., Ramirez, D., Rood, M. J., Grevillot, G., Hay, K. J. and Thurston, D. L. (2006). "Adsorption and electrothermal desorption of organic vapors using activated carbon adsorbents with novel morphologies." Carbon **44**(13): 2715-2723.

20. Niknaddaf, S., Atkinson, J. D., Shariaty, P., Jahandar Lashaki, M., Hashisho, Z., Phillips, J. H., Anderson, J. E. and Nichols, M. (2016). "Heel formation during volatile organic compound desorption from activated carbon fiber cloth." Carbon **96**: 131-138.

21. Nugent, P., Giannopoulou, E. G., Burd, S. D., Elemento, O., Giannopoulou, E. G., Forrest, K., Pham, T., Ma, S., Space, B., Wojtas, L., Eddaoudi, M. and Zaworotko, M. J. (2013). "Porous materials with optimal adsorption thermodynamics and kinetics for co2 separation." Nature **495**(7439): 80-84.

22. Park, S., Kwon, Y. P., Kwon, H. C., Lee, J. H., Lee, H. W. and Lee, J. C. (2007). "Electrothermal properties of porous ceramic fiber media containing carbon materials." Journal of Nanoscience and Nanotechnology **7**(11): 3776-3779.

23. Pełech, I., Narkiewicz, U., Kaczmarek, A. and Jędrzejewska, A. (2014). "Preparation and characterization of multi-walled carbon nanotubes grown on transition metal catalysts." Polish Journal of Chemical Technology **16**(1): 117-122.

24. Ramirez, D., Emamipour, H., Vidal, E. X., Rood, M. J. and Hay, K. J. (2011). "Capture and recovery of methyl ethyl ketone with electrothermal-swing adsorption systems." Journal of Environmental Engineering **137**(9): 826-832.

25. Ribeiro, R. P. P. L., Grande, C. A. and Rodrigues, A. E. (2014). "Electric Swing Adsorption for Gas Separation and Purification: A Review." Separation Science and Technology (Philadelphia) **49**(13): 1985-2002.

26. Russell, J. and Cohn, R. (2012). Joule Heating, Book on Demand.

27. Shariaty, P., Jahandar Lashaki, M., Hashisho, Z., Sawada, J., Kuznicki, S. and Hutcheon, R. (2017). "Effect of ETS-10 ion exchange on its dielectric properties and adsorption/microwave regeneration." Separation and Purification Technology **179**: 420-427.

28. Subrenat, A., Baléo, J. N., Le Cloirec, P. and Blanc, P. E. (2001). "Electrical behaviour of activated carbon cloth heated by the joule effect: Desorption application." Carbon **39**(5): 707-716.

29. Sullivan, P. D., Rood, M. J., Dombrowski, K. D. and Hay, K. J. (2004). "Capture of organic vapors using adsorption and electrothermal regeneration." Journal of Environmental Engineering **130**(3): 258-267.

30. Sullivan, P. D., Rood, M. J., Hay, K. J. and Qi, S. (2001). "Adsorption and electrothermal desorption of hazardous organic vapors." Journal of Environmental Engineering **127**(3): 217-223.

Chapter 7. ENHANCED MICROWAVE HEATING REGENERATION OF DEALUMINATED ZEOLITE Y WITH MODIFIED DIELECTRIC PROPERTIES

7.1. Chapter Overview

The previous chapters described modifying the electrical properties of dealuminated zeolite Y with minimal change to its adsorption properties. Since dielectric properties in solids depend on ionic conduction, we decided to evaluate the dielectric properties of the modified dealuminated zeolite Y sample with tuned electrical resistivity and compare it to original sample. Also, the performance of microwave regeneration of the modified dealuminated zeolite Y was evaluated and compared to conventional regeneration of original zeolite.

7.2. Introduction

Microwave heating is considered as a promising alternative to conventional heating methods (e.g. hot gas, steam) for thermal regeneration of adsorbents (Chowdhury et al. 2012, Fayaz et al. 2015, Mao et al. 2015, Pinchukova et al. 2015, Li et al. 2017). In this technique, direct adsorbent and adsorbate heating minimizes heat losses and energy consumption to reach target regeneration efficiency (Reuß et al. 2002, Witkiewicz and Nastaj 2014). Previous researches showed that compared to conventional thermal regeneration methods, microwave heating has lower energy consumption, higher desorption rate, and shorter desorption duration (Ania et al. 2005, Hashisho et al. 2008, Cherbański and Molga 2009, Cherbański et al. 2011, Chowdhury et al. 2012, Fayaz et al. 2015, Mao et al. 2015, Pinchukova et al. 2015, Li et al. 2017). Microwave heating could also overcome conventional temperature swing and pressure swing regeneration techniques (e.g. steam,

hot gas, indirect resistive heating, and vacuum regeneration) drawbacks, such as high energy consumption, long duration, and/or altering the physical/chemical properties of the adsorbents and adsorbates.(Ania et al. 2005, Hashisho et al. 2008, Cherbański and Molga 2009, Cherbański et al. 2011, Chowdhury et al. 2012, Fayaz et al. 2015, Kamravaei et al. 2017)

During microwave heating, microwave energy dissipates in a material as thermal energy or heat according to its dielectric properties. The response of a material to microwave irradiation depends on its complex permittivity (ε^*), defined as follows (Metaxas and Meredith 1983):

$$\varepsilon^* = \varepsilon' - \varepsilon'' j \qquad \text{Eq. 10}$$

The dielectric constant (ε', real) is related to a material's ability to store energy. The dielectric loss factor (ε'', imaginary) describes the dissipation of energy as heat. The loss tangent ($\tan\delta = \frac{\varepsilon''}{\varepsilon'}$) is also commonly used to describe the losses within the material due to development of the internal field within the affected medium by microwaves penetration, a consequence of which is volumetric heating (Metaxas and Meredith 1983). Therefore, material's loss tangent could affect the volumetric power density ($P_{(z)avg.}, \frac{\mathbf{W}}{\mathbf{m^3}}$), which is the average microwave power converted into heat per unit volume (National Research Council 1994):

$$P_{(z)_{ave.}} = 2\pi f \varepsilon_0 \varepsilon' \tan\delta \, E_{(z)}{}^2 \qquad \text{Eq. 11}$$

where λ_0 is wavelength (m), f is wave frequency (1/s), ε_0 is free space permittivity (8.854×10^{-12} F/m), and $E_{(z)}$ is the internal electric field strength (V/m) in the material (National Research Council 1994). Materials, therefore, can be selectively heated with microwaves depending on their dielectric properties. A "lossy" material (high tan δ) can be heated more readily than a low-loss (low tan δ) material.

Microwave penetration inside an adsorbent, which highly depends on its dielectric properties, is another important parameter for industrial application of microwave regeneration. Microwave penetration can be quantified using the Penetration Depth (d_E) which is defined as the characteristic length at which ~63% of the incident microwave power is dissipated (Bathen 2003):

$$d_E \approx \frac{\lambda_0}{2.\pi} \times \frac{\sqrt{\varepsilon'}}{\varepsilon''} \qquad \text{Eq. 12}$$

where λ_0 is wavelength in vacuum (m).

Very low (<1cm) and very high (>100cm) d_E values are not favorable for industrial applications. Low d_E would result in penetration of the microwave into thin layer of the adsorbent bed, while high d_E means low microwave absorption by the adsorbent bed and ineffective microwave heating (Bathen 2003).

Due to their unique structural characteristics, molecular sieves have been widely used for different applications, such as CO_2 capture and storage process (CCS) (Ben-Mansour et al. 2016), VOCs abatement systems (Kim and Ahn 2012), natural gas separation/purification, and gas drying applications (Nugent et al. 2013, Eyer et al. 2014). Although several researches (Reuß et al. 2002, Witkiewicz and Nastaj 2014, Pinchukova et al. 2015, Nigar et al. 2016, Kamravaei et al. 2017) previously demonstrated potential application of microwave heating for regeneration of different molecular sieves, their low dielectric properties (Reuß et al. 2002, Witkiewicz and Nastaj 2014, Kamravaei et al. 2017) resulted in low microwave absorption and small penetration depth of microwaves in adsorbents, which ultimately lead to high energy consumption to reach complete regeneration (Witkiewicz and Nastaj 2014).

Previous investigations proposed microwave heating for regeneration of molecular sieves when loaded with polar adsorbates. It was concluded that microwave-assisted desorption can be effective

(in terms of regeneration efficiency and energy consumption) for adsorption systems in which at least one component, adsorbent or adsorbate, can absorb and dissipate microwave energy into heat (Reuß et al. 2002, Witkiewicz and Nastaj 2014, Shariaty et al. 2017). Therefore, unlike non-polar adsorbates, microwave desorption of polar adsorbates from microwave transparent adsorbents (e.g. molecular sieves) can be readily achieved due to direct dissipation of microwave energy in the adsorbate (Reuß et al. 2002, Witkiewicz and Nastaj 2014, Kamravaei et al. 2017).

Limited works systematically investigated the performance of microwave regeneration of microwave transparent adsorbents to achieve complete desorption of adsorbates. Using highly microwave transparent adsorbent, complete regeneration is challenging even when the adsorbent is saturated with a polar adsorbate. In this case, while the majority of adsorbate can be desorbed due to direct microwave heating, remaining adsorbate at the end of regeneration cannot absorb enough microwaves to compensate for the low dielectric properties of the adsorbent. Consequently, it is expected to result in longer duration and higher energy consumption requirement for adsorbent complete regeneration. Microwave regeneration of microwave transparent adsorbents saturated with nonpolar adsorbates is even more challenging. Since nonpolar adsorbates cannot directly absorb microwave energy, the microwave regeneration can just be achieved by heating the adsorbent to suitable regeneration temperature. Microwave transparent adsorbents, however, either cannot be heated to desorption temperature or very high microwave energy would be required to reach the target regeneration temperature (Kamravaei et al. 2017). Hence, there is a need to overcome this drawback and allow microwave regeneration of microwave transparent adsorbents regardless of the properties of the adsorbate. A method, therefore, is required to tailor the adsorbent dielectric properties without compromising its adsorption properties.

Different forms of carbon addition have been previously used for improving the dielectric properties of polymers, ceramic matrices, and elastomers. Specifically, application of black fillers including carbon nanotube has been reported as an effective method to enhance the material dielectric properties (Wang and Dang 2005, Bokobza 2007, Shin and Hong 2012, Qing et al. 2014, Wu et al. 2016, Zhao et al. 2016, He et al. 2017). While all these reports have used pre-synthesized carbon nanotube and physically mixed it with initial solutions of polymers, ceramic matrices, and elastomers, the same principles could be used for molecular sieves modification. However, in this case, the carbon addition can be done, post synthesis, through carbon nanotube growth on the molecular sieve. A modification method recently introduced to tune electrical conductivity of molecular sieves while maintaining their adsorption properties by low temperature carbon nanotube (CNT) addition (Hashisho and Shariaty 2016). Since ionic conduction is an important mechanism for microwave heating of solids (Rybakov et al. 2006, Polaert et al. 2010), it is expected that any change in electrical conductivity of the solid materials could correspondingly alter their dielectric properties.

The objective of this work is then to evaluate the microwave regeneration properties of a microwave transparent adsorbent following its modification through carbon nanotube addition. Dealuminated zeolite Y was used as an adsorbent and its properties were characterized using SEM micrographs, XRD patterns, N_2 and methyl ethyl ketone (MEK) adsorption isotherms, dielectric properties, in addition to temperature and power profiles during microwave heating. The adsorbent was saturated with MEK as a polar test adsorbate and its regeneration properties were evaluated by comparing the microwave regeneration of the modified adsorbent with microwave and conventional conduction-convection heating of the original adsorbent before modification.

Furthermore, the modified sample was then tested for its microwave regeneration when saturated with cyclohexane as a non-polar adsorbate, and compared with original zeolite.

7.3. Materials and Methods

7.3.1. Sample Preparation

Dealuminated zeolite Y (CBV-901, Zeolyst, average particle size of 7 μm) was the base material for this study. Previously reported low temperature CNT deposition was used as a modification method (Hashisho and Shariaty 2016), as summarized below:

Solution of $Co(NO_3)_2.6H_2O$ (≥ 98%, Sigma-Aldrich) and CBV-901 (1:1 wt) was prepared. The solution was sonicated at room temperature for 1 h and then dried at 90 ºC overnight. Collected powder was then placed in a tubular boat without fore or aft edges (to enhance the gas/solid contact) and put in a tube furnace. The sample was heated at 20 ºC/min in 0.5 standard (25ºC and 1 atm) liter per minute (SLPM) N_2 to reach 300 ºC followed by 15 min calcination in 0.5 SLPM air and 15 min metal catalyst formation in 0.5 SLPM of 10% H_2 in N_2. The temperature was further increased at 20 ºC/min in 0.5 SLPM N_2 to reach 400 ºC followed by 30 min CNT deposition in 0.5 SLPM CH_4 at this temperature.

Modified (CNT/CBV-901) and original (CBV-901) zeolite were pressed at 5 kPSI and the cake was then crushed and sieved to 20 – 50 mesh for adsorption/regeneration tests.

7.3.2. Material Characterization

Bulk Elemental Analysis*:* Added carbon was measured using Organic Elemental Analysis (OEA) (Flash 2000, Thermo Fisher Scientific Inc.) with furnace and gas chromatograph column temperatures of 950 and 65 ^{0}C, respectively. He (carrier gas), He (reference), and O_2 flow rates

were 140, 250, and 100 ml/min, respectively. A 5 sec oxygen dose was used and the run time was 12 min.

Scanning Electron Microscopy (SEM)*: Field emission* SEM was completed using a JAMP-9500F Auger microprobe (JEOL). The accelerating voltage, emission current, working distance, and sample rotation were 15 kV, 8 nA, 24 mm, and 30^{o}, respectively. A M5 lens with 0.6% energy resolution was used for Auger spectroscopy and imaging. Samples were also analyzed using SEM (Vega-3, Tescan) equipped with energy dispersive x-ray spectroscopy (EDX) and backscatter SEM (BSEM, Oxford Instruments) detectors to determine and differentiate between the existing elements in SEM pictures.

X-Ray Diffraction (XRD)*:* Powder XRD patterns were acquired with a Rigaku Ultima IV unit equipped with a D/Tex detector and Fe filter. Results were obtained using a cobalt tube (38 kV, 38 mA) with average Kα wavelength of 1.790260 Å. Samples were run from 5 to 90° on a continuous scan using a top-pack mount at 2° 2θ/min and step size of 0.02°.

Raman Spectroscopy*:* All Raman spectra were acquired at room temperature using a Nicolet Almega XR micro-Raman Analysis System. Laser wavelength was set to 532 nm (2.33 eV). Maximum power of 24 mW was used for this spectroscopic study. All Raman spectra were collected by fine-focusing a 50 × microscope objective and five 10 seconds exposure.

N_2 Adsorption Isotherm*:* Micropore surface analysis (IQ2MP, Quantachrome) with N_2 (relative pressures from 10^{-7} to 0.995) at 77 K was used to characterize physical properties of original and modified samples. 60 – 70 mg of sample was degassed at 120 °C for 5 h to remove moisture before analysis.

MEK Adsorption Isotherm: Adsorption isotherms of MEK (99.9%, Fisher Chemicals) were obtained gravimetrically using a sorption analyzer (TA Instruments, model VTI-SA) at 25 °C with

N_2 carrier gas and varying concentrations of MEK (99.9%, Fisher Chemicals). The system logged the equilibrium weight of the sample (5–7 mg) in response to a step change in the concentration of the adsorbate (relative pressure range of 0.01–0.9). Equilibrium was assumed when the weight changed by < 0.001 wt% in 5 min.

For both N_2 and MEK adsorption capacities, the obtained adsorption capacities were normalized based on the weight of the original zeolite before modification.

Dielectric Properties Measurement: The system used to acquire adsorbents dielectric properties consists of a Vector Network Analyzer (VNA, supplied by Rohde and Schwarz), equipped with an open-ended coaxial probe (Keycom), and data acquisition software. Adsorbent samples were placed in a quartz tube (2 cm inner diameter, 2 cm length) and reflection coefficients of the electromagnetic waves from the samples at each frequency were measured at 25 °C and 1 atm. The sample affects the phase and magnitude of the reflected power observed by the VNA, from which the complex permittivity is calculated by the software based on the difference between the obtained measurements for test sample and blank sample (calibration material).

7.3.3. Adsorption/Regeneration Experiments

VOC adsorption

The adsorption setup consisted of an adsorption tube, adsorbate vapor generation system, gas detection system, and data acquisition system (Figure 6-1.a). Quartz and stainless steel tubes were used for conductive and microwave heating regeneration, respectively. Note that different adsorption tube materials were used to allow the lowest energy requirement for each regeneration technique. Each tube was filled with 2.0 ± 0.1 g of dry zeolite. Fritted quartz disk and glass wool was used to hold the adsorbent bed in place in quartz and stainless steel tube, respectively.

The adsorbate vapor generation system consisted of a syringe pump (KD Scientific, KDS-220) that injected liquid VOC into a dry, 5 SLPM air stream to achieve a concentration of 500 ppmv. The air flow rate was set using a mass flow controller (Alicat Scientific). The gas detection system consisted of a flame-ionization detector (FID, Baseline-Mocon Inc., series 9000) that monitored VOC concentration at the adsorption tube's outlet. The FID was calibrated before each test using the adsorbate stream generated with the vapor generation system. When the outlet concentration matched the inlet concentration, the adsorbent was considered to be saturated. The adsorbent was fully loaded during all adsorption experiments, requiring 60 min of exposure to the 5 SLPM, 500 ppmv VOC laden air stream. MEK and Cyclohexane were selected as polar and non-polar test adsorbates, respectively. The data acquisition system consisted of a LabVIEW program (National Instruments) and a data logger (National Instruments, Compact DAC) equipped with analogue input modules for recording temperature and outlet VOC concentration. After adsorbent saturation, the adsorption capacity was determined gravimetrically using the following equation:

$$Adsorption\ capacity\% = \frac{W_{AA} - W_{BA}}{W_{BA}} \times 100 \qquad \text{Eq. 13}$$

where W_{BA} and W_{AA} are weight of adsorbent bed before and after adsorption, respectively. Adsorption capacities for modified zeolite were normalized based on the weight of the original zeolite used for modification.

Regeneration

After adsorption, microwave heating and conventional conduction base indirect resistive heating were used for regenerating the saturated adsorbents. The power was adjusted to reach a regeneration temperature of 160 ^{o}C within similar duration (15 min) for both methods. The

regeneration setups are described elsewhere and are briefly described below (Chowdhury et al. 2012, Fayaz et al. 2015, Kamravaei et al. 2017, Kamravaei et al. 2017).

Microwave heating regeneration (Chowdhury et al. 2012, Fayaz et al. 2015, Kamravaei et al. 2017): The setup consisted of a 2kW power supply (SM745G.1, Alter), a 2kW variable output microwave generator (MH2.0W S, National Electronics) equipped with a 2.45GHz magnetron, an isolator (National Electronics), a three-stub tuner (National Electronics), and a waveguide applicator connected to a sliding short (IBF Electronic GmbH & Co. KG). A dual channel microwave power meter (E4419B, Agilent), two power sensors (8481 A, Agilent), and a dual directional coupler with 60db attenuation (Mega Industries) were used to measure forward and reverse power during regeneration. A fiber optic sensor with a signal conditioner (Reflex, Neoptix) measured the temperature. A data acquisition and control (DAC) system (Compact DAC, National Instruments) equipped with LabVIEW (National Instruments) recorded power during heating. The schematic diagram of the setup is demonstrated in Figure 7-1.b.

Conventional conduction-convection heating regeneration (Chowdhury et al. 2012, Fayaz et al. 2015, Kamravaei et al. 2017): The heat application module consisted of a heating tape (Omega) wrapped around the stainless-steel tube. Insulation tape (Omega) was wrapped around the heating tape to minimize heat loss. A 0.9-mm OD type K thermocouple (Omega) inserted at the center (radially) of the adsorbent bed was used to measure its temperature during regeneration. The DAC system was interfaced to thermocouple and a solid state relay to control the power application to achieve the set point temperature. This is referred to as conventional regeneration. The schematic diagram of the setup is demonstrated in Figure 7-1.c.

During each regeneration test, the data logger was interfaced to the FID and thermocouple to record outlet VOC concentration and adsorbent bed temperature. A N_2 flow of 0.5 SLPM was also used to purge the adsorbent bed during regeneration experiments.

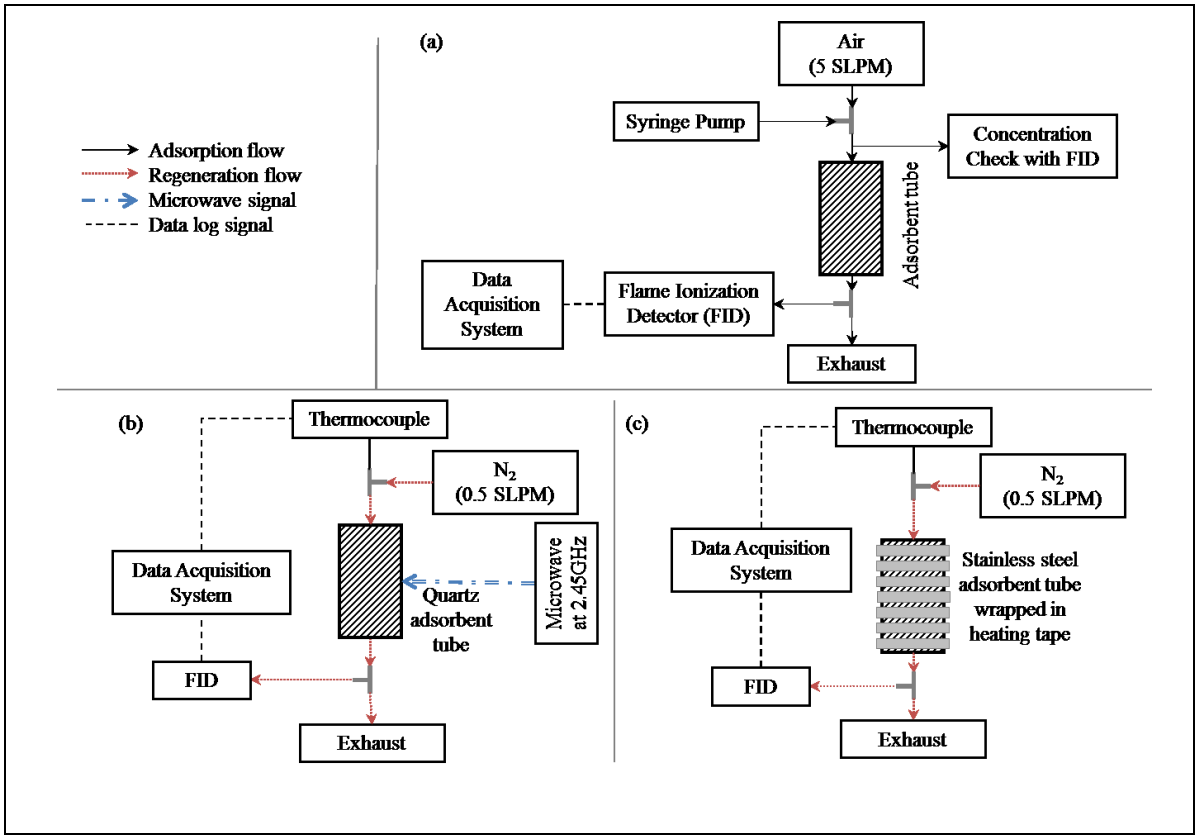

Figure 7-1. Schematic diagram of (a) adsorption, (b) microwave heating regeneration, and (c) conventional heating regeneration setups

7.4. Results and Discussion

Adsorption and physical properties

The adsorption and physical properties of dealuminated zeolite Y were measured before and after modification. The modification resulted in addition of 11 wt% carbon in the form of carbon nanotubes, as confirmed by SEM and presence of D (1343 cm^{-1}), G (1573 cm^{-1}), and G' (2671 cm^{-1}) bands in the Raman spectroscopy (Figure 7-2), which is in agreement with previously reported values (Triantafyllidis et al. 2008, Hashisho and Shariaty 2016). SEM for the modified sample further confirms low population of added carbon nanotubes directly attached on the zeolite crystals, which makes them still accessible for adsorption. XRD patterns also showed similar crystalline structure of the zeolite before and after modification with additional peaks due to formation of carbon nanotubes (Figure 7-2.c).

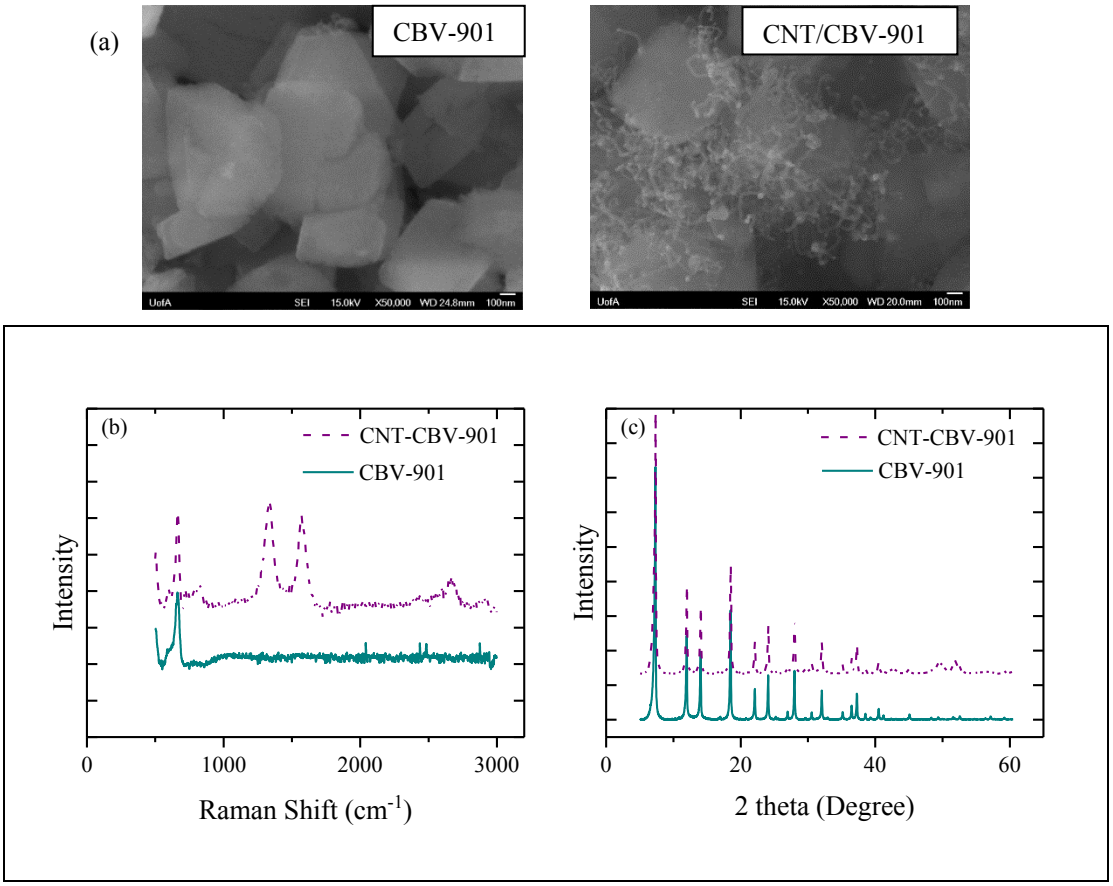

Figure 7-2. SEM pictures (a), Raman spectroscopy (b), and XRD pattern (c) of modified and original zeolite

The N_2 and MEK adsorption isotherms of the modified samples were ~11 and 9 % lower than that of the original zeolite, respectively. However, after normalization based on the weight of the original zeolite before modification, similar results were obtained for modified and original zeolite (Figure 7-3). This confirms that the applied modification has almost no effect on adsorption properties of the zeolite.

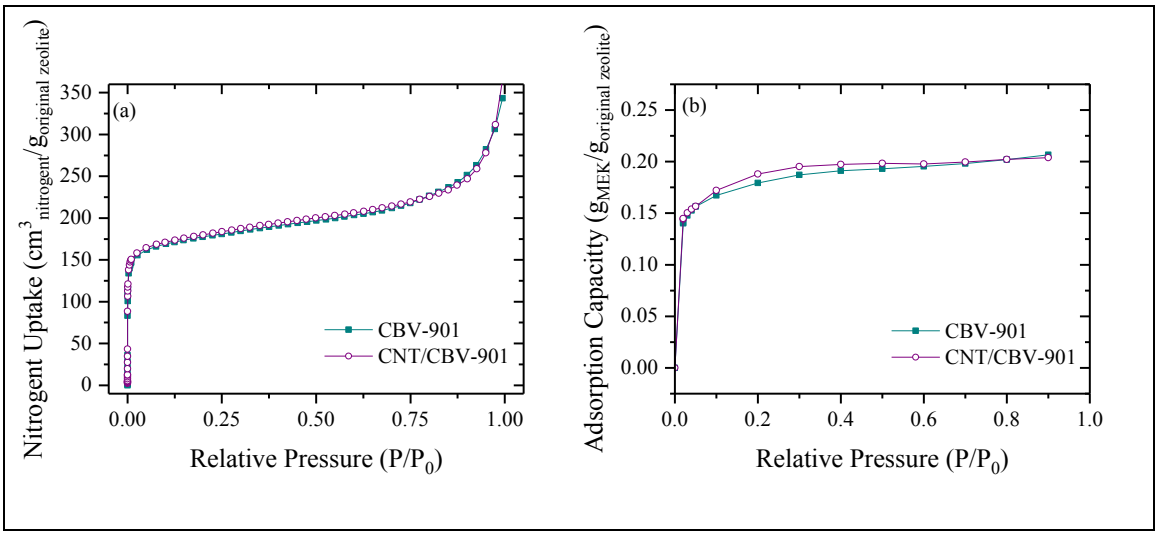

Figure 7-3- Nitrogen (a) and MEK (b) adsorption isotherms for original (CBV-901) and modified (CNT/CBV-901) zeolite

Dielectric properties measurements also showed significant (more than one order of magnitude) increase in the dielectric constant, loss factor and loss tangent for zeolite as a result of modification (Figure 7-4.a). The dielectric properties for modified sample are comparable with that for activated carbon samples ($15< \varepsilon'< 40$, $3< \varepsilon''<20$, and $0.1<\tan\delta<0.5$) (Atwater and Wheeler Jr 2003). This resulted in similar behavior of modified zeolite in microwave field. Additionally, calculating penetration depth (d_E) for zeolite before and after modification showed that modification tuned zeolite dielectric properties (from 755 to 26cm) in a way to have suitable penetration depth within industrial rage of 1-100 cm (Bathen 2003). Hence, modified zeolite can be readily used in microwave heating application and could lead to effective microwave heating of the total volume of the adsorbent bed.

Temperature profiles during microwave heating of the zeolite before and after modification also confirmed the increase in zeolite dielectric properties. As illustrated in Figure 7-4.b and c, microwave heating of modified zeolite resulted in almost 3 times higher microwave absorption

(60% vs 21%) and more than 9 times faster heating rate (94 vs 10 ^{o}C/min) when using the same microwave applied power of 60W. The increase in dielectric properties of zeolite after modification was expected because of enhanced electrical conductivity (resistivity decreased from $>10^{7}$ Ω.m for original zeolite to 1.1 Ω.m for modified zeolite). The addition of carbon nanotubes to the zeolite crystals resulted in increased net charge of the zeolite lattice and led to changes in hindered ionic conduction and/or ionic relaxation, which are responsible for the dielectric response of zeolites (Rybakov et al. 2006, Polaert et al. 2010).

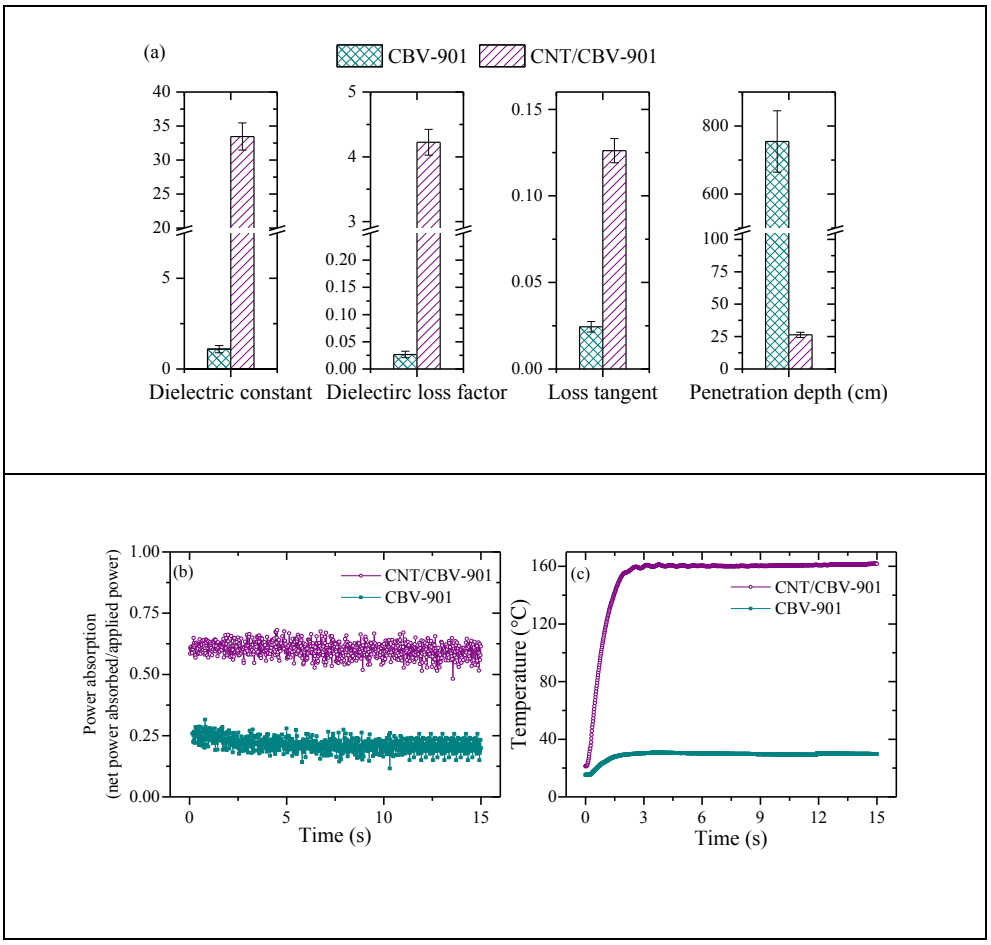

Figure 7-4- Dielectric properties at 2.45GHz and 25^{o}C (a), microwave power absorption (b), and microwave temperature profile (c) of original (CBV-901) and modified (CNT/CBV-901) zeolite

Microwave Regeneration

To better understand the effect of modification on the microwave regeneration of zeolite, three separate adsorption/regeneration tests were completed using polar adsorbate, MEK, which is preferred for microwave regeneration of original zeolite. Each test was performed for 5 consecutive cycles for better comparison of the effectiveness of each regeneration method. All samples were saturated with MEK prior to regeneration step. The saturation was achieved when outlet and inlet MEK concentrations were the same. The obtained adsorption capacities for both modified and original samples in all cycles were similar and equal to 8±1 wt% (gram MEK adsorbed/gram original zeolite).

Microwave regeneration was used for both modified and original zeolite. Conventional conduction-convection heating regeneration was also performed for original zeolite as a baseline method. All regeneration tests were completed aiming for the same regeneration temperature (160 ^{o}C) and duration (15 min). For microwave heating of original zeolite, however, the target temperature was not reached due to low dielectric loss factor of this sample (Figure 7-4.a).

Figure 7-5.a and b show the temperature and desorption profiles obtained for all regeneration tests. As expected, microwave regeneration of the modified zeolite resulted in faster heating (16 and 5 times) and higher desorption rate (4 and 8 times) compared to microwave and conventional heating regeneration of original zeolite. Microwave regeneration of modified zeolite and conventional regeneration of the original zeolite resulted in complete regeneration within 15 min duration, while 81% regeneration efficiency was achieved for microwave regeneration of original zeolite for the same regeneration duration (Figure 7-7).

Furthermore, it can be seen that although the temperature during microwave heating of original zeolite did not reached more than 35 ^{o}C, its desorption rate at the beginning of the regeneration

period was still more (2 times) than conventional heating (Figure 7-5.b). Desorption profile and calculated regeneration efficiency, however, illustrated removal of a large fraction of the adsorbed MEK despite the low temperature of the adsorbent bed. This agrees with previous reports that in microwave regeneration of transparent adsorbents saturated with polar adsorbates, the regeneration could take place due to direct microwave heating of adsorbates (Reuß et al. 2002, Witkiewicz and Nastaj 2014, Shariaty et al. 2017). This can be further seen in the temperature and power absorption profiles during microwave heating (Figure 7-5.a and c) whereby the temperature and microwave power absorption for original zeolite decreased after most of the adsorbates desorbed. This decrease is due to the inability of the remaining polar adsorbates to compensate for the low dielectric properties of the adsorbent and heat the bulk adsorbent bed. This led to longer duration and more energy consumption for complete regeneration of the adsorbent in this case.

To further confirm the previous statement, the microwave regeneration was continued until complete regeneration was achieved as indicated by a stable, near zero effluent MEK concentration. The results indicated ~2 times longer duration for complete microwave regeneration of original zeolite compared to modified zeolite. This is due to decrease in power absorption as a result of desorbing the majority of adsorbed MEK during the first half of the regeneration period which led to slower desorption of MEK in the second half.

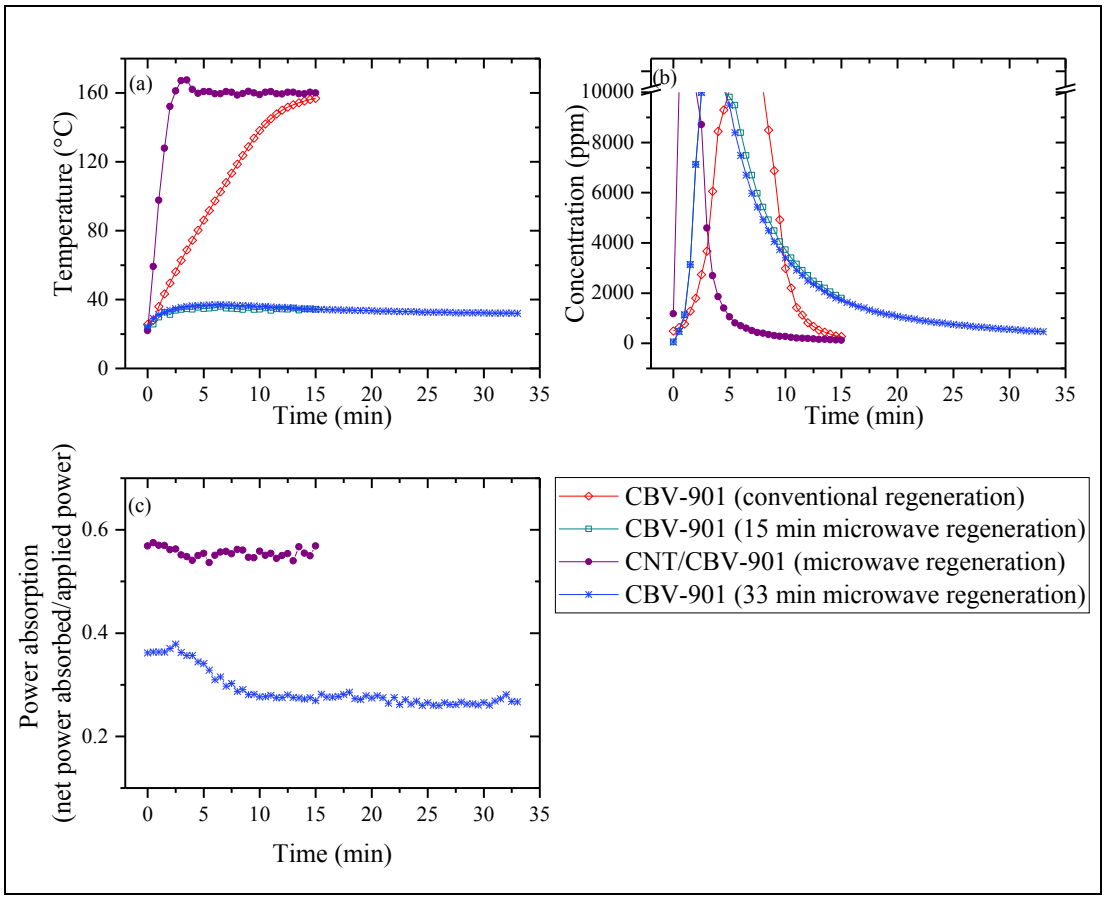

Figure 7-5- Temperature (a) and desorption (b) profile for different regeneration experiments. (c) also presents microwave power absorption during microwave regeneration of original (CBV-901) and modified (CNT/CBV-901) zeolite saturated with MEK

Additionally, to show that modification could make microwave heating a suitable regeneration method even for non-polar adsorbates, the microwave regeneration properties of original and modified zeolite were measured after saturation with cyclohexane, a non-polar adsorbate. The adsorption capacity, normalization based on the weight of the original zeolite, was similar for both modified and original zeolites (7.5±1 wt%) confirming that the zeolite modification has negligible effect on zeolite's adsorption properties. As in the case of MEK, temperature of original zeolite saturated with cyclohexane could not reach more than 30 ºC (Figure 7-6.a), while modified zeolite

could easily reach target temperature of 160 ºC with relatively high heating rate of 73 ºC/min. Unlike the case of polar adsorbate, very low desorption rate was achieved during microwave regeneration of original zeolite saturated with non-polar adsorbate (Figure 7-6. b), and desorption was continued even after 60 min. This resulted in a 67% regeneration efficiency for 60min of microwave heating. In case of modified zeolite, however, similar desorption profile (fast desorption profile) as polar adsorbate was obtained. This confirms that microwave regeneration of zeolite after modification does not rely on the polarity of adsorbate. The power absorption during microwave regeneration for both original and modified zeolite was stable, suggesting that the adsorbate negligibly contributed to microwave absorption.

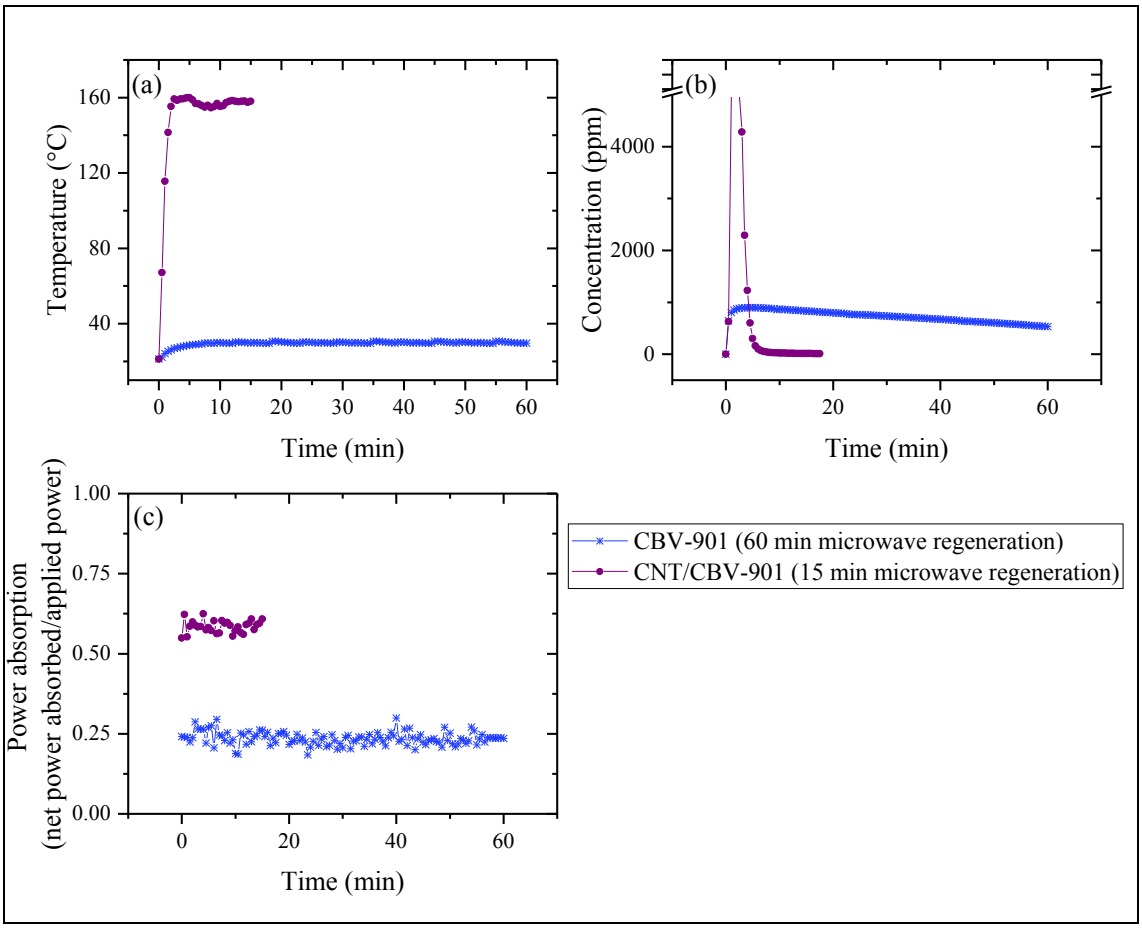

Figure 7-6. Temperature (a) and desorption (b) profile for different regeneration experiments. (c) also presents microwave power absorption during microwave regeneration of original (CBV-901) and modified (CNT/CBV-901) zeolite saturated with cyclohexane

Microwave power was recorded during regeneration of original and modified zeolite, and total energy consumption was calculated for all regeneration tests (Figure 7-7). Obtained results showed 7.5 and 4.2 times less energy consumption for microwave regeneration of the modified zeolite (for both polar and non-polar adsorbates) compared to microwave and conventional regeneration of original zeolite (using polar adsorbate), respectively. Also, poor performance of microwave regeneration of original zeolite saturated with non-polar adsorbate resulted in 67% regeneration

efficiency after 60min while consuming 174 kJ (i.e. long duration, high energy consumption, and low efficiency).

Continuing microwave regeneration of original zeolite saturated with polar adsorbate to achieve complete regeneration significantly increased energy consumption, relative to that of modified zeolite saturated with MEK. This confirms the previous statement that for microwave transparent adsorbents the majority of a polar adsorbate can be desorbed due to direct microwave heating, however, remaining the adsorbate at the end of regeneration cannot absorb enough microwaves to compensate for the low dielectric properties of the adsorbent. Therefore, this results in a longer and more energy consuming process for complete regeneration. Consequently, this further justify implementing the modification method for effective regeneration of microwave transparent adsorbents.

(a)

		Regeneration efficiency
		gr desorbed/ gr adsorbed
(1)	CBV-901 (conventional regeneration)	100%
(2)	CBV-901 (15 min microwave regeneration)	81%
(3)	CNT/CBV-901 (microwave regeneration)	100%
(4)	CBV-901 (33 min microwave regeneration)	100%

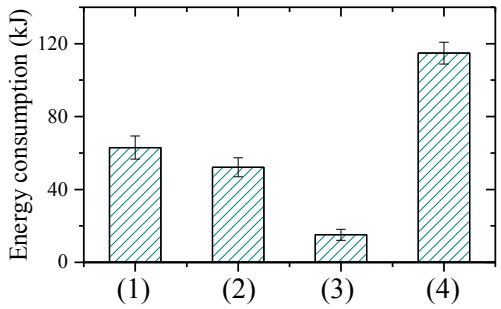

(b)

		Regeneration efficiency
		gr desorbed/gr adsorbed
(5)	CBV-901 (60 min microwave regeneration)	67%
(6)	CNT/CBV-901 (15 min microwave regeneration)	100%

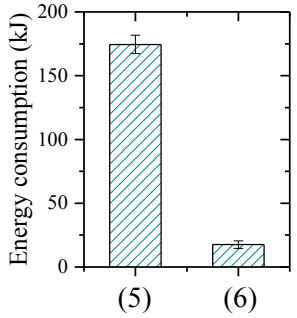

Figure 7-7- Energy consumed and regeneration efficiency obtained during regeneration experiments for (a) polar (MEK) and (b) non-polar adsorbate (cyclohexane)

7.5. Conclusion

A method for addition of carbon nanotube through low temperature catalytic decomposition of CH_4 was used to modify dealuminated zeolite Y aiming for improved dielectric properties. The modification led to addition of 11wt% carbon as nanotubes (confirmed by Raman spectroscopy and SEM pictures) to the zeolite without compromising the adsorption properties. Improved dielectric constant, dielectric loss factor, loss tangent, and penetration depth were obtained for modified samples (more than an order of magnitude increase) which resulted in faster heating rate (~10 times) and larger power absorption (~3 times) during microwave heating compared to original zeolite. Microwave regeneration of the modified sample resulted in faster heating (16 and 5 times) and higher desorption rate (4 and 8 times) compared to microwave and conventional

conduction-convection regeneration of original zeolite. Also, poor performance of microwave regeneration of original zeolite saturated with non-polar adsorbate was found, as indicated by low regeneration efficiency of 67% after 60min regeneration. Microwave regeneration properties of modified zeolite to achieve complete desorption of polar adsorbate (MEK) showed shorter duration (about half) and less energy consumption (7.5 times) compared to original zeolite. Finally, microwave regeneration of modified zeolite saturated with polar or non-polar adsorbates resulted in 4.2 times less energy consumption compared to conventional regeneration of original zeolite. The results obtained indicate that the modification method allows for more effective use of microwave heating for regeneration of microwave transparent adsorbents, for poplar and nonpolar adsorbates.

7.6. Acknowledgements

We would like to acknowledge financial support for this research from the Natural Science and Engineering Research Council (NSERC) of Canada and Alberta Innovates Graduate Student Scholarship program. We also acknowledge Dr. Mojgan Daneshmand and Mohammad H. Zarifi for their help and advices in dielectric properties measurements.

7.7. References

1. Ania, C. O., Parra, J. B., Menéndez, J. A. and Pis, J. J. (2005). "Effect of microwave and conventional regeneration on the microporous and mesoporous network and on the adsorptive capacity of activated carbons." Microporous and Mesoporous Materials **85**(1-2): 7-15.

2. Atwater, J. E. and Wheeler Jr, R. R. (2003). "Complex permittivities and dielectric relaxation of granular activated carbons at microwave frequencies between 0.2 and 26 GHz." Carbon **41**(9): 1801-1807.

3. Bathen, D. (2003). "Physical waves in adsorption technology - An overview." Separation and Purification Technology **33**(2): 163-177.

4. Ben-Mansour, R., Habib, M. A., Bamidele, O. E., Basha, M., Qasem, N. A. A., Peedikakkal, A., Laoui, T. and Ali, M. (2016). "Carbon capture by physical adsorption: Materials, experimental investigations and numerical modeling and simulations - A review." Applied Energy **161**: 225-255.

5. Bokobza, L. (2007). "Multiwall carbon nanotube elastomeric composites: A review." Polymer **48**(17): 4907-4920.

6. Cherbański, R., Komorowska-Durka, M., Stefanidis, G. D. and Stankiewicz, A. I. (2011). "Microwave swing regeneration Vs temperature swing regeneration - Comparison of desorption kinetics." Industrial & Engineering Chemistry Research **50**(14): 8632-8644.

7. Cherbański, R. and Molga, E. (2009). "Intensification of desorption processes by use of microwaves-An overview of possible applications and industrial perspectives." Chemical Engineering and Processing: Process Intensification **48**(1): 48-58.

8. Chowdhury, T., Shi, M., Hashisho, Z., Sawada, J. A. and Kuznicki, S. M. (2012). "Regeneration of Na-ETS-10 using microwave and conductive heating." Chemical Engineering Science **75**: 282-288.

9. Eyer, S., Stadie, N. P., Borgschulte, A., Emmenegger, L. and Mohn, J. (2014). "Methane preconcentration by adsorption: A methodology for materials and conditions selection." Adsorption **20**(5-6): 657-666.

10. Fayaz, M., Shariaty, P., Atkinson, J. D., Hashisho, Z., Phillips, J. H., Anderson, J. E. and Nichols, M. (2015). "Using microwave heating to improve the desorption efficiency of high molecular weight VOC from beaded activated carbon." Environmental Science and Technology **49**(7): 4536-4542.

11. Hashisho, Z., Emamipour, H., Rood, M. J., Hay, K. J., Kim, B. J. and Thurston, D. (2008). "Concomitant adsorption and desorption of organic vapor in dry and humid air streams using microwave and direct electrothermal swing adsorption." Environmental Science and Technology **42**(24): 9317-9322.

12. Hashisho, Z. and Shariaty, P. (2016). Method for Tailoring Electrical Resistivity of Molecular Sieve Absorbents for Resistive Heating Application. **US Provisional application 62/419,798**.

13. He, Y., Gao, J., Gong, X. and Xu, J. (2017). "The role of carbon nanotubes in promoting the properties of carbon black-filled natural rubber/butadiene rubber composites." Results in Physics.

14. Kamravaei, S., Shariaty, P., Jahandar Lashaki, M., Atkinson, J. D., Hashisho, Z., Phillips, J. H., Anderson, J. E. and Nichols, M. (2017). "Effect of Beaded Activated Carbon Fluidization on Adsorption of Volatile Organic Compounds." Industrial & Engineering Chemistry Research **56**(5): 1297-1305.

15. Kamravaei, S., Shariaty, P., Jahandar Lashaki, M., Atkinson, J. D., Hashisho, Z., Phillips, J. H., Anderson, J. E. and Nichols, M. (2017). "Effect of Beaded Activated Carbon Fluidization on Adsorption of Volatile Organic Compounds." Industrial and Engineering Chemistry Research **56**(5): 1297-1305.

16. Kim, K. J. and Ahn, H. G. (2012). "The effect of pore structure of zeolite on the adsorption of VOCs and their desorption properties by microwave heating." Microporous and Mesoporous Materials **152**: 78-83.

17. Li, C., Zhang, L., Xia, H., Peng, J., Cheng, S., Shu, J., Zhang, Q. and Jiang, X. (2017). "Analysis of devitalization mechanism and chemical constituents for fast and efficient regeneration of spent carbon by means of ultrasound and microwaves." Journal of Analytical and Applied Pyrolysis **124**: 42-50.

18. Mao, H., Zhou, D., Hashisho, Z., Wang, S., Chen, H. and Wang, H. H. (2015). "Constant power and constant temperature microwave regeneration of toluene and acetone loaded on microporous activated carbon from agricultural residue." Journal of Industrial and Engineering Chemistry **21**: 516-525.

19. Metaxas, A. C. and Meredith, R. J. (1983). Industrial Microwave Heating, P. Peregrinus.

20. National Research Council (1994). Microwave processing of materials, The National Academies Press..

21. Nigar, H., Garcia-Baños, B., Peñaranda-Foix, F. L., Catalá-Civera, J. M., Mallada, R. and Santamaría, J. (2016). "Amine-functionalized mesoporous silica: A material capable of CO2 adsorption and fast regeneration by microwave heating." AIChE Journal **62**(2): 547-555.

22. Nugent, P., Giannopoulou, E. G., Burd, S. D., Elemento, O., Giannopoulou, E. G., Forrest, K., Pham, T., Ma, S., Space, B., Wojtas, L., Eddaoudi, M. and Zaworotko, M. J. (2013). "Porous materials with optimal adsorption thermodynamics and kinetics for co2 separation." Nature **495**(7439): 80-84.

23. Pinchukova, N. A., Voloshko, A. Y., Baumer, V. N., Shishkin, O. V. and Chebanov, V. A. (2015). "The use of microwave irradiation for zeolite regeneration in a continuous ethanol dewatering process." Chemical Engineering and Processing: Process Intensification **95**: 151-158.

24. Polaert, I., Estel, L., Huyghe, R. and Thomas, M. (2010). "Adsorbents regeneration under microwave irradiation for dehydration and volatile organic compounds gas treatment." Chemical Engineering Journal **162**(3): 941-948.

25. Qing, Y., Wang, X., Zhou, Y., Huang, Z., Luo, F. and Zhou, W. (2014). "Enhanced microwave absorption of multi-walled carbon nanotubes/epoxy composites incorporated with ceramic particles." Composites Science and Technology **102**: 161-168.

26. Reuß, J., Bathen, D. and Schmidt-Traub, H. (2002). "Desorption by microwaves: Mechanisms of multicomponent mixtures." Chemical engineering and Technology **25**(4): 381-384.

27. Rybakov, K. I., Semenov, V. E., Egorov, S. V., Eremeev, A. G., Plotnikov, I. V. and Bykov, Y. V. (2006). "Microwave heating of conductive powder materials." Journal of Applied Physics **99**(2).

28. Shariaty, P., Jahandar Lashaki, M., Hashisho, Z., Sawada, J., Kuznicki, S. and Hutcheon, R. (2017). "Effect of ETS-10 Ion Exchange on Its Dielectric Properties and Adsorption/Microwave Regeneration." Separation and Purification Technology **179**(Supplement C): 420-427.

29. Shin, J. H. and Hong, S. H. (2012). "Microstructure and mechanical properties of single wall carbon nanotube reinforced yttria stabilized zircona ceramics." Materials Science and Engineering A **556**: 382-387.

30. Triantafyllidis, K. S., Karakoulia, S. A., Gournis, D., Delimitis, A., Nalbandian, L., Maccallini, E. and Rudolf, P. (2008). "Formation of carbon nanotubes on iron/cobalt oxides supported on zeolite-Y: Effect of zeolite textural properties and particle morphology." Microporous and Mesoporous Materials **110**(1): 128-140.

31. Wang, L. and Dang, Z. M. (2005). "Carbon nanotube composites with high dielectric constant at low percolation threshold." Applied Physics Letters **87**(4).

32. Witkiewicz, K. and Nastaj, J. (2014). "Modeling of Microwave-Assisted Regeneration of Selected Adsorbents Loaded with Water or Toluene." Drying Technology **32**(11): 1369-1385.

33. Wu, K., Lei, C., Yang, W., Chai, S., Chen, F. and Fu, Q. (2016). "Surface modification of boron nitride by reduced graphene oxide for preparation of dielectric material with enhanced dielectric constant and well-suppressed dielectric loss." Composites Science and Technology **134**: 191-200.

34. Zhao, P., Wang, S., Kadlec, A., Li, Z. and Wang, X. (2016). "Properties of cement-sand-based piezoelectric composites with carbon nanotubes modification." Ceramics International.

Chapter 8. CONCLUSIONS AND RECOMMENDATIONS

8.1. Dissertation Overview

Microwave and resistive heating regenerations have several advantages over conventional methods for regeneration of adsorbents. Their application, however, for regeneration of inorganic adsorbents is limited due to their dependence on adsorbents electric and dielectric properties. One of the renowned categories within inorganic adsorbents is molecular sieves. Adsorptive separation using molecular sieves is a well-developed technique in the industry for gas separation and purification as well as for gaseous pollutants emission control. This research aimed at improving electric and dielectric properties of molecular sieves and efficiently implementing resistive and microwave heating for their regeneration.

8.2. Summary of Findings

Chapter 3 described the effect of ion-exchange of Engelhard Titanosilicate, ETS-10, (test molecular sieve), on its adsorption, dielectric, and microwave regeneration properties using water (polar molecule) as adsorbate. All ion exchanged ETS-10 samples showed increased water adsorption capacity and regeneration efficiency compared to untreated ETS-10. Exchanging ETS-10 with cations also resulted in a decrease in its cation mobility, basicity, and the dielectric properties. This led to increasing the difference between the dielectric properties of the adsorbent and polar adsorbate (e.g. water), resulting in better microwave regeneration efficiency for ion exchanged samples. These improvements may outweigh the increase in energy consumption required to regenerate the adsorbent. Larger adsorption capacity and higher regeneration efficiency compared to untreated ETS-10 may justify the use of ion exchanged adsorbents. Based on capacity

and regeneration efficiency alone, Li-ETS-10 and Ba-ETS-10 are strong candidates for microwave regeneration when loaded with water (e.g. drying applications). Li-ETS-10, however, requires 30% less energy during regeneration and has ~5 times smaller penetration depth compared to Ba-ETS-10, which make it more favorable adsorbent for industrial use.

Effect of carbon addition on the electrical resistivity of dealuminated zeolite Y was investigated in chapter 4. The resistivity of CBV-901 decreased from > 10^7 to 2.8 Ω.m (suitable for resistive heating) by physically mixing the zeolite with 40 wt% carbon powders. While this method significantly decreases zeolite resistivity, the resistivity was decreased even more by adding carbon directly to the zeolite's structure in the form of CNT. CNT growth increased the carbon content of zeolite to 31.4 wt% and decreased its resistivity by eight orders of magnitude (t from > 10^7 o 0.7 Ω.m) while preserving majority of zeolite pores for adsorption. This zeolite modified by CNT growth was successfully heated by resistive heating at 120 ºC /min. The results from this work show the potential for using CNT addition for decreasing the resistivity of highly resistive adsorbents to a level suitable for resistive heating. This technique, however, could be further optimized to reduce its effect on the adsorption properties of the adsorbent.

Chapter 5 evaluated different conditions for CNT growth on the surface of zeolites, as a technique to modify dealuminated zeolite Y and reduce its electrical resistivity. Specifically, temperature and duration of calcination, cobalt catalyst formation, and CH_4 thermal decomposition influenced CNT abundance, diameter, and length, respectively. The optimum condition for CNT deposition was found as 300ºC for 15 minutes (calcination), 300ºC for 15 minutes (cobalt catalyst formation), and 400ºC for 30 minutes (CH_4 thermal decomposition). This condition led to more than 6 orders of magnitude reduction in CBV-901 resistivity with minor impact (<2%) on its adsorption properties. The relatively mild thermal treatment makes this technique applicable for

inorganic adsorbents even with low thermal stability with no additional change in their adsorption and structural properties. Finally, the zeolite modified under the optimum condition was successfully heated using resistive heating, which proves the effectiveness of the applied modification method for tuning the electrical resistivity of the zeolite.

In chapter 6, thermal regeneration of dealuminated zeolite Y was investigated using two different heating methods, resistive and conventional conduction-convection heating (named as conductive heating). The electrical resistivity of the zeolite was initially modified by carbon nanotube addition under optimum thermal condition. The performance of resistive and conductive heating regeneration was then compared. Using the same regeneration duration for both methods, resistive heating demonstrated 94% less energy consumption, 4 times higher heating rate, and 4 times higher desorption rate to reach complete regeneration. This proves resistive heating as a potential alternative for conventional methods for regenerating zeolite adsorbents. Implementing the proposed modification method on other inorganic adsorbents could ultimately allow for resistive heating of adsorbents as a more efficient regeneration method compared to conventional thermal regeneration techniques, without compromising its adsorption performance.

In chapter 7, adsorption/microwave heating regeneration performance of dealuminated zeolite Y was evaluated before and after its modification with CNT deposition. Higher dielectric constant, dielectric loss factor, and loss tangent were obtained for modified adsorbent (more than an order of magnitude increase) which resulted in faster heating rate (~10 times) and higher power absorption (~3 times) during microwave heating compared to original zeolite. Microwave regeneration of the modified sample resulted in faster heating (16 and 5 times) and higher desorption rate (4 and 8 times) compared to microwave and conductive regeneration of original zeolite sample. Also, poor performance of microwave heating of original zeolite saturated with

non-polar adsorbate resulted in low regeneration efficiency, long duration, and high energy consumption. Obtained microwave regeneration properties of modified zeolite after complete desorption of polar adsorbate (MEK) showed shorter duration (about half) and less energy consumption (7.5 times) compared to original zeolite. Finally, microwave regeneration of modified zeolite saturated with both polar and non-polar adsorbates resulted in 4.2 times less energy consumption compared to conductive regeneration of original zeolite. The results obtained indicate that the modification method allows for more effective use of microwave heating for regeneration of microwave transparent adsorbents, for polar and nonpolar adsorbates.

8.3. Recommendations for Future Work

An optimum method to tailor the dielectric and electric properties of molecular sieve adsorbents was achieved in this research at a lab scale, as a proof of concept. Therefore, a scaled-up system should be prepared for further study of adsorption and resistive or microwave heating regeneration of modified adsorbents. Also, a method should be developed to prepare modified adsorbents in a form (e.g. adsorbent beads, monolith, honeycomb, etc.) that can be efficiently incorporated into a scaled-up adsorption/regeneration system to treat high gas flow rates compared to lab scale system. Hence, the following recommendations can be made for future research:

1. *Develop an efficient pilot scale modification system:* The method should be optimized for pilot scale production of the modified adsorbents. Therefore, the key factors should be investigated (e.g. gas/solid ratio, heating rate) and tuned considering the dimension of the new system and increased quantity of base zeolite material (from 1gr to 1kg). The optimum thermal condition should also be investigated.

2. *Prepare monolith from the modified adsorbents:* While resistive/microwave heating could be applied to granular adsorbent bed, configuring the adsorbent into a structured bed (i.e. a monolith or hollow tube) provide an effective configuration for adsorption/regeneration system. Such a configuration provides better path for electric current for resistive heating, better microwave propagation (avoiding any hot spot formation) for microwave heating, fast mass and heat transfer allowing faster adsorption and regeneration (heating and cooling), and lower pressure drop compared to packed beds.
3. *Evaluate the performance of the prepared adsorbents for adsorption and resistive or microwave heating regeneration:* Performance of prepared monoliths (with different types of molecular sieves) should be tested for their ability to adsorb different compounds (e.g. VOCs and CO_2) followed by regeneration using resistive or microwave heating. The adsorption capacity, energy consumption, regeneration efficiency, desorption rate, and composition of the desorbed stream should be measured during resistive, microwave, and conventional heating method (hot gas or steam) for regeneration of the saturated adsorbents.

BIBLIOGRAPHY

1. Abrioux, C., Coasne, B., Maurin, G., Henn, F., Boutin, A., Di Lella, A., Nieto-Draghi, C. and Fuchs, A. H. (2008). "A molecular simulation study of the distribution of cation in zeolites." Adsorption **14**(4-5): 743-754.

2. Adams, F., de Jong, M. and Hutcheon, R. (1992). "Sample shape correction factors for cavity perturbation measurements." Journal of Microwave Power and Electromagnetic Energy **27**(3): 131-135.

3. Al-Baghli, N. A. and Loughlin, K. F. (2005). "Adsorption of methane, ethane, and ethylene on titanosilicate ETS-10 zeolite." Journal of Chemical Engineering Data **50**(3): 843-848.

4. Alsdorf, E., Lohse, U. and Feist, M. (1985). "Thermoanalytical and adsorption investigations on dealuminated Y-zeolites of different preparation." Thermochimica Acta **93**: 553-556.

5. Álvaro, M., Cabeza, J. F., Fabuel, D., García, H., Guijarro, E. and De Juan, J. L. M. (2006). "Electrical conductivity of zeolite films: Influence of charge balancing cations and crystal structure." Chemistry of Materials **18**(1): 26-33.

6. Anderson, M. W., Terasaki, O., Ohsuna, T., Phllippou, A., MacKay, S. P., Ferreira, A., Rocha, J. and Lidin, S. (1994). "Structure of the microporous titanosilicate ETS-10." Nature **367**(6461): 347-351.

7. Ania, C. O., Parra, J. B., Menéndez, J. A. and Pis, J. J. (2005). "Effect of microwave and conventional regeneration on the microporous and mesoporous network and on the adsorptive capacity of activated carbons." Microporous and Mesoporous Materials **85**(1-2): 7-15.

8. Anna, M., Albert, G. N. and Esko, I. K. (2003). "The role of metal nanoparticles in the catalytic production of single-walled carbon nanotubes—a review." Journal of Physics: Condensed Matter **15**(42): S3011.

9. Anson, A., Lin, C. C. H., Kuznicki, S. M. and Sawada, J. A. (2009). "Adsorption of carbon dioxide, ethane, and methane on titanosilicate type molecular sieves." Chemical Engineering Science **64**(16): 3683-3687.

10. Anson, A., Lin, C. C. H., Kuznicki, T. M. and Kuznicki, S. M. (2010). "Separation of ethylene/ethane mixtures by adsorption on small-pored titanosilicate molecular sieves." Chemical Engineering Science **65**(2): 807-811.

11. Anson, A., Wang, Y., Lin, C. C. H., Kuznicki, T. M. and Kuznicki, S. M. (2008). "Adsorption of ethane and ethylene on modified ETS-10." Chemical Engineering Science **63**(16): 4171-4175.

12. Atkinson, J. D., Zhang, Z., Yan, Z. and Rood, M. J. (2013). "Evolution and impact of acidic oxygen functional groups on activated carbon fiber cloth during NO oxidation." Carbon **54**: 444-453.

13. Atwater, J. E. and Wheeler Jr, R. R. (2003). "Complex permittivities and dielectric relaxation of granular activated carbons at microwave frequencies between 0.2 and 26 GHz." Carbon **41**(9): 1801-1807.

14. Auerbach, S. M., Carrado, K. A. and Dutta, P. K. (2003). Handbook of Zeolite Science and Technology, CRC Press.

15. Avila, A. M., Yang, F., Shi, M. and Kuznicki, S. M. (2011). "Extraction of ethane from natural gas at high pressure by adsorption on Na-ETS-10." Chemical Engineering Science **66**(13): 2991-2996.

16. Bansal, R. C. and Goyal, M. (2005). Activated Carbon Adsorption, CRC Press.

17. Bathen, D. (2003). "Physical waves in adsorption technology—an overview." Separation and Purification Technology **33**(2): 163-177.

18. Bathen, D. (2003). "Physical waves in adsorption technology - An overview." Separation and Purification Technology **33**(2): 163-177.

19. Bellat, J. P., Paulin, C., Jeffroy, M., Boutin, A., Paillaud, J. L., Patarin, J., Lella, A. D. and Fuchs, A. (2009). "Unusual hysteresis loop in the adsorption-desorption of water in NaY zeolite at very low pressure." Journal of Physical Chemistry C **113**(19): 8287-8295.

20. Ben-Mansour, R., Habib, M. A., Bamidele, O. E., Basha, M., Qasem, N. A. A., Peedikakkal, A., Laoui, T. and Ali, M. (2016). "Carbon capture by physical adsorption: Materials, experimental investigations and numerical modeling and simulations - A review." Applied Energy **161**: 225-255.

21. Bokobza, L. (2007). "Multiwall carbon nanotube elastomeric composites: A review." Polymer **48**(17): 4907-4920.

22. Bueche, F. (1973). "A new class of switching materials." Journal of Applied Physics **44**(1): 532-533.

23. Camarinha, E. D., Lito, P. F., Antunes, B. M., Otero, M., Lin, Z., Rocha, J., Pereira, E., Duarte, A. C. and Silva, C. M. (2009). "Cadmium(II) removal from aqueous solution using microporous titanosilicate ETS-10." Chemical Engineering Journal **155**(1-2): 108-114.

24. Cao, Y., Yu, H., Tan, J., Peng, F., Wang, H., Li, J., Zheng, W. and Wong, N. B. (2013). "Nitrogen-, phosphorous- and boron-doped carbon nanotubes as catalysts for the aerobic oxidation of cyclohexane." Carbon **57**: 433-442.

25. Cejka, J., Corma, A. and Zones, S. (2010). Zeolites and Catalysis: Synthesis, Reactions and Applications, Wiley.

26. Cherbański, R., Komorowska-Durka, M., Stefanidis, G. D. and Stankiewicz, A. I. (2011). "Microwave swing regeneration Vs temperature swing regeneration - Comparison of desorption kinetics." Industrial & Engineering Chemistry Research **50**(14): 8632-8644.

27. Cherbański, R. and Molga, E. (2009). "Intensification of desorption processes by use of microwaves-An overview of possible applications and industrial perspectives." Chemical Engineering and Processing: Process Intensification **48**(1): 48-58.

28. Choi, J. H., Kim, S. D., Kwon, Y. J. and Kim, W. J. (2006). "Adsorption behaviors of ETS-10 and its variant, ETAS-10 on the removal of heavy metals, Cu2+, Co2+, Mn2+ and Zn2+ from a waste water." Microporous and Mesoporous Materials **96**(1-3): 157-167.

29. Chowdhury, T., Shi, M., Hashisho, Z. and Kuznicki, S. M. (2013). "Indirect and direct microwave regeneration of Na-ETS-10." Chemical Engineering Science **95**: 27-32.

30. Chowdhury, T., Shi, M., Hashisho, Z., Sawada, J. A. and Kuznicki, S. M. (2012). "Regeneration of Na-ETS-10 using microwave and conductive heating." Chemical Engineering Science **75**: 282-288.

31. Ciambelli, P., Sannino, D., Sarno, M., Fonseca, A. and Nagy, J. B. (2005). "Selective formation of carbon nanotubes over Co-modified beta zeolite by CCVD." Carbon **43**(3): 631-640.

32. Coss, P. M. and Cha, C. Y. (2000). "Microwave regeneration of activated carbon used for removal of solvents from vented air." Journal of the Air and Waste Management Association **50**(4): 529-535.

33. Crittenden, B. and Thomas, W. J. (1998). Adsorption Technology and Design, Elsevier Science.

34. Das, S., Mukhopadhyay, A. K., Datta, S. and Basu, D. (2009). "Prospects of microwave processing: An overview." Bulletin of Materials Science **32**(1): 1-13.

35. De Alwis, A. A. P. and Fryer, P. J. (1990). "The use of direct resistance heating in the food industry." Journal of Food Engineering **11**(1): 3-27.

36. Dechow, F. J. (1989). Separation and purification techniques in biotechnology, Noyes Publications.

37. Dehdashti, A., Khavanin, A., Rezaee, A., Assilian, H. and Motalebi, M. (2011). "Application of microwave irradiation for the treatment of adsorbed volatile organic compounds on granular activated carbon." Iranian Journal of Environmental Health Science and Engineering **8**(1): 85-94.

38. Dombrowski, K. D., Lehmann, C. M. B., Sullivan, P. D., Ramirez, D., Rood, M. J. and Hay, K. J. (2004). "Organic vapor recovery and energy efficiency during electric regeneration of an activated carbon fiber cloth adsorber." Journal of Environmental Engineering **130**(3): 268-275.

39. Donohue, M. D. and Aranovich, G. L. (1998). "Classification of Gibbs adsorption isotherms." Advances in Colloid and Interface Science **76**: 137-152.

40. Downarowicz, D. (2015). "Adsorption characteristics of propan-2-ol vapours on activated carbon Sorbonorit 4 in electrothermal temperature swing adsorption process." Adsorption **21**(1-2): 87-98.

41. Emamipour, H., Johnsen, D. L., Rood, M. J., Jain, M. and Skandan, G. (2015). "Novel activated carbon fiber cloth filter with functionalized silica nanoparticles for adsorption of toxic industrial chemicals." Adsorption **21**(4): 265-272.

42. Eyer, S., Stadie, N. P., Borgschulte, A., Emmenegger, L. and Mohn, J. (2014). "Methane preconcentration by adsorption: A methodology for materials and conditions selection." Adsorption **20**(5-6): 657-666.

43. Fan, R. J., Sun, Q., Zhang, L., Zhang, Y. and Lu, A. H. (2014). "Photoluminescent carbon dots directly derived from polyethylene glycol and their application for cellular imaging." Carbon **71**: 87-93.

44. Fayaz, M., Shariaty, P., Atkinson, J. D., Hashisho, Z., Phillips, J. H., Anderson, J. E. and Nichols, M. (2015). "Using microwave heating to improve the desorption efficiency of high molecular weight VOC from beaded activated carbon." Environmental Science and Technology **49**(7): 4536-4542.

45. Gallego, J., Sierra, G., Mondragon, F., Barrault, J. and Batiot-Dupeyrat, C. (2011). "Synthesis of MWCNTs and hydrogen from ethanol catalytic decomposition over a Ni/La2O3 catalyst produced by the reduction of LaNiO3." Applied Catalysis A: General **397**(1–2): 73-81.

46. Garrido Pedrosa, A. M., Souza, M. J. B., Melo, D. M. A. and Araujo, A. S. (2006). "Cobalt and nickel supported on HY zeolite: Synthesis, characterization and catalytic properties." Materials Research Bulletin **41**(6): 1105-1111.

47. Giraudet, S., Boulinguiez, B. and Le Cloirec, P. (2014). "Adsorption and electrothermal desorption of volatile organic compounds and siloxanes onto an activated carbon fiber cloth for biogas purification." Energy and Fuels **28**(6): 3924-3932.

48. Guéret, C., Daroux, M. and Billaud, F. (1997). "Methane pyrolysis: thermodynamics." Chemical Engineering Science **52**(5): 815-827.

49. Hashisho, Z., Emamipour, H., Rood, M. J., Hay, K. J., Kim, B. J. and Thurston, D. (2008). "Concomitant adsorption and desorption of organic vapor in dry and humid air streams using microwave and direct electrothermal swing adsorption." Environmental Science and Technology **42**(24): 9317-9322.

50. Hashisho, Z., Rood, M. and Botich, L. (2005). "Microwave-swing adsorption to capture and recover vapors from air streams with activated carbon fiber cloth." Environmental Science and Technology **39**(17): 6851-6859.

51. Hashisho, Z., Rood, M. J., Barot, S. and Bernhard, J. (2009). "Role of functional groups on the microwave attenuation and electric resistivity of activated carbon fiber cloth." Carbon **47**(7): 1814-1823.

52. Hashisho, Z. and Shariaty, P. (2016). Method for Tailoring Electrical Resistivity of Molecular Sieve Absorbents for Resistive Heating Application. **US Provisional application 62/419,798**.

53. He, Y., Gao, J., Gong, X. and Xu, J. (2017). "The role of carbon nanotubes in promoting the properties of carbon black-filled natural rubber/butadiene rubber composites." Results in Physics.

54. Hu, M. M., Emamipour, H., Johnsen, D. L., Rood, M. J., Song, L. and Zhang, Z. (2017). "Monitoring and Control of an Adsorption System Using Electrical Properties of the Adsorbent for Organic Compound Abatement." Environmental Science and Technology **51**(13): 7581-7589.

55. Hutcheon, R. M., de Jong, M. and Adams, F. P. (1992). "A System for Rapid Measurements of RF and Microwave Properties Up to 1400°C." Journal of Microwave Power and Electromagnetic Energy **27(2)**: 87.

56. IUPAC-Recommendation (1994). "Recommendations for the characterization of porous solids (Technical Report)." Pure and Applied Chemistry **66**(8): 1739-1758.

57. Jacobs, P. A., Flanigen, E. M., Jansen, J. C. and van Bekkum, H. (2001). Introduction to Zeolite Science and Practice, Elsevier Science.

58. Janas, D. and Koziol, K. K. (2014). "A review of production methods of carbon nanotube and graphene thin films for electrothermal applications." Nanoscale **6**(6): 3037-3045.

59. Jänchen, J., Ackermann, D., Stach, H. and Brösicke, W. (2004). "Studies of the water adsorption on Zeolites and modified mesoporous materials for seasonal storage of solar heat." Solar Energy **76**(1–3): 339-344.

60. Jha, V. K., Matsuda, M. and Miyake, M. (2008). "Sorption properties of the activated carbon-zeolite composite prepared from coal fly ash for Ni2+, Cu2+, Cd2+ and Pb2+." Journal of Hazardous Materials **160**(1): 148-153.

61. Jiang, Z., Nolan, A., Walton, J. G. A., Lilienkampf, A., Zhang, R. and Bradley, M. (2014). "Photoluminescent carbon dots from 1,4-addition polymers." Chemistry - A European Journal **20**(35): 10926-10931.

62. Johnsen, D. L., Mallouk, K. E. and Rood, M. J. (2011). "Control of electrothermal heating during regeneration of activated carbon fiber cloth." Environmental Science and Technology **45**(2): 738-743.

63. Johnsen, D. L. and Rood, M. J. (2012). "Temperature control during regeneration of activated carbon fiber cloth with resistance-feedback." Environmental Science and Technology **46**(20): 11305-11312.

64. Johnsen, D. L., Zhang, Z., Emamipour, H., Yan, Z. and Rood, M. J. (2014). "Effect of isobutane adsorption on the electrical resistivity of activated carbon fiber cloth with select physical and chemical properties." Carbon **76**(0): 435-445.

65. Jones, D. A., Lelyveld, T. P., Mavrofidis, S. D., Kingman, S. W. and Miles, N. J. (2002). "Microwave heating applications in environmental engineering - A review." Resources, Conservation and Recycling **34**(2): 75-90.

66. Jullien, A. G. a. R. (1989). The Solid State: From Superconductors to Superalloys. New York, Oxford Science Publications.

67. Kamravaei, S., Shariaty, P., Jahandar Lashaki, M., Atkinson, J. D., Hashisho, Z., Phillips, J. H., Anderson, J. E. and Nichols, M. (2017). "Effect of Beaded Activated Carbon Fluidization on Adsorption of Volatile Organic Compounds." Industrial & Engineering Chemistry Research **56**(5): 1297-1305.

68. Kaneto, K., Tsuruta, M., Sakai, G., Cho, W. Y. and Ando, Y. (1999). "Electrical conductivities of multi-wall carbon nano tubes." Synthetic Metals **103**(1–3): 2543-2546.

69. Karimifard, S., Reza, M. and Moghaddam, A. (2016). "The effects of microwave regeneration on adsorptive performance of functionalized carbon nanotubes." Water Science and Technology **73**(11): 2638-2643.

70. Khachatryan, S. V. and Gevorgyan, T. A. (2010). "Dielectric properties of natural, modified, and irradiated zeolites." Technical Physics **55**(5): 732-734.

71. Khatri, I., Kishi, N., Zhang, J., Soga, T., Jimbo, T., Adhikari, S., Aryal, H. R. and Umeno, M. (2010). "Synthesis and characterization of carbon nanotubes via ultrasonic spray pyrolysis method on zeolite." Thin Solid Films **518**(23): 6756-6760.

72. Kim, J. H., Ikoma, Y. and Niwa, M. (1999). "Control of the pore-opening size of HY zeolite by CVD of silicon alkoxide." Microporous and Mesoporous Materials **32**(1-2): 37-44.

73. Kim, K.-J. and Ahn, H.-G. (2012). "The effect of pore structure of zeolite on the adsorption of VOCs and their desorption properties by microwave heating." Microporous and Mesoporous Materials **152**(0): 78-83.

74. Kim, K. J. and Ahn, H. G. (2012). "The effect of pore structure of zeolite on the adsorption of VOCs and their desorption properties by microwave heating." Microporous and Mesoporous Materials **152**: 78-83.

75. Kraus, M., Kopinke, F. D. and Roland, U. (2011). "Influence of moisture content and temperature on the dielectric permittivity of zeolite NaY." Physical Chemistry Chemical Physics **13**(9): 4119-4125.

76. Kumar, M. and Ando, Y. (2005). "Controlling the diameter distribution of carbon nanotubes grown from camphor on a zeolite support." Carbon **43**(3): 533-540.

77. Kurzweil, P., Maunz, W. and Plog, C. (1995). "Impedance of zeolite-based gas sensors." Sensors and Actuators B: Chemical **25**(1-3): 653-656.

78. Kuznicki, S. M. (1991). Large-pored crystalline titanium molecular sieve zeolites.

79. Legras, B., Polaert, I., Estel, L. and Thomas, M. (2012). "Effect of alcaline cations in zeolites on their dielectric properties." Journal of Microwave Power and Electromagnetic Energy **46**(1): 5-11.

80. Li, C., Zhang, L., Xia, H., Peng, J., Cheng, S., Shu, J., Zhang, Q. and Jiang, X. (2017). "Analysis of devitalization mechanism and chemical constituents for fast and efficient regeneration of spent carbon by means of ultrasound and microwaves." Journal of Analytical and Applied Pyrolysis **124**: 42-50.

81. Li, J., Lu, R., Dou, B., Ma, C., Hu, Q., Liang, Y., Wu, F., Qiao, S. and Hao, Z. (2012). "Porous graphitized carbon for adsorptive removal of benzene and the electrothermal regeneration." Environmental Science and Technology **46**(22): 12648-12654.

82. Li, Y. and Chung, T. S. (2008). "Exploratory development of dual-layer carbon-zeolite nanocomposite hollow fiber membranes with high performance for oxygen enrichment and natural gas separation." Microporous and Mesoporous Materials **113**(1-3): 315-324.

83. Liang, Y., Zhang, H., Yi, B., Zhang, Z. and Tan, Z. (2005). "Preparation and characterization of multi-walled carbon nanotubes supported PtRu catalysts for proton exchange membrane fuel cells." Carbon **43**(15): 3144-3152.

84. Ling, J., Ntiamoah, A., Xiao, P., Webley, P. A. and Zhai, Y. (2015). "Effects of feed gas concentration, temperature and process parameters on vacuum swing adsorption performance for CO2 capture." Chemical Engineering Journal **265**: 47-57.

85. Lu, D., Kondo, J. N., Domen, K., Begum, H. A. and Niwa, M. (2004). "Ultra-fine tuning of microporous opening size in zeolite by CVD." Journal of Physical Chemistry B **108**(7): 2295-2299.

86. Lu, L., Shao, Q., Huang, L. and Lu, X. (2007). "Simulation of adsorption and separation of ethanol–water mixture with zeolite and carbon nanotube." Fluid Phase Equilibria **261**(1–2): 191-198.

87. Luo, L., Ramirez, D., Rood, M. J., Grevillot, G., Hay, K. J. and Thurston, D. L. (2006). "Adsorption and electrothermal desorption of organic vapors using activated carbon adsorbents with novel morphologies." Carbon **44**(13): 2715-2723.

88. Lv, L., Tsoi, G. and Zhao, X. S. (2004). "Uptake equilibria and mechanisms of heavy metal ions on microporous titanosilicate ETS-10." Industrial & Engineering Chemistry Research **43**(24): 7900-7906.

89. Magnowski, N. B. K., Avila, A. M., Lin, C. C. H., Shi, M. and Kuznicki, S. M. (2011). "Extraction of ethane from natural gas by adsorption on modified ETS-10." Chemical Engineering Science **66**(8): 1697-1701.

90. Mao, H., Zhou, D., Hashisho, Z., Wang, S., Chen, H. and Wang, H. H. (2015). "Constant power and constant temperature microwave regeneration of toluene and acetone loaded on microporous activated carbon from agricultural residue." Journal of Industrial and Engineering Chemistry **21**: 516-525.

91. Metaxas, A. C. and Meredith, R. J. (1983). Industrial Microwave Heating, P. Peregrinus.

92. Miyake, M., Kimura, Y., Ohashi, T. and Matsuda, M. (2008). "Preparation of activated carbon-zeolite composite materials from coal fly ash." Microporous and Mesoporous Materials **112**(1-3): 170-177.

93. Mohamad Nor, N., Sukri, M. F. F. and Mohamed, A. R. (2016). "Development of high porosity structures of activated carbon via microwave-assisted regeneration for H2S removal." Journal of Environmental Chemical Engineering **4**(4): 4839-4845.

94. Moisala, A., Nasibulin, A. G. and Kauppinen, E. I. (2003). "The role of metal nanoparticles in the catalytic production of single-walled carbon nanotubes - A review." Journal of Physics Condensed Matter **15**(42): S3011-S3035.

95. Monneyron, P., Manero, M. H. and Foussard, J. N. (2003). "Measurement and modeling of single- and multi-component adsorption equilibria of VOC on high-silica zeolites." Environmental Science and Technology **37**(11): 2410-2414.

96. Moteki, T., Murakami, Y., Noda, S., Maruyama, S. and Okubo, T. (2011). "Zeolite Surface As a Catalyst Support Material for Synthesis of Single-Walled Carbon Nanotubes." The Journal of Physical Chemistry C **115**(49): 24231-24237.

97. Nak, C. J., Young, J. L., Park, J. H., Lim, H., Shin, C. H., Cheong, H. and Kyung, B. Y. (2009). "New insights into ETS-10 and titanate quantum wire: A comprehensive characterization." Journal of the American Chemical Society **131**(36): 13080-13092.

98. Nakada, K. and Ishii, A. (2011). DFT Calculation for Adatom Adsorption on Graphene.

99. Nath, D. C. D. and Sahajwalla, V. (2011). "Application of fly ash as a catalyst for synthesis of carbon nanotube ribbons." Journal of Hazardous Materials **192**(2): 691-697.

100. Nath, D. C. D. and Sahajwalla, V. (2011). "Growth mechanism of carbon nanotubes produced by pyrolysis of a composite film of poly (vinyl alcohol) and fly ash." Applied Physics A: Materials Science and Processing **104**(2): 539-544.

101. National Research Council (1994). Microwave processing of materials, The National Academies Press.

102. Nigar, H., Garcia-Baños, B., Peñaranda-Foix, F. L., Catalá-Civera, J. M., Mallada, R. and Santamaría, J. (2016). "Amine-functionalized mesoporous silica: A material capable of CO2 adsorption and fast regeneration by microwave heating." AIChE Journal **62**(2): 547-555.

103. Nigar, H., Navascués, N., de la Iglesia, O., Mallada, R. and Santamaría, J. (2015). "Removal of VOCs at trace concentration levels from humid air by Microwave Swing Adsorption, kinetics and proper sorbent selection." Separation and Purification Technology **151**: 193-200.

104. Niknaddaf, S., Atkinson, J. D., Shariaty, P., Jahandar Lashaki, M., Hashisho, Z., Phillips, J. H., Anderson, J. E. and Nichols, M. (2016). "Heel formation during volatile organic compound desorption from activated carbon fiber cloth." Carbon **96**: 131-138.

105. Nugent, P., Giannopoulou, E. G., Burd, S. D., Elemento, O., Giannopoulou, E. G., Forrest, K., Pham, T., Ma, S., Space, B., Wojtas, L., Eddaoudi, M. and Zaworotko, M. J. (2013). "Porous materials with optimal adsorption thermodynamics and kinetics for co2 separation." Nature **495**(7439): 80-84.

106. Ohgushi, T., Sakai, Y., Adachi, Y. and Satoh, H. (2009). "Comparisons between measured and calculated properties in the microwave heating of Na-A, K-A, and Na,Ca-A zeolites." Journal of Physical Chemistry C **113**(19): 8206-8210.

107. Ohsuna, T., Terasaki, O., Watanabe, D., Anderson, M. W. and Lidin, S. (1994). "Microporous titanosilicate ETS-10: electron microscopy study." Studies in Surface Science and Catalysis **84**: 413-420.

108. Olivier, J. P. (1998). "Improving the models used for calculating the size distribution of micropore volume of activated carbons from adsorption data." Carbon **36**(10): 1469-1472.

109. Palma, V. and Meloni, E. (2016). "Microwave assisted regeneration of a catalytic diesel soot trap." Fuel **181**: 421-429.

110. Pan, R. R., Fan, F. L., Li, Y. and Jin, X. J. (2016). "Microwave regeneration of phenol-loaded activated carbons obtained from: Arundo donax and waste fiberboard." RSC Advances **6**(39): 32960-32966.

111. Park, S., Kwon, Y. P., Kwon, H. C., Lee, J. H., Lee, H. W. and Lee, J. C. (2007). "Electrothermal properties of porous ceramic fiber media containing carbon materials." Journal of Nanoscience and Nanotechnology **7**(11): 3776-3779.

112. Park, S., Kwon, Y. P., Kwon, H. C., Lee, J. H., Lee, H. W. and Lee, J. C. (2009). "Electrothermal properties of regenerable carbon contained porous ceramic fiber media." Journal of Electroceramics **22**(1-3): 315-318.

113. Park, S. W., Yun, Y. H., Kim, S. D., Yang, S. T., Ahn, W. S., Seo, G. and Kim, W. J. (2010). "CO2 retention ability on alkali cation exchanged titanium silicate, ETS-10." Journal of Porous Materials **17**(5): 589-595.

114. Pełech, I., Narkiewicz, U., Kaczmarek, A. and Jędrzejewska, A. (2014). "Preparation and characterization of multi-walled carbon nanotubes grown on transition metal catalysts." Polish Journal of Chemical Technology **16**(1): 117-122.

115. Petkovska, M., Tondeur, D., Grevillot, G., Granger, J. and Mitrovic, M. (1991). "Temperature-swing gas separation with electrothermal desorption step." Separation Science and Technology **26**(3): 425-444.

116. Pinchukova, N. A., Voloshko, A. Y., Baumer, V. N., Shishkin, O. V. and Chebanov, V. A. (2015). "The use of microwave irradiation for zeolite regeneration in a continuous ethanol dewatering process." Chemical Engineering and Processing: Process Intensification **95**: 151-158.

117. Polaert, I., Estel, L., Huyghe, R. and Thomas, M. (2010). "Adsorbents regeneration under microwave irradiation for dehydration and volatile organic compounds gas treatment." Chemical Engineering Journal **162**(3): 941-948.

118. Qi, J., Benipal, N., Chadderdon, D. J., Huo, J., Jiang, Y., Qiu, Y., Han, X., Hu, Y. H., Shanks, B. H. and Li, W. (2015). "Carbon nanotubes as catalysts for direct carbohydrazide fuel cells." Carbon **89**: 142-147.

119. Qing, Y., Wang, X., Zhou, Y., Huang, Z., Luo, F. and Zhou, W. (2014). "Enhanced microwave absorption of multi-walled carbon nanotubes/epoxy composites incorporated with ceramic particles." Composites Science and Technology **102**: 161-168.

120. Ramirez, D., Emamipour, H., Vidal, E. X., Rood, M. J. and Hay, K. J. (2011). "Capture and recovery of methyl ethyl ketone with electrothermal-swing adsorption systems." Journal of Environmental Engineering **137**(9): 826-832.

121. Resasco, D. E., Alvarez, W. E., Pompeo, F., Balzano, L., Herrera, J. E., Kitiyanan, B. and Borgna, A. (2002). "A Scalable Process for Production of Single-walled Carbon Nanotubes (SWNTs) by Catalytic Disproportionation of CO on a Solid Catalyst." Journal of Nanoparticle Research **4**(1): 131-136.

122. Reuß, J., Bathen, D. and Schmidt-Traub, H. (2002). "Desorption by microwaves: Mechanisms of multicomponent mixtures." Chemical engineering and Technology **25**(4): 381-384.

123. Ribeiro, R. P. P. L., Grande, C. A. and Rodrigues, A. E. (2011). "Adsorption of water vapor on carbon molecular sieve: Thermal and electrothermal regeneration study." Industrial and Engineering Chemistry Research **50**(4): 2144-2156.

124. Ribeiro, R. P. P. L., Grande, C. A. and Rodrigues, A. E. (2014). "Electric Swing Adsorption for Gas Separation and Purification: A Review." Separation Science and Technology (Philadelphia) **49**(13): 1985-2002.

125. Rocha, J. and Anderson, M. W. (2000). "Microporous titanosilicates and other novel mixed octahedral-tetrahedral framework oxides." European Journal of Inorganic Chemistry(5): 801-818.

126. Roussy, G. and Chenot, P. (1981). Selective Energy Supply to Adsorbed Water and Non Classical Thermal Process During Microwave Dehydration of Zeolite. 16th Annual Symposium on Microwave Power., Toronto, Canada.

127. Roussy, G. and Chenot, P. (1981). "Selective energy supply to adsorbed water and nonclassical thermal process during microwave dehydration of zeolite." Journal of Physical Chemistry **85**(15): 2199-2203.

128. Roussy, G., Zoulalian, A., Charreyre, M. and Thiebaut, J. M. (1984). "How microwaves dehydrate zeolites." Journal of physical Chemistry **88**(23): 5702-5708.

129. Russell, J. and Cohn, R. (2012). Joule Heating, Book on Demand.

130. Rybakov, K. I., Semenov, V. E., Egorov, S. V., Eremeev, A. G., Plotnikov, I. V. and Bykov, Y. V. (2006). "Microwave heating of conductive powder materials." Journal of Applied Physics **99**(2).

131. Sano, N., Kodama, T. and Tamon, H. (2013). "Direct synthesis of carbon nanotubes on stainless steel electrode for enhanced catalyst efficiency in a glucose fuel cell." Carbon **55**: 365-368.

132. Sarno, M., Tamburrano, A., Arurault, L., Fontorbes, S., Pantani, R., Datas, L., Ciambelli, P. and Sarto, M. S. (2013). "Electrical conductivity of carbon nanotubes grown inside a mesoporous anodic aluminium oxide membrane." Carbon **55**: 10-22.

133. Sengupta, J. and Jacob, C. (2009). "Growth temperature dependence of partially Fe filled MWCNT using chemical vapor deposition." Journal of Crystal Growth **311**(23–24): 4692-4697.

134. Shariaty, P., Jahandar Lashaki, M., Hashisho, Z., Sawada, J., Kuznicki, S. and Hutcheon, R. (2017). "Effect of ETS-10 ion exchange on its dielectric properties and adsorption/microwave regeneration." Separation and Purification Technology **179**: 420-427.

135. Shi, M., Avila, A. M., Yang, F., Kuznicki, T. M. and Kuznicki, S. M. (2011). "High pressure adsorptive separation of ethylene and ethane on Na-ETS-10." Chemical Engineering Science **66**(12): 2817-2822.

136. Shi, M., Lin, C. C. H., Kuznicki, T. M., Hashisho, Z. and Kuznicki, S. M. (2010). "Separation of a binary mixture of ethylene and ethane by adsorption on Na-ETS-10." Chemical Engineering Science **65**(11): 3494-3498.

137. Shin, J. H. and Hong, S. H. (2012). "Microstructure and mechanical properties of single wall carbon nanotube reinforced yttria stabilized zircona ceramics." Materials Science and Engineering A **556**: 382-387.

138. Sing, K. S. W. (1998). "Adsorption methods for the characterization of porous materials." Advances in Colloid and Interface Science **76**: 3-11.

139. Singleton, J. (2001). Band Theory and Electronic Properties of Solids. New York, Oxford University Press.

140. Snyder, J. D. and Leesch, J. G. (2001). "Methyl bromide recovery on activated carbon with repeated adsorption and electrothermal regeneration." Industrial and Engineering Chemistry Research **40**(13): 2925-2933.

141. Song, X. H., Teo, W. S. and Wang, K. (2012). "Synthesis and characterization of activated carbons prepared from benzene CVD on zeolite y." Journal of Porous Materials **19**(2): 211-215.

142. Subrenat, A., Baléo, J. N., Le Cloirec, P. and Blanc, P. E. (2001). "Electrical behaviour of activated carbon cloth heated by the joule effect: Desorption application." Carbon **39**(5): 707-716.

143. Subrenat, A. and Le Cloirec, P. (2004). "Adsorption onto activated carbon cloths an electrothermal regeneration: Its potential industrial applications." Journal of Environmental Engineering **130**(3): 249-257.

144. Sullivan, P. D., Rood, M. J., Dombrowski, K. D. and Hay, K. J. (2004). "Capture of organic vapors using adsorption and electrothermal regeneration." Journal of Environmental Engineering **130**(3): 258-267.

145. Sullivan, P. D., Rood, M. J., Grevillot, G., Wander, J. D. and Hay, K. J. (2004). "Activated carbon fiber cloth electrothermal swing adsorption system." Environmental Science and Technology **38**(18): 4865-4877.

146. Sullivan, P. D., Rood, M. J., Hay, K. J. and Qi, S. (2001). "Adsorption and electrothermal desorption of hazardous organic vapors." Journal of Environmental Engineering **127**(3): 217-223.

147. Takagi, D., Hibino, H., Suzuki, S., Kobayashi, Y. and Homma, Y. (2007). "Carbon Nanotube Growth from Semiconductor Nanoparticles." Nano Letters **7**(8): 2272-2275.

148. Tanchuk, B., Sawada, J. A., Rezaei, S. and Kuznicki, S. M. (2013). "Adsorptive drying of CO2 using low grade heat and humid, ambient air." Separation and Purification Technology **120**: 354-361.

149. Triantafyllidis, K. S., Karakoulia, S. A., Gournis, D., Delimitis, A., Nalbandian, L., Maccallini, E. and Rudolf, P. (2008). "Formation of carbon nanotubes on iron/cobalt oxides supported on zeolite-Y: Effect of zeolite textural properties and particle morphology." Microporous and Mesoporous Materials **110**(1): 128-140.

150. Uda, A., Morita, S. and Ozaki, Y. (2013). "Thermal degradation of a poly(vinyl alcohol) film studied by multivariate curve resolution analysis." Polymer (United Kingdom) **54**(8): 2130-2137.

151. Uma, S., Rodrigues, S., Martyanov, I. N. and Klabunde, K. J. (2004). "Exploration of photocatalytic activities of titanosilicate ETS-10 and transition metal incorporated ETS-10." Microporous and Mesoporous Materials **67**(2-3): 181-187.

152. Varghese, K. S., Pandey, M. C., Radhakrishna, K. and Bawa, A. S. (2012). "Technology, applications and modelling of ohmic heating: a review." Journal of Food Science and Technology **51**(10): 2304-2317.

153. Waghmode, S. B., Vetrivel, R., Hegde, S. G., Gopinath, C. S. and Sivasanker, S. (2003). "Physicochemical investigations of the basicity of the cation exchanged ETS-10 molecular sieves." Journal of Physical Chemistry B **107**(33): 8517-8523.

154. Wang, L. and Dang, Z. M. (2005). "Carbon nanotube composites with high dielectric constant at low percolation threshold." Applied Physics Letters **87**(4).

155. Witkiewicz, K. and Nastaj, J. (2014). "Modeling of Microwave-Assisted Regeneration of Selected Adsorbents Loaded with Water or Toluene." Drying Technology **32**(11): 1369-1385.

156. Wu, K., Lei, C., Yang, W., Chai, S., Chen, F. and Fu, Q. (2016). "Surface modification of boron nitride by reduced graphene oxide for preparation of dielectric material with enhanced dielectric constant and well-suppressed dielectric loss." Composites Science and Technology **134**: 191-200.

157. Yang, H., Xu, S., Jiang, L. and Dan, Y. (2012). "Thermal decomposition behavior of poly (vinyl alcohol) with different hydroxyl content." Journal of Macromolecular Science, Part B: Physics **51**(3): 464-480.

158. Yuen, F. K. and Hameed, B. H. (2009). "Recent developments in the preparation and regeneration of activated carbons by microwaves." Advances in Colloid and Interface Science **149**(1): 19-27.

159. Zanetti, J. E. and Egloff, G. (1917). "The Thermal Decomposition of Benzene." Journal of Industrial & Engineering Chemistry **9**(4): 350-356.

160. Zarifi, M. H., Shariaty, P., Hashisho, Z. and Daneshmand, M. (2017). "A non-contact microwave sensor for monitoring the interaction of zeolite 13X with CO2 and CH4 in gaseous streams." Sensors and Actuators, B: Chemical **238**: 1240-1247.

161. Zhang, L., Zhao, B., Wang, X., Liang, Y., Qiu, H., Zheng, G. and Yang, J. (2014). "Gas transport in vertically-aligned carbon nanotube/parylene composite membranes." Carbon **66**: 11-17.

162. Zhao, P., Wang, S., Kadlec, A., Li, Z. and Wang, X. (2016). "Properties of cement-sand-based piezoelectric composites with carbon nanotubes modification." Ceramics International.

163. Zheng, T., Wang, Q., Shi, Z., Zhang, Z. and Ma, Y. (2016). "Microwave regeneration of spent activated carbon for the treatment of ester-containing wastewater." RSC Advances **6**(65): 60815-60825.